NUREG/CR-6914, Vol. 6
LA-UR-05-9177

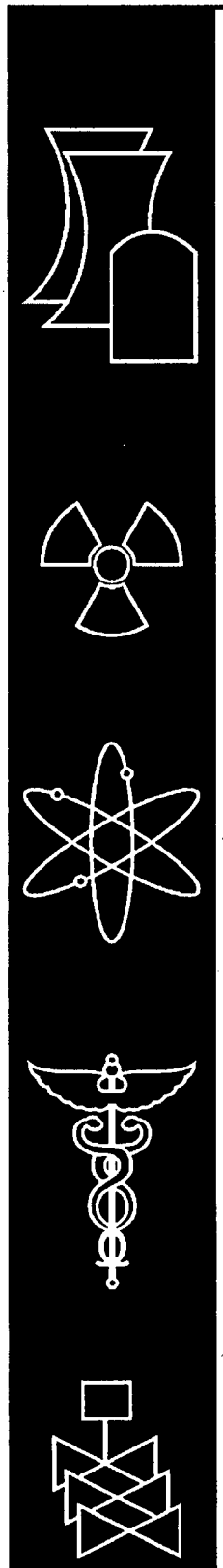

# Integrated Chemical Effects Test Project: Test #5 Data Report

**Los Alamos National Laboratory**

**U.S. Nuclear Regulatory Commission**
**Office of Nuclear Regulatory Research**
**Washington, DC 20555-0001**

## AVAILABILITY OF REFERENCE MATERIALS IN NRC PUBLICATIONS

### NRC Reference Material

As of November 1999, you may electronically access NUREG-series publications and other NRC records at NRC's Public Electronic Reading Room at http://www.nrc.gov/reading-rm.html. Publicly released records include, to name a few, NUREG-series publications; *Federal Register* notices; applicant, licensee, and vendor documents and correspondence; NRC correspondence and internal memoranda; bulletins and information notices; inspection and investigative reports; licensee event reports; and Commission papers and their attachments.

NRC publications in the NUREG series, NRC regulations, and *Title 10, Energy*, in the Code of *Federal Regulations* may also be purchased from one of these two sources.

1. The Superintendent of Documents
   U.S. Government Printing Office
   Mail Stop SSOP
   Washington, DC 20402–0001
   Internet: bookstore.gpo.gov
   Telephone: 202-512-1800
   Fax: 202-512-2250
2. The National Technical Information Service
   Springfield, VA 22161–0002
   www.ntis.gov
   1–800–553–6847 or, locally, 703–605–6000

A single copy of each NRC draft report for comment is available free, to the extent of supply, upon written request as follows:

Address: U.S. Nuclear Regulatory Commission
Office of Administration
Mail, Distribution and Messenger Team
Washington, DC 20555-0001
E-mail: DISTRIBUTION@nrc.gov
Facsimile: 301–415–2289

Some publications in the NUREG series that are posted at NRC's Web site address http://www.nrc.gov/reading-rm/doc-collections/nuregs are updated periodically and may differ from the last printed version. Although references to material found on a Web site bear the date the material was accessed, the material available on the date cited may subsequently be removed from the site.

### Non-NRC Reference Material

Documents available from public and special technical libraries include all open literature items, such as books, journal articles, and transactions, *Federal Register* notices, Federal and State legislation, and congressional reports. Such documents as theses, dissertations, foreign reports and translations, and non-NRC conference proceedings may be purchased from their sponsoring organization.

Copies of industry codes and standards used in a substantive manner in the NRC regulatory process are maintained at—

The NRC Technical Library
Two White Flint North
11545 Rockville Pike
Rockville, MD 20852–2738

These standards are available in the library for reference use by the public. Codes and standards are usually copyrighted and may be purchased from the originating organization or, if they are American National Standards, from—

American National Standards Institute
11 West 42nd Street
New York, NY 10036–8002
www.ansi.org
212–642–4900

Legally binding regulatory requirements are stated only in laws; NRC regulations; licenses, including technical specifications; or orders, not in NUREG-series publications. The views expressed in contractor-prepared publications in this series are not necessarily those of the NRC.

The NUREG series comprises (1) technical and administrative reports and books prepared by the staff (NUREG–XXXX) or agency contractors (NUREG/CR–XXXX), (2) proceedings of conferences (NUREG/CP–XXXX), (3) reports resulting from international agreements (NUREG/IA–XXXX), (4) brochures (NUREG/BR–XXXX), and (5) compilations of legal decisions and orders of the Commission and Atomic and Safety Licensing Boards and of Directors' decisions under Section 2.206 of NRC's regulations (NUREG–0750).

NUREG/CR-6914, Vol. 6
LA-UR-05-9177

# Integrated Chemical Effects Test Project: Test #5 Data Report

Manuscript Completed: August 2006
Date Published: December 2006

Principal Investigator: J. Dallman

Prepared by
J. Dallman, B. Letellier, J. Garcia, J. Madrid, W. Roesch
Los Alamos National Laboratory
Los Alamos, NM 87545

D. Chen, K. Howe
University of New Mexico
Department of Civil Engineering
Albuquerque, NM 87110

L. Archuleta, F. Sciacca
OMICRON Safety and Risk Technologies, Inc.
2500 Louisiana Blvd. NE, Suite 410
Albuquerque, NM 87110

B.P. Jain, NRC Project Manager

**Prepared for**
**Division of Fuel, Engineering and Radiological Research**
**Office of Nuclear Regulatory Research**
**U.S. Nuclear Regulatory Commission**
**Washington, DC 20555-0001**
**NRC Job Code Y6999**

**NUREG/CR-6914, Volume 6, has been reproduced from the best available copy.**

# INTEGRATED CHEMICAL EFFECTS TEST PROJECT: TEST #5 DATA REPORT

## ABSTRACT

A 30-day test was conducted in the Integrated Chemical Effects Test (ICET) project test apparatus. The test simulated the chemical environment present inside a pressurized water reactor containment water pool after a loss-of-coolant accident. The initial chemical environment contained 6.48 kg of boric acid, 10.0 kg of sodium tetraborate, and 0.284 g of lithium hydroxide. 90.8 mL of hydrochloric acid was added during the last two hours of the four-hour spray phase. The test was conducted for 30 days at a constant temperature of 60°C (140°F). The materials tested within this environment included representative amounts of submerged and unsubmerged aluminum, copper, concrete, zinc, carbon steel, and insulation samples (100% fiberglass). Representative amounts of concrete dust and latent debris were also added to the test solution. Water was circulated through the bottom portion of the test chamber during the entire test to achieve representative flow rates over the submerged specimens. The test solution pH varied from 8.2 to 8.4 for the duration of the test. The test solution turbidity decreased to approximately 2 NTU after 7 days. The turbidity at 60°C decreased to approximately 1 NTU the following day and remained near 1 NTU for the duration of the test. However, when the solution was cooled to 23°C, the turbidity increased to 5 NTU at Day 19 and remained near that value for the duration of the test. After the water samples had cooled to room temperature for several days, precipitates were visible in the water. These formed wispy patterns when the sample bottles were turned upside down and took 2–3 days to settle again. The submerged metallic coupons all developed thin particulate deposits that dulled their color and roughened their surface. Post-test examinations showed that the submerged aluminum coupons lost approximately 3% of their weight, but there were very little weight changes on the other coupons. The unsubmerged coupons exhibited some streaking, but little or no weight changes. The bottom of the tank contained very little sediment at the end of the test. The test solution at 60°C remained Newtonian for the entire test. When cooled to 25°C, the solution exhibited shear thinning, and the viscosity generally increased at all shear rates as the test progressed. Aluminum concentration rose to over 50 mg/L by Day 11 and fluctuated between 33 and 55 mg/L for the duration of the test.

# CONTENTS

# Appendices

# FIGURES

## TABLES

# INTEGRATED CHEMICAL EFFECTS TEST PROJECT: TEST #5 DATA REPORT

## EXECUTIVE SUMMARY

The U.S. Nuclear Regulatory Commission (NRC) Office of Nuclear Regulatory Research has developed a comprehensive research program to support resolution of Generic Safety Issue (GSI)-191. GSI-191 addresses the potential for debris accumulation on pressurized water reactor (PWR) sump screens, with the consequent loss of net-positive-suction-head margin in the emergency core-cooling system (ECCS) pump. Among the GSI-191 research program tasks is the experimental investigation of chemical effects that may exacerbate sump-screen clogging.

The Integrated Chemical Effects Test (ICET) project represents a joint effort by the U.S. NRC and the nuclear utility industry, undertaken through the Memorandum of Understanding on Cooperative Nuclear Safety between the NRC and Electric Power Research Institute, Addendum on Integral Chemical Effects Testing for PWR ECCS Recirculation. The ICET project simulates the chemical environment present inside a containment water pool after a loss-of-coolant accident and monitors the chemical system for an extended time to identify the presence, composition, and physical characteristics of chemical products that form during the test. The ICET test series is being conducted by Los Alamos National Laboratory at the University of New Mexico, with the assistance of professors and students in the civil engineering department.

This report describes the ICET experimental apparatus and surveys the principal findings of Test #5. This interim data report summarizes both primary and representative findings that were available at the time the report was prepared. The NRC and the nuclear power industry may conduct additional analyses to enhance the understandings obtained from this test.

All of the ICET tests were conducted in environments that simulate expected containment pool conditions during recirculation. The tests are conducted for 30 days at a constant temperature of 60°C (140°F). The materials tested within each environment include representative amounts of submerged and unsubmerged aluminum, copper, concrete, zinc, carbon steel, and insulation samples. Representative amounts of concrete dust and latent debris are also added to the test solution. Tests consist of an initial 4-hour spray phase to simulate containment spray interaction with the unsubmerged samples. Water is circulated through the bottom portion of the test chamber during the entire test to achieve representative flow rates over the submerged specimens. Test #5 had a different initial boron concentration and a buffering agent that was different from the other 4 tests. Boric acid (6.48 kg), sodium tetraborate (10.0 kg), and lithium hydroxide (0.284 g) were added and dissolved in the ICET tank solution. That resulted in the initial test solution having a boron concentration of 2400 mg/L. Also, 90.8 mL of hydrochloric acid was added during the last two hours of the spray phase.

ICET Test #5 was conducted using sodium tetraborate as a buffering agent, with a target pH of 8 to 8.5. Insulation samples consisted of scaled amounts of NUKON™ fiberglass. In addition, the test apparatus contained 373 metal coupon samples and 1 concrete sample. Process control consisted of monitoring online measurements of recirculation flow rate, test solution

temperature, and pH. Flow rate and temperature were controlled to maintain the desired values of 25 gpm and 140°F. Daily water samples were obtained for measurements of pH, turbidity, total suspended solids, kinematic viscosity, and shear-dependent viscosity and for analytical laboratory evaluations of the chemical elements present. In addition, microscopic evaluations were conducted on water sample filtrates, fiberglass, coupons, and sediment.

The test ran for 30 days, and all conditions were maintained within the accepted flow and temperature ranges, with one exception. On Day 5, the addition of cold makeup water caused the test solution temperature to drop to 57.7°C, which is 0.3°C below the target minimum. The minimum temperature was below 58.0°C for less than 10 minutes. At the start of the test, the measured pH was 8.4. During the addition of hydrochloric acid, the pH dropped slightly to 8.3, and it remained between 8.2 and 8.4 for the duration of the test.

Daily measurements of the constant-shear kinematic viscosity of the test solution revealed an approximately constant value at both test temperature and room temperature. Measurements of the shear-dependent viscosity indicated that at 60°C the test solution remained Newtonian for the entire test. At 25°C, the test solution exhibited shear thinning, and the viscosity generally increased at all shear rates as the test progressed. Light, wispy precipitates were visible after the test solution sat at room temperature for several days.

Analyses of the test solution showed that aluminum in the solution rose above 50 mg/L on Day 11 and fluctuated between 33 and 55 mg/L for the duration of the test. Calcium, silica, and sodium were prevalent in the solution.

Examinations of fiberglass taken from the test apparatus revealed chemical byproducts and web-like deposits that spanned individual fibers. Flocculent deposits were also observed. The amounts of these deposits did not increase significantly over the duration of the test, and the web-like deposits were absent in the Day-30 samples. The deposits were likely formed by chemical precipitation. In addition to flocculent deposits, some samples had significant amounts of particulate deposits on their exteriors that were likely physically attached.

The submerged metallic coupons all developed thin particulate deposits that dulled their color and roughened their surface. Post-test examinations showed that the submerged aluminum coupons lost approximately 3% of their weight, but there were very little weight changes on the other coupons. The unsubmerged coupons exhibited some streaking, but little or no weight changes.

The ICET series is being conducted under an approved quality assurance (QA) program, and QA procedures and project instructions were reviewed and approved by the project sponsors. Analytical laboratory results are generated under a quality control program approved by the Environmental Protection Agency, and other laboratory analyses were performed using standard practices.

# ACKNOWLEDGMENTS

The principal authors of this report gratefully acknowledge the assistance of the following persons, without whom successful completion of the fifth Integrated Chemical Effects Test could not have been accomplished. Mr. John Gisclon, representing the Electric Power Research Institute, contributed much practical, timely advice on preparation of the quality assurance (QA) experimental project instructions and the addition of sodium tetraborate. Mr. Michael Niehaus from Sandia National Laboratories provided a characterization of time-dependent shear-rate viscosity measurements for the circulating solution. Mr. Luke Bartlein, of Los Alamos National Laboratory's Nuclear Design and Risk Analysis group (D-5), provided timely tagging of all test pictures and analytical images. Mr. Jim Young, of group PS-1, provided valuable reviews and inputs to QA documentation and practices, and a QA review of this report. The authors also express their gratitude for the contributions and continued participation of numerous NRC staff members who reviewed the project instructions and preliminary data to ensure relevance to plant safety, high-quality defensible results, and timely execution of this test. Dr. Alicia Aragon of Sandia National Laboratories provided a very thorough review of the report and many helpful suggestions.

The authors acknowledge Ms. Eileen Patterson and Lisa Rothrock of IM-1, Los Alamos National Laboratory, and Ms. Katsura Fujiike of OMICRON for their editing support. Ms. Nancy Butner provided invaluable assistance with project management, budget analysis and reporting, contract administration, and final report preparation.

# ACRONYMS AND ABBREVIATIONS

| | |
|---|---|
| CPVC | Chlorinated Polyvinyl Chloride |
| CS | Coated Steel |
| DAS | Data Acquisition System |
| ECCS | Emergency-Core-Cooling System |
| EDS | Energy-Dispersive Spectroscopy |
| ESEM | Environmental Scanning Electron Microscopy |
| F | Filtered |
| GS | Galvanized Steel |
| GSI | Generic Safety Issue |
| ICET | Integrated Chemical Effects Test |
| ICP | Inductively Coupled Plasma |
| ICP-AES | Inductively Coupled Plasma—Atomic Emission Spectroscopy |
| IOZ | Inorganic Zinc |
| LOCA | Loss-of-Coolant Accident |
| NRC | Nuclear Regulatory Commission |
| NTU | Nephelometric Turbidity Unit |
| PI | Project Instruction |
| PWR | Pressurized Water Reactor |
| QA | Quality Assurance |
| RO | Reverse Osmosis |
| SEM | Scanning Electron Microscopy |
| SS | Stainless Steel |
| TEM | Transmission Electron Microscopy |
| TSP | Trisodium Phosphate |
| TSS | Total Suspended Solids |
| U | Unfiltered |
| UNM | University of New Mexico |
| US | Uncoated Steel |
| UV | Ultraviolet |
| WD | Working Distance |
| XRD | X-Ray Diffraction |
| XRF | X-Ray Fluorescence |

# 1. INTRODUCTION

The Integrated Chemical Effects Test (ICET) project represents a joint effort by the United States Nuclear Regulatory Commission (NRC) and the nuclear utility industry to simulate the chemical environment present inside a containment water pool after a loss-of-coolant accident (LOCA) and to monitor the chemical system for an extended time to identify the presence, composition, and physical characteristics of chemical products that may form. The ICET series is being conducted by Los Alamos National Laboratory (LANL) at the University of New Mexico (UNM), with the assistance of professors and students in the civil engineering department.

## 1.1. Objective and Test Conditions

Containment buildings of pressurized water reactors (PWRs) are designed to accommodate the energy release following a postulated accident. They also permit recirculation of reactor coolant and emergency-core-cooling-system (ECCS) water to the decay heat removal (DHR) heat exchangers. The water collected in the sump from the reactor coolant system, the safety injection system, and the containment spray system is recirculated to the reactor core to remove residual heat. The sump contains a screen to protect system structures and components in the containment spray and ECCS flow paths from the effects of debris that could be transported to the sump. Concerns have been raised that fibrous insulation material could form a mat on the screen, obstructing flow, and that chemical reaction products such as gelatinous or crystalline precipitants could migrate to the screen, causing further blockage and increased head losses across the debris bed. Another potential adverse chemical effect includes increased bulk fluid viscosity that could also increase head losses through a debris bed.

The primary objectives for the ICET series are (1) to determine, characterize, and quantify chemical reaction products that may develop in the containment sump under a representative post-LOCA environment and (2) to determine and quantify any gelatinous material that could be produced during the post-LOCA recirculation phase.

The ICET series was conceived as a limited-scope suite of five different 30-day tests with different constituents. The conditions selected for each test are shown in Table 1-1. Test #5 had a different initial boron concentration and a buffering that was different from the other four tests. A 107-gallon solution containing 2800 mg/L of boron, and 0.7 mg/L of lithium hydroxide was mixed with a 143-gallon solution containing 18.5 g/L of sodium tetraborate (borax). That resulted in the initial test solution having a boron concentration of 2400 mg/L. Also, 90.8 mL of hydrochloric acid was added during the last two hours of the spray phase. The resulting pH was an intermediate value of 8–8.5. All tests in the series included metal coupons where the surface areas were scaled to those in representative PWR containment and sump systems. A complete rationale for the selection of these test conditions is provided in Ref. 1.

**Table 1-1. Test Series Parameters**

| Run | Temp (°C) | TSP[a] | NaOH | Sodium Tetraborate | pH | Boron (mg/L) | Notes |
|---|---|---|---|---|---|---|---|
| 1 | 60 | N/A | Yes | N/A | 10 | 2800 | 100% fiberglass insulation test. High pH, NaOH concentration as required by pH |
| 2 | 60 | Yes | N/A | N/A | 7 | 2800 | 100% fiberglass insulation test. Low pH, TSP concentration as required by pH. |
| 3 | 60 | Yes | N/A | N/A | 7 | 2800 | 80% calcium silicate/20% fiberglass insulation test. Low pH, TSP concentration as required by pH |
| 4 | 60 | N/A | Yes | N/A | 10 | 2800 | 80% calcium silicate/20% fiberglass insulation test. High pH, NaOH concentration, as required by pH. |
| 5 | 60 | N/A | N/A | Yes | 8 to 8.5 | 2400 | 100% fiberglass insulation test. Intermediate pH, sodium tetraborate (borax) buffer. |

[a]TSP = trisodium phosphate.

The ICET apparatus consists of a large stainless-steel (SS) tank with heating elements, spray nozzles, and associated recirculation pump and piping to simulate the post-LOCA chemical environment. Samples of structural metals, concrete, and insulation debris are scaled in proportion to their relative surface areas found in containment and in proportion to a maximum test dilution volume of 250 gal. of circulating fluid. Representative chemical additives, temperature, and material combinations are established in each test; the system is then monitored while corrosion and fluid circulation occur for a duration comparable to the ECCS recirculation mission time.

## 1.2. Information Presented in This Report

This report surveys the principal findings of ICET Test #5. As an interim data report, this exposition summarizes both primary and representative findings, but it cannot be considered comprehensive. For example, only a small selection of photographs out of several hundred is presented here. In addition, this report presents observations and data without in-depth analyses or interpretations. However, trends and typical behaviors are noted where appropriate. Section 2 of this report reviews the test procedures followed for Test #5. Analytical techniques used in evaluating test results are also briefly reviewed in Section 2. Section 3 presents key test results for Test #5, including representative and noteworthy results of water sampling, fiberglass insulation samples, metallic and concrete coupon samples, tank sediment, deposition products, and water property analyses. The results for Test #5 are presented in both graphical and narrative form. Section 4 presents a summary of key observations for Test #5. This report also includes several appendices that capture additional Test #5 images and information. The data presented in the appendices are largely qualitative, consisting primarily of environmental scanning

electron microscopy (ESEM), scanning electron microscopy (SEM), transmission electron microscopy (TEM) micrographs, and energy-dispersive spectroscopy (EDS) spectra.

# 2. TEST PROCEDURES

The functional description and physical attributes of the ICET apparatus were presented in detail in the ICET Test #1 report (Ref. 2). The experimental apparatus is briefly described below, followed by a review of the test operation and analytical techniques used to evaluate the test results.

## 2.1. Chemical Test Apparatus Functional Description

The test apparatus was designed to meet the functional requirements of the Project Test Plan (Ref. 1). Functional aspects of the test apparatus are as follows:

1. The central component of the system is a test tank. The test apparatus was designed to prevent solids from settling in the test piping.

2. The test tank can maintain both a liquid and vapor environment, as would be expected in post-LOCA containment.

3. The test loop controls the liquid temperature at 140°F (±5°F).

4. The system circulates water at flow rates that simulate spray flow rates per unit area of containment cross section.

5. The test tank provides for water flow over submerged test coupons that is representative of containment pool fluid velocities expected at plants.

6. Piping and related isolation valves are provided such that a section of piping can be isolated without interrupting the test.

7. The pump discharge line is split in two, one branch directing the spray header in the tank's vapor space and the other returning to the liquid side of the tank. Each branch is provided with an isolation valve, and the spray line includes a flow meter.

8. The recirculation piping includes a flow meter.

9. The pump circulation flow rate is controlled at the pump discharge to be within ±5% of the flow required to simulate fluid velocities in the tank. Flow is controlled manually.

10. The tank accommodates a rack of immersed sample coupons, including the potential reaction constituents identified in the test plan.

11. The tank also accommodates six racks of sample coupons that are exposed to a spray of liquid that simulates the chemistry of a containment spray system. Provision is made for these racks to be visually inspected.

12. The coupon racks provide sufficient space between the test coupons to preclude galvanic interactions among the coupons. The different metallic test coupons are also electrically isolated from each other and the test stand to prevent galvanic effects resulting from metal-to-metal contact between specimens or between the test tank and the specimens.

13. The fluid volumes and sample surface areas are based on scaling considerations that relate the test conditions to actual plant conditions.

14. All components of the test loop are made of corrosion-resistant material (for example, SS for metallic components).

The as-built test loop consists of a test tank, a recirculation pump, 2 flow meters, 10 isolation valves, and pipes that connect the major components, as shown schematically in Figure 2-1. P, T, and pH represent pressure, temperature, and pH probes, respectively.

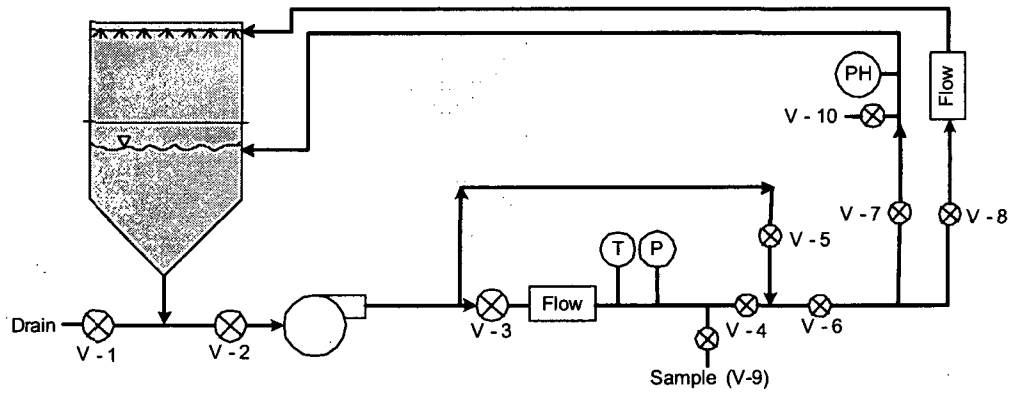


**Figure 2-1. Test loop process flow diagram.**

## 2.2. Pre-Test Preparation

### 2.2.1. Test Loop Cleaning

In preparation for Test #5, the experiment test loop was thoroughly cleaned to remove all Test #4 deposits and residues. In addition to visual inspections, the test apparatus was flushed and cleaned per the written direction given in the pre-test operations project instruction (PI) (Ref. 3). The system was flushed with ammonium hydroxide, followed by ethanol, and then nitric acid until it was visually clean and the water conductivity was <50 μS/cm.

### 2.2.2. Test Coupons and Samples

Each ICET experiment exposes metallic and concrete coupons to anticipated post-LOCA environments. Each coupon is approximately 12 in. square. The metallic coupons are approximately 1/16 in. thick, except for the inorganic zinc-coated steel coupons, which are approximately 3/32 in. thick. The concrete coupons (one per test) are approximately

1-1/2 in. thick. Insulation materials are also exposed. For Test #5, NUKON™ fiberglass insulation samples were included in the test. As with previous tests, Test #5 subjected seven racks of coupons to the specified environment, with one being submerged in the test tank and the remaining six being held in the tank's gas/vapor space. The Test #5 coupons of each type were as shown in Table 2-1.

**Table 2-1. Quantity of Each Coupon Type in Test #5**

| Material | No. of Coupons |
|---|---|
| Coated Steel (CS) | 77 |
| Aluminum (Al) | 59 |
| Galvanized Steel (GS) | 134 |
| Copper (Cu) | 100 |
| Uncoated Steel (US) | 3 |
| Concrete | 1 |

Note: Inorganic zinc (IOZ)-coated steel and CS are the same coupon type.

The arrangement of the coupon racks in the test tank is schematically illustrated in Figure 2-2. The figure shows a side view of the ICET tank, with the ends of the seven chlorinated polyvinyl chloride (CPVC) racks illustrated. The normal water level is indicated by the blue line in the figure. Rack #1 is the only submerged rack, and it sits on angle iron. It is centered in the tank so that flow from the two headers reaches it equally. Racks #2–#4 are positioned above the water line, supported by angle iron in the tank. Racks #5–#7 are positioned at a higher level, also supported by angle iron. Racks #2–#7 are exposed to spray. In the figure, north is to the right, and south is to the left. Directions are used only to identify such things as rack locations and sediment locations.

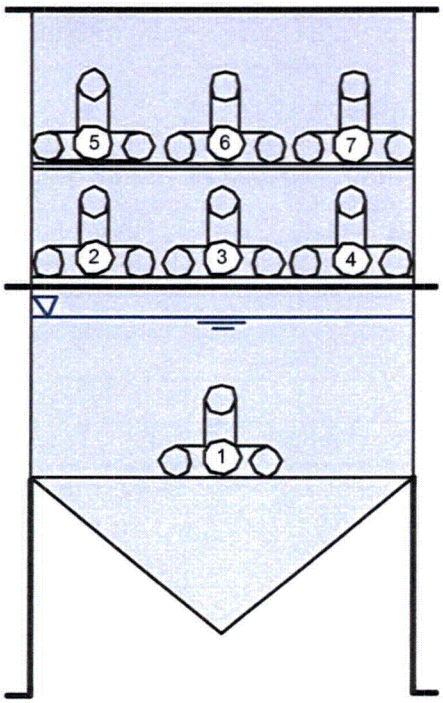


**Figure 2-2. Coupon rack configuration in the ICET tank. The blue line represents the surface of the test solution.**

Figure 2-3 shows the configuration of a typical unsubmerged coupon rack loaded with metal coupons in the ICET tank. The loading pattern of the racks was nearly identical, varying by only one or two coupons. Shown in the figure from left to right, the coupons are arranged as follows: 4 Cu, 4 Al, 4 IOZ, 7 GS, 4 Cu, 3 Al, 4 IOZ, 7 GS, 4 Cu, 3 Al, 4 IOZ, and 7 GS.

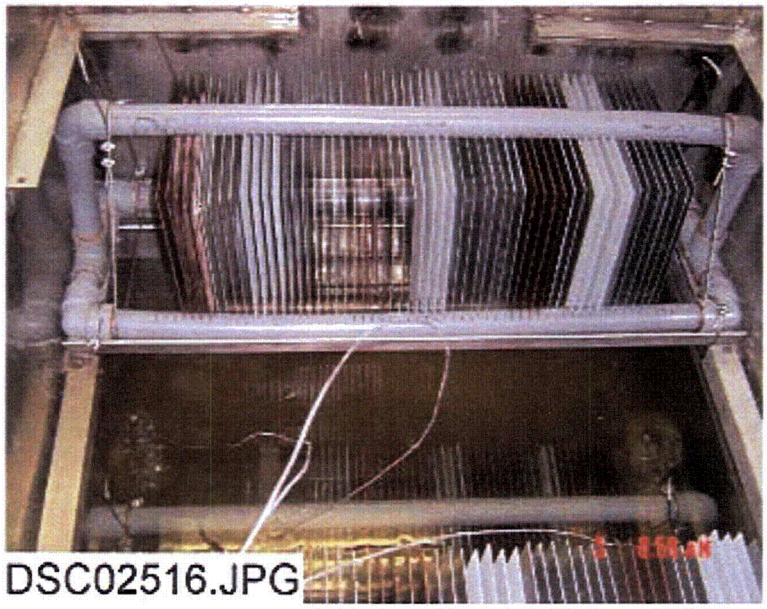


**Figure 2-3. A typical loaded coupon rack in the ICET tank.**

Several fiberglass samples were placed in the ICET tank. Samples were either submerged or held above the water level. The unsubmerged fiberglass samples were positioned so they would be exposed to sprays. The fiberglass samples were contained in SS wire mesh that allowed water flow while confining the fiberglass material. Both loosely packed and more tightly packed samples were used. In addition, some submerged fiberglass samples were located where they would be exposed to relatively high-flow conditions, and others were located in quiescent regions of the tank. Figure 2-4 shows the so-called "sacrificial" fiberglass samples in wire mesh pouches attached to the submerged coupon rack (Rack 1 in Figure 2-2). Each pouch contains approximately 5 g of fiberglass. Those samples were attached with SS wire; removed from the tank on Days 4, 15, and 30; and examined. As shown in the figure, bigger insulation bags were wrapped around the sacrificial specimens during the test. In addition, small, sacrificial samples called fiber pucks were added to the solution. The fiber pucks are described in Ref. 4. Subsection 2.4.1.1 contains descriptions of other fiberglass samples.

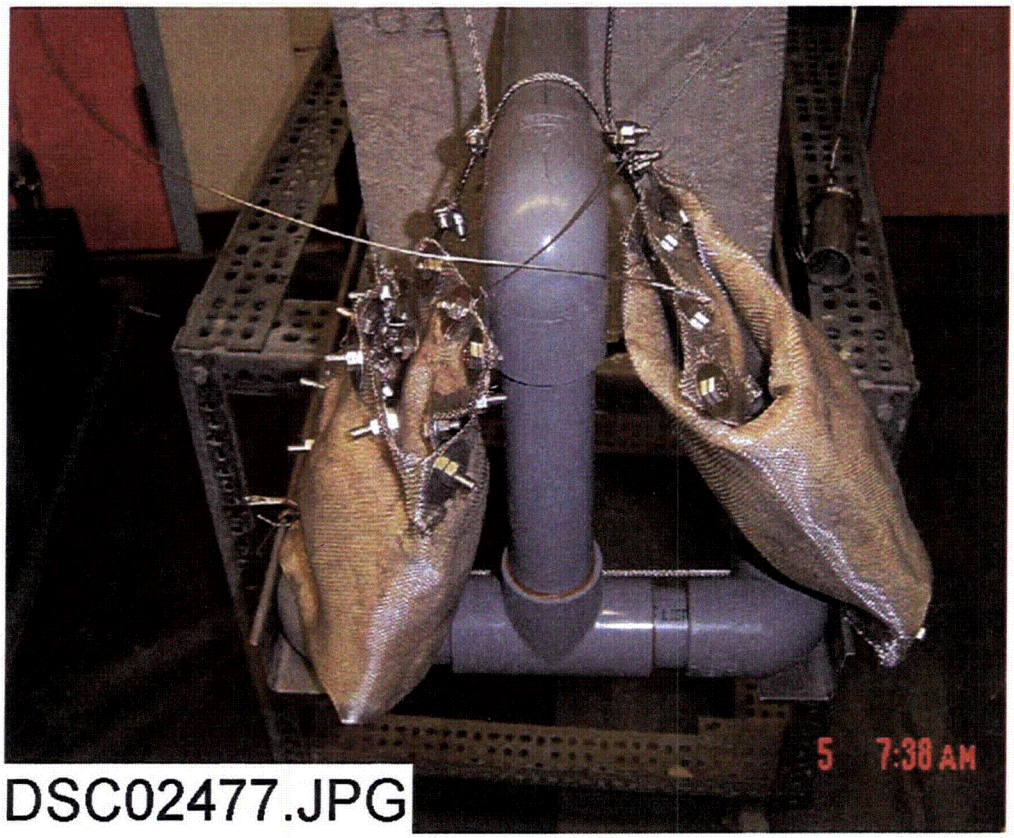


**Figure 2-4. Fiberglass samples attached to a coupon rack.**

### 2.2.3. Quality Assurance Program

A project quality assurance (QA) manual was developed to satisfy the contractual requirements that apply to the ICET project. Specifically, those requirements were to provide credible results by maintaining an appropriate level of QA in the areas of test loop design, sampling, chemicals, operation, and analysis. These requirements were summarized in the contract requirement that QA was to be consistent with the intent of the appropriate sections of 10CFR50, Appendix B.

The 18 criteria of 10CFR50, Appendix B, were addressed separately in the QA manual, and the extents to which they apply to the ICET project were delineated. A resultant set of QA procedures was developed. In addition, test-specific PIs were written to address specific operational topics that required detailed step-by-step guidance. PIs generally applicable to all tests were written for the following topics and were followed for Test #5:

- Data Acquisition System (DAS)
- Coupon Receipt, Preparation, Inspection, and Storage
- DAS Alarm Response
- Chemical Sampling and Analysis
- TEM Examination of Test Samples

- SEM Characterization of Test Samples
- Viscosity Measurements
- Post-Test Operations

Project instructions specific to Test #5 were written for the following:

- Pre-Test Operations, Test #5
- Test Operations, Test #5 (fiberglass and sodium tetraborate at pH 8)

The pre-test, test, and post-test operations PIs that were used in Test #5 are included in Appendix I.

### 2.2.4. Test Parameters

ICET test parameters were selected based on literature surveys and the results of surveys of United States nuclear power plants. Quantities of test materials were selected to preserve the scaling of representative ratios between material surface areas and total cooling-water volumes. Chemical additives also simulate the post-LOCA sump environment. The Project Test Plan (Ref. 1) is the basis for the following information in this section.

The materials included in the tests are zinc, aluminum, copper, carbon steel, concrete, and insulation materials such as fiberglass and calcium silicate. The amounts of each material are given in Table 2-2 in the form of ratios (material surface area to water volume), with three exceptions: concrete dust, which is presented as a ratio of mass to water volume, and fiberglass and calcium silicate, which are presented as a ratio of insulation volume to water volume. Also shown in the table are the percentages of material that are submerged and unsubmerged in the test chamber.

**Table 2-2. Material Quantity/Sump Water Volume Ratios for the ICET Tests**

| Material | Value of Ratio for the Test (Ratio Units) | Percentage of Submerged Material (%) | Percentage of Unsubmerged Material (%) |
|---|---|---|---|
| Zinc in Galvanized Steel | 8.0 ($ft^2/ft^3$) | 5 | 95 |
| Inorganic Zinc Primer Coating (non–top coated) | 4.6 ($ft^2/ft^3$) | 4 | 96 |
| Inorganic Zinc Primer Coating (top coated) | 0.0 ($ft^2/ft^3$) | – | – |
| Aluminum | 3.5 ($ft^2/ft^3$) | 5 | 95 |
| Copper (including Cu-Ni alloys) | 6.0 ($ft^2/ft^3$) | 25 | 75 |
| Carbon Steel | 0.15 ($ft^2/ft^3$) | 34 | 66 |
| Concrete (surface) | 0.045 ($ft^2/ft^3$) | 34 | 66 |
| Concrete (particulate) | 0.0014 ($lbm/ft^3$) | 100 | 0 |
| Insulation Material (fiberglass or calcium silicate) | 0.137 ($ft^3/ft^3$) | 75 | 25 |

The physical and chemical parameters that are critical for defining the tank environment and that have a significant effect on sump-flow blockage potential and gel formation have been identified in Ref. 1. These physical and chemical parameters are summarized as follows:

Physical Parameters

| | | |
|---|---|---|
| • Water volume in the tank | 949 L | 250 gal. |
| • Circulation flow | 0–200 L/min | 0–50 gpm |
| • Spray flow | 0–20 L/min | 0–5 gpm |
| • Sump temperature | 60°C | 140°F |

Chemistry Parameters

| | |
|---|---|
| • $H_3BO_3$ concentration | 2800 mg/L as boron |
| • $Na_3PO_4 \cdot 12H_2O$ concentration | As required to reach pH 7 in the simulated sump fluid |
| • NaOH concentration | As required to reach pH 10 in the simulated sump fluid |
| • Sodium tetraborate (borax) | As required to reach boron concentration of 2400 mg/L |
| • Hydrochloric acid (HCl) concentration | 42.8 mg/L |
| • Lithium hydroxide (LiOH) concentration | 0.3 mg/L as Li |

The parameters planned for each ICET test run are described in Table 1-1.

## 2.3. Test Operation

### 2.3.1. Description

Preparation of ICET Test #5 (Run 5 in Table 1-1) began with 248 gal. of reverse osmosis (RO) water heated to 65°C. (Adding the metal coupons and insulation samples reduces the water temperature by approximately 5°C, so the water was heated initially to 65°C.) With 25 gpm circulating through the loop, the predetermined quantities of boric acid (6.48 kg), sodium tetraborate (10.0 kg), and lithium hydroxide (0.284 g) were added and dissolved in the ICET tank solution. After the chemicals were added and observed to be well mixed, a baseline grab sample and measurements of the test solution were taken. Then the pre-measured latent debris and concrete dust were added to the tank solution. After the solution circulated for 10 minutes, the pump was stopped and the coupon racks and insulation samples were put into the tank (see Section 2.2.2).

The test commenced with initiation of the tank sprays (3.5 gpm). After two hours, 2 gallons of RO water containing 90.8 mL of hydrochloric acid were metered into the spray. The sprays were terminated after 4 hours. The test ran uninterrupted for 30 days.

The experiment commenced at 11:00 a.m. on Tuesday, July 26, 2005, and it ended on August 25, 2005. During the test, grab samples were taken daily for wet chemistry and inductively coupled plasma – atomic emission spectroscopy (ICP-AES) analyses. Water loss due to water sample removals and evaporation was made up with RO water. Water samples, insulation, and metal coupons were analyzed after the test. Sampling and analyses were conducted in accordance with approved project instructions (Refs. 3, 4, and 5).

### 2.3.2. Process Control

During the test, critical process control parameters were monitored to ensure that the test conditions met the functional test requirements. Recirculation flow rate and temperature were controlled throughout the test. The solution pH was expected to reach a value of approximately 8 to 8.5 after the spray phase ended. The predetermined amounts of chemicals were added to achieve 2400 mg/L of boron, and pH was not controlled.

Recirculation flow in the test loop was controlled by adjusting the pump speed. Fine tuning was achieved by manually adjusting a valve located downstream of the recirculation pump. In-line flow meters were used to measure the flow rate in the recirculation line and the spray line.

Titanium-jacketed immersion electric heaters controlled the water temperature. The heaters were thermostatically controlled to automatically maintain the desired temperature.

## 2.4. Analytical Methods

Data collected during Test #5 included the in-line measurements of temperature, pH, and loop flow rate. During the daily water grab sample analysis, bench-top measurements were obtained for temperature, pH, turbidity, total suspended solids (TSS), and kinematic viscosity. The concentration of hydrogen in the tank atmosphere was also measured and could be used as an indicator of chemical reactions taking place. Water, fiberglass, and metal coupon samples were taken to other laboratory locations for additional analyses. These analyses included shear-rate viscosity, ESEM, SEM, EDS, TEM, ICP-AES, x-ray fluorescence (XRF), and x-ray diffraction (XRD). EDS provided a semi-quantitative elemental analysis after calibration of the instrument's x-ray signal using an internal element standard. Descriptions of the principles of operation and limitations of these analytical methods were provided in the Test #1 report (Ref. 2).

### 2.4.1. Data Compilation and Nomenclature

This section provides a brief guide to assist the reader in interpreting the ICET Test #5 information and data presented in the following sections and in the appendices. Standardized nomenclature is defined first to clarify the origin of samples that are described in the data sets. The appendices are listed, and a description is provided of how they were compiled.

#### 2.4.1.1. Nomenclature

Many spatially unique but physically similar sample types were collected in ICET Test #5. To ensure that consistent interpretations and comparisons of data sets are made, it is imperative that a standardized nomenclature be adopted when referring to each sample type. Many different qualitative descriptions of these samples might be equally suitable, but different adjectives convey different connotations to each observer. Therefore, the following definitions establish the convention used in this report when making generic references to sample type.

White Precipitate — The behavior of the solution at test temperature and upon cooling is observed during testing. Precipitates and their prominence indicate chemical interactions occurring in the solution. White precipitate formed in Test #1 water solution samples drawn from the test loop. Upon cooling below the test temperature, Test #1 daily water samples extracted from the tank formed a visible white material that is referred to as a precipitate. While less prominent from Test #1, there was a precipitate that formed in Test #5. After the test solution sat at room temperature for several days, a light, wispy precipitate was visible after the sample bottle was agitated. The precipitate could not be seen again until the sample sat for several days. The precipitate was not concentrated enough to allow samples to be obtained for analysis.

| | |
|---|---|
| Latent Debris | Commercial power plant containments gradually accumulate dust, dirt, and fibrous lint that are generically referred to as latent debris. This classification distinguishes resident material from debris generated during an accident scenario. At the beginning of Test #5, measured quantities of crushed concrete and soil (sand and clay) were added to simulate the latent debris present in containment. These materials were examined via SEM/EDS to establish a baseline composition for comparison with sediment samples (see "Sediment" below). |
| Sediment | Surrogate latent debris particulates and fugitive fiberglass fragments that were initially suspended in water at the beginning of Test #5 gradually settled to the bottom of the tank. At the conclusion of the test, only a small amount of sediment remained on the tank bottom. It was recovered as completely as possible. |
| Powder | At the conclusion of Test #5, fine, yellow particulate deposits were found on the submerged CPVC coupon rack. They were referred to as powder and examined by SEM/EDS. These deposits are also referred to as deposition products (see Appendix D). |
| Fiberglass | The principal debris type introduced in Test #5 was shredded fiberglass insulation. This debris was bundled in 3-in.-thick bags (or blankets) of fiberglass confined in SS mesh to prevent ingestion through the pump and to better control the placement of debris in various flow regimes. Fiberglass samples are designated by their placement in high-flow and low-flow areas of the tank. Fiberglass in the "big envelope" sat on the tank bottom in a low-flow area of the tank. Additional 4-in.-square envelopes of fiberglass were also prepared for extraction during the course of the test. These samples are referred to as "sacrificial" samples. The "birdcage" sample was constructed so that the fiberglass within was loose and not compacted. The birdcage fiberglass sat on the tank bottom and was removed on Day 30. Some amount of fiber, especially short-fiber fragments, escaped the mesh bags and was deposited in other locations within the tank. This material is referred to as "fugitive" fiberglass. Two additional fiberglass samples were added after the test began and the water clarity improved, to investigate what deposited after the tank solution stablized. A sacrificial sample was placed directly in front of one of the flow headers (high-flow area) on Day 6. A sacrificial sample enclosed in nylon mesh was placed in a low-flow area also on Day 6. |
| Drain Screen | A 12-in.-tall screen made of coarse SS mesh (1/8-in. holes) wrapped into a 2-in.-diam cylinder was inserted into the outlet drain at the bottom of the tank to protect the pump from ingesting |

| | |
|---|---|
| | large debris items. Two inches of the screen were inserted into the tank outlet to provide a solid base and stability. A 6-in.-tall drain collar was installed around the drain screen. This drain collar was a cylinder of fiberglass held in SS mesh. The drain collar was exposed to higher-velocity water flow than other samples in the tank. The drain collar fiberglass was examined as a separate debris location to identify any apparent differences with other sample locations. |
| Gelatinous Material | This term generically refers to any observed sample constituent with amorphous, hydrated, or noncrystalline physical characteristics. When Test #5 was shut down, there was no evidence of gel-like precipitates in the tank or piping. |
| Water Sample | Daily water samples were extracted from the ICET tank for elemental concentration analyses. After the sample line was properly flushed, some of this water was extracted directly from the tap. An equal amount of water was also generally collected through a micropore filter. Thus, daily water samples were designated as filtered (F) and unfiltered (U), and a corresponding filter paper exists in the sample archive for each daily sample that was collected. |
| High-Volume Filter | If white precipitates are observed in the tests, larger quantities of test solution are periodically extracted for filtration to determine whether suspended chemical products are present in the test liquid under in situ conditions. The intent of this exercise is to maintain the liquid temperature while forcing the liquid through a micropore filter under vacuum. Because the precipitates were not present in Test #5, these high-volume filter samples were not obtained. |
| Filter Paper | Many different samples of tank solution were fractionated by micropore filtration into a liquid supernate and a solid filtrate that existed at the time and temperature conditions of the filtering process. These samples included (1) daily water samples filtered during extraction, (2) daily water samples filtered after cooling to room temperature, and (3) high-volume water samples. |
| Chemical Deposits | Sacrificial fiberglass samples that were extracted at Day 4, Day 15, and Day 30 showed evidence of chemical products forming on and between fiber strands. These products are referred to as "deposits," although the exact physical mechanism of formation is not well understood. The physical appearance suggests growth, agglomeration, or crystallization on and around the fiber strands over time rather than capture or impaction of particles from the bulk solution. This observation is supported by the fact that the |

small sacrificial fiberglass samples were located in a region of lower-velocity water flow (i.e., in the interior of larger blankets).

Concrete Sample — Several chips of concrete (1/4–3/4 in. diam) were broken from the primary slab of submerged concrete and introduced to the tank in a small SS envelope at the start of the test. Examinations of these chips were conducted to determine if concrete surfaces provide a preferential site for gel formation.

Although these terms have been defined, the reader may note minor inconsistencies in the caption labels used in this document. The caption labels use the same descriptions that were applied in laboratory notebooks to improve traceability of the data.

### 2.4.1.2. Usage

The 9 appendices listed below are provided to present data collected for the sample types and analysis methods listed below. In addition, an appendix is provided with pertinent Test #5 project instructions.

| | |
|---|---|
| Appendix A | ESEM/EDS Data for Test #5, Day-4 Fiberglass in a Low-Flow Zone |
| Appendix B | ESEM Day-15 Fiberglass |
| Appendix C | ESEM Day-30 Fiberglass |
| Appendix D | SEM/EDS Data for Test #5, Day-30 Deposition Products |
| Appendix E | SEM Day-30 Coupons |
| Appendix F | SEM/EDS Data for Test #5, Day-30 Sediment |
| Appendix G | TEM Data for Test #5 Solution Samples |
| Appendix H | UV Absorbance Spectrum – Day-30 Solution Samples |
| Appendix I | ICET Test #5: Pre-Test, Test, and Post-Test Project Instructions |

These data are largely qualitative in nature, consisting primarily of ESEM, SEM, TEM micrographs, and EDS spectra. Each appendix subsection represents a separate session of laboratory work that can be traced to a batch of samples that were processed in chronological order. This organizational scheme preserves the connection with laboratory notebooks and timelines that naturally developed during operation; however, in a few cases, results for a given sample type may be mixed across two or more appendices because of the order in which the individual samples were analyzed.

ESEM analyses were added to the ICET diagnostic suite for the first time during Test #2 as a means of examining hydrated chemical products. This equipment operates as an electron microscope, but it does not require a high-vacuum condition in the sample chamber. Thus, a sample need only be thoroughly drained of free water content before examination rather than fully desiccated, making the ESEM ideal for examinations of

biological and environmental specimens. The complementary EDS capability that is often found with equipment of this type is not presently functional at UNM, so duplicate examinations are often performed on the same ICET sample first using ESEM to obtain images of hydrated structural details and then using SEM/EDS to obtain representative elemental compositions. Throughout the report, ESEM analyses are also indicated by the descriptions of "hydrated" and "low-vacuum" findings.

Transcriptions of the logbooks are provided for each appendix to better document commonalities that existed among the samples at the time of analysis. Interpretation and understanding of the images and their accompanying EDS spectra will be greatly improved by frequent reference to the logbook sample descriptions and sequences. Typically, a relatively large quantity of a test sample was delivered for SEM or TEM analysis, and then several small sub-samples of each item were examined. Note that each sub-sample was assigned a sequential reference number during the laboratory session. These reference numbers have been cited in the figure captions whenever possible to preserve the connection between the micrographs and the notebook descriptions. Electronic file names have also been stamped on the images to permit retrieval of the original data files that are archived elsewhere. Individual data sets for a given sample item have been collated into a typical sequence of (1) visual image, (2) EDS spectra, and (3) semi-quantitative mass composition.

For most of the EDS spectra, semi-quantitative mass compositions are also presented. These results are obtained from a commercial algorithm that decomposes the spectra into the separate contributions of each element. Several caveats, as enumerated below, should be considered when interpreting the numeric compositions thus obtained; however, despite these caveats, semi-quantitative EDS analysis offers a natural complement to micrographic examination as a survey technique for identifying trends in composition.

1. The spectral deconvolution algorithm is based on a library of unique signatures of each element that were obtained for pure samples using a standard beam setting that may not identically match the conditions applied for the test item.
2. The operator must select a limited number of elements to be used in the proportional mass balance. These candidates are chosen from among the peaks that are observed in the spectrum; however, the composition percentages can vary, depending on which elements are included in the list. In a few cases, two or more alternative compositions have been generated by selecting a different set of elements from the same spectrum to illustrate the sensitivity of this technique to operator input.
3. The spectral unfolding algorithm is a statistical technique having a precision that depends on the relative quality of the data in each peak. Compositions with high $R^2$ correlation coefficients and total-mass normalization factors closer to unity represent the more-reliable estimates. The precision obtained in the fit depends on the duration of the scan and the number of counts received in each energy bin.

4. All sub-samples examined in the SEM microprobe facility are coated with a thin layer of either carbon or gold/palladium alloy to prevent the sub-samples from accumulating a charge from the impinging electron beam. Spectral peaks visible for gold (Au) and palladium (Pd) are not indigenous to the samples.
5. The EDS spectral analysis software contains a peak-recognition algorithm and an automated cursor that scans across the spectrum to locate each peak. An accompanying library of elemental energy signatures is also provided to suggest what constituents might be contributing to a given energy bin, but the operator must judge what label to assign to the spectral image. It is possible that some peaks near closely neighboring elements have been mislabeled in these images. However, every effort was made to choose from candidate elements that were most likely to be present in the test material. In a few cases, the spectral peaks were not labeled by the SEM operator. These spectra should be viewed as corroborating evidence for similar samples that are definitively labeled. Careful comparisons of the energy scales in combination with a library of electron-scattering energies can also be used to infer the origin of the more-prominent peaks that are present in unlabeled spectra.
6. Unless an obvious spatial heterogeneity is being examined, the exact location of an EDS spectrum is not always relevant because the operator chooses arbitrary sites that are visually judged to be representative. It is not possible to sample a surface comprehensively on a microscopic basis and compute average compositions. In many cases, two or three replicate spectra are provided for this purpose, but SEM/EDS is most effective as a survey diagnostic.
7. EDS analysis is not particularly sensitive to the presence of boron for several reasons: (a) boron has a low atomic mass that does not interact well with electrons in the beam, (b) the emission lines are very close to those of carbon, and (c) the beam-port material has a high absorption cross section for these emission energies. Therefore, the correction factors used in the semi-quantitative composition analysis are quite large, as are the uncertainties in the estimated percentage of total composition for this element. There may be spectra presented in the appendices in which the lowest energy peaks are labeled as either B (boron) and/or C (carbon).

EDS locations were chosen manually at regions of specific interest. In many cases, multiple spectra were collected from a single sample and an annotated image is provided to identify the specific location. These annotated images are not generally noted in the laboratory logbook entries, but they are provided in proper sequence within the appendices.

Appendix G presents TEM data for water samples extracted from the ICET solution at Day 4, Day 15, and Day 30. The purpose of this examination was to determine whether the physical structure of any suspended products exhibits crystalline or amorphous characteristics. These data are also qualitative in nature, consisting generally of a set of high-resolution micrographs followed by companion electron diffraction images. The TEM sample holder consists of a carbon grid that is "lacey," or filamentary, in nature.

This grid is visible as a relatively large-scale structure in the background of most images. Surface tension in a droplet of liquid suspends the particulates of interest across the grid so that the electron beam can illuminate the sample through the holes without interference from a substrate. Crystalline material will exhibit diffraction patterns unique to the molecular arrangement. Amorphous material that is diffuse or disorganized in structure will not exhibit regular diffraction patterns that can be identified.

Water samples submitted for TEM analysis are not temperature controlled because the temperature cannot be maintained during the examination. A tiny drop of the test solution was transferred to a copper mesh and dried in air for TEM analysis.

In a few cases, data file names that were noted by the operator in the laboratory log were not successfully saved in electronic form. These cases are noted in the transcribed log sheets, but the corresponding images are unavailable and therefore are not presented in the data sequence.

# 3. TEST RESULTS

This section describes the results obtained from Test #5. Some visual observations are first presented as an overview. This overview is followed by more-detailed information organized by the type of samples/data collected. Data and photographs are provided here for the (1) water samples, (2) NUKON™ fiberglass samples, (3) metallic and concrete coupons, (4) sediment, and (5) deposition products. Then, TEM images, UV absorbance spectrum and shear-dependent viscosity measurements of water samples are also discussed.

## 3.1. General Observations

These observations are taken from the project daily log book. They were meant to capture visual observations of the test solution and/or test samples during the daily sampling activities.

Shortly after the latent debris and crushed concrete were introduced into the tank, the inline flow meter quit working. The unit was removed from the piping, rinsed with RO water, and returned to the piping. The flow meter then operated normally. Four hours after the sprays were activated, the tank solution was very turbid. It was difficult to observe the submerged coupons from the lower view window.

On Day 1, after approximately 24 hours of testing, the water clarity was still poor. The tank solution was a yellow-brown color.

On Day 5, 5 gallons of RO make-up water were added to the tank through the top using a recycle funnel.

On Day 6, the water clarity had improved enough that the opposite side of the tank could be seen through the submerged view window. The eight remaining fiber-pucks (see ICET-PI-018, Rev. 0 in Appendix I), the small fiberglass sample encased in the nylon mesh bag, and the small high-flow fiberglass header sample were placed into the tank at that time.

On Day 10, very small particles were observed on all of the submerged galvanized steel coupons. All other submerged samples appeared to be free of deposits.

On Day 13, 5 gallons of RO make-up water were added to the tank through the top using a recycle funnel.

On Day 17, it was observed that a slight amount of precipitate had settled in the UNM-archived test solution bottle labeled "ICET5-0803-0900-U" (Day 8 sample). In addition, 3 gallons of RO make-up water were added to the tank through the top using a recycle funnel.

On Day 21, four fiber-pucks that had been placed in the tank in the low-flow area on Day 6 were removed. They were placed in a re-closable plastic bag with a small volume of test solution. The bag was enclosed in a 5-gallon bucket and put into an oven set at 60°C.

On Day 22, it was observed that the submerged aluminum coupons had a light coating. The submerged aluminum coupons had a rough, dull surface similar to the inorganic zinc-coated steel coupons.

On Day 22, 5 gallons of RO make-up water were added to the tank through the top using a recycle funnel.

On Day 28, 5 gallons of RO make-up water were added to the tank through the top using a recycle funnel.

After the test was completed, observations of the sample bottles were made. Beginning with the Day 2 water sample, white precipitates were observed after the samples had been at room temperature for several days. These precipitates settled to the bottom of the sample bottles. When the bottles were gently turned upside down, the precipitates formed wispy patterns in the solution. They were resuspended when the bottles were shaken and could not be seen. It takes 2–3 days for the precipitates to settle again in the sample bottles.

### 3.1.1. Control of Test Parameters

**Recirculation flow rate:** Excluding the spray phase, the average recirculation flow rate was 94.6 L/min (25.0 gpm). Recorded recirculation flow rate had a standard deviation of 0.72 L/min, with a range of 94.3–99.1 L/min (24.9–26.1 gpm).

**Temperature:** Temperature is recorded at three submerged locations in the ICET tank. The average recorded temperature at these locations was 60.6°C, 60.8°C, and 60.8°C (141.1°F, 141.4°F, and 141.4°F). The standard deviation in temperature recorded by all three thermocouples was within ±0.4°C (± 0.7°F), with a maximum range of 57.7°C–61.7°C (135.8°F–143.0°F). The temperature went below 58°C for less than 10 minutes, when make-up water was added quickly to the tank on Day 5. Make-up water was subsequently added at a slower rate to ensure that the temperature did not drop below 58°C.

**pH:** Before time zero, 6.48 kg of boric acid, 10.0 kg of borax, and 0.284 g of lithium hydroxide were dissolved into the ICET tank. The in-line pH probe, which produced the data in Figure 3-1, provides only an estimated pH measurement. The measured bench-top probe pH was 8.4 at 60°C. During the addition of the HCl, the pH of the system dropped slightly to a value of 8.3. The pH remained in the range of 8.2–8.4 for the duration of the test. This can be seen in Figure 3-2.

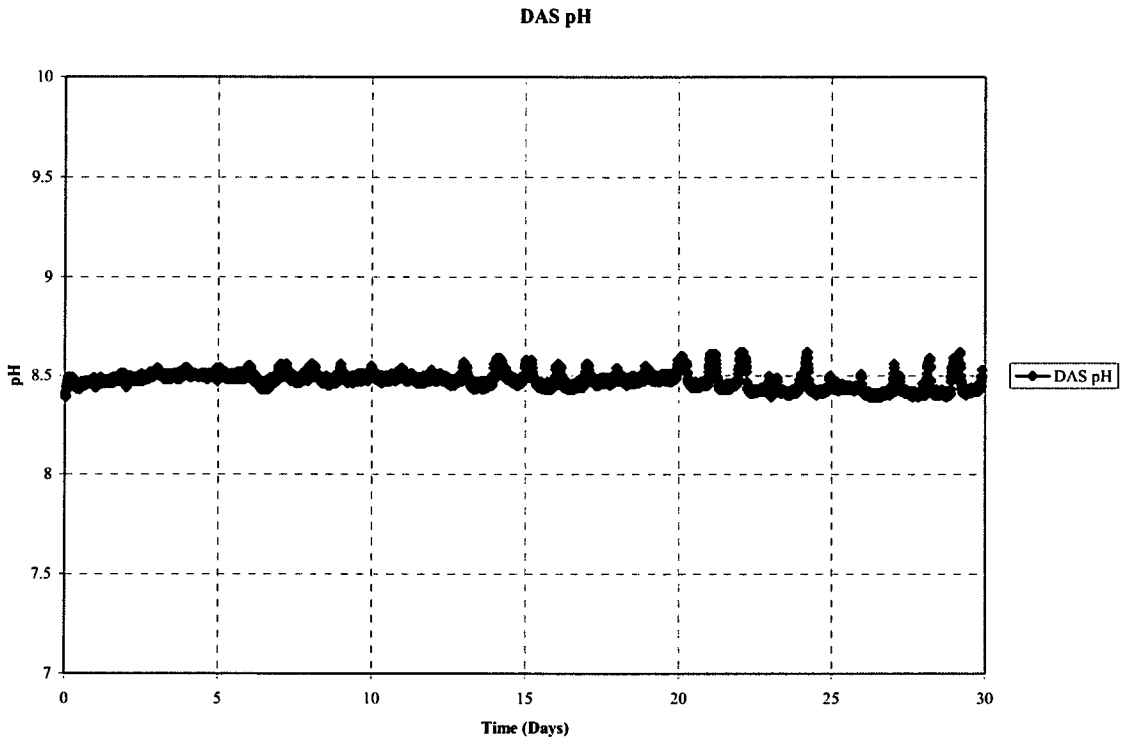


**Figure 3-1. In-line pH measurements.**

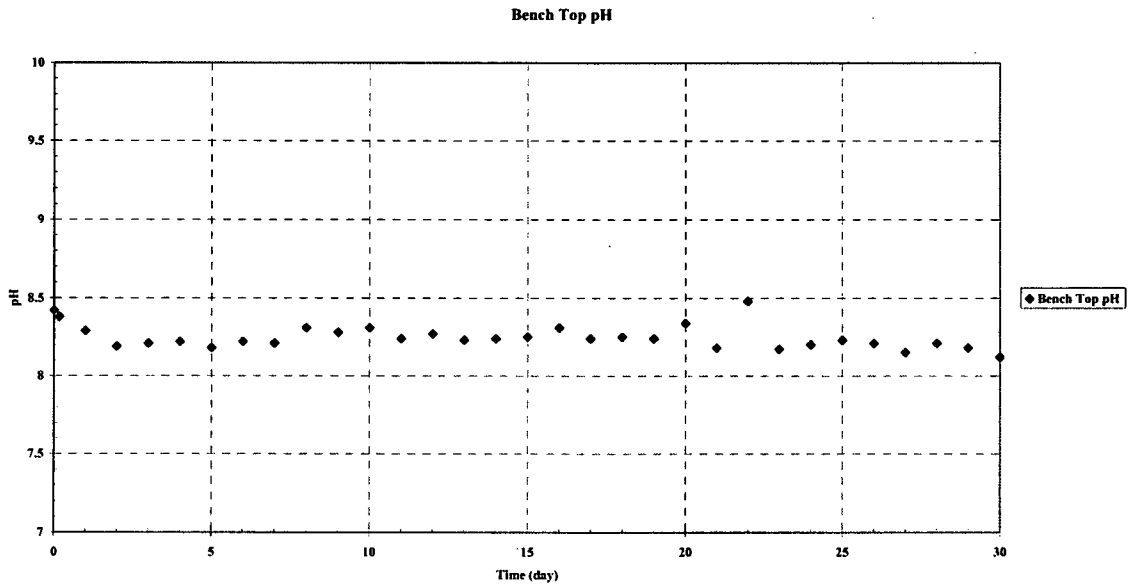


**Figure 3-2. Bench-top pH meter results.**

### 3.1.2. Hydrogen Generation

Hydrogen remained at or below 0.15% of the daily samples' air volume (from the tank atmosphere) for the duration of the test as shown in Figure 3-3. All of the measured values were well below the hydrogen safety action threshold of 0.4%.

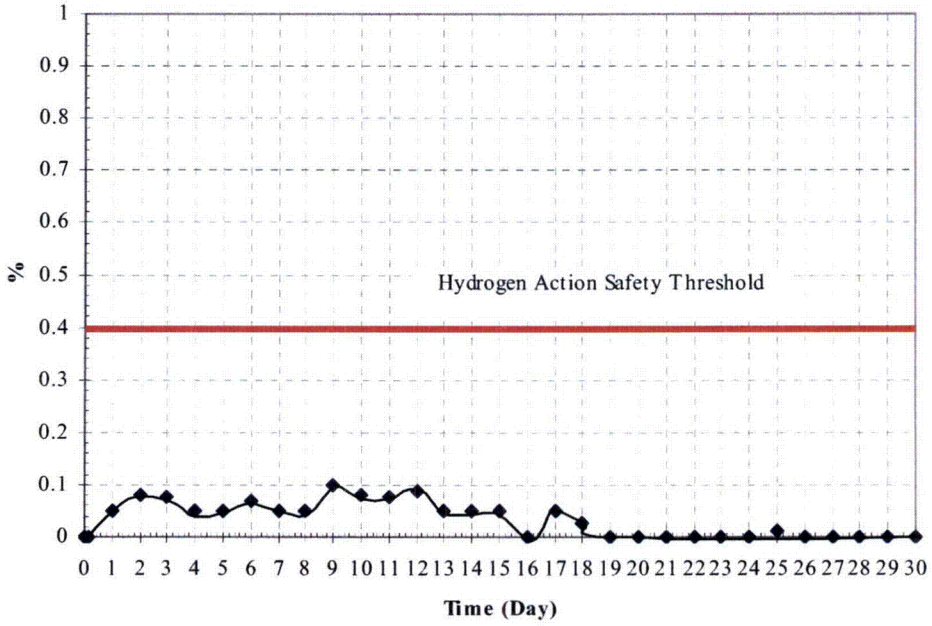


**Figure 3-3. Hydrogen generation.**

## 3.2. Water Samples

### 3.2.1. Wet Chemistry

Wet chemistry analyses included turbidity, TSS, and kinematic viscosity.

**Turbidity:** The baseline turbidity values, which were taken before the latent debris and concrete dust were added, for the 23°C and 60°C water samples were 0.81 NTU and 0.77 NTU. After the addition of latent debris and concrete dust, the tank solution turbidity was 14.1 NTU. The daily turbidity values are shown in Figure 3-5.

Due to the cloudy nature of the water in the tank after the recirculation pump was turned on, turbidity values were measured at 60°C over the initial 4-hour spray phase, in addition to regular daily monitoring. Figure 3-4 shows the turbidity during this time period. The x-axis on the graph represents the time in hours after the spray nozzles were turned on. As can be seen, a slight decrease in turbidity occurred from the time zero value to 12.4 NTU at 4 hours.

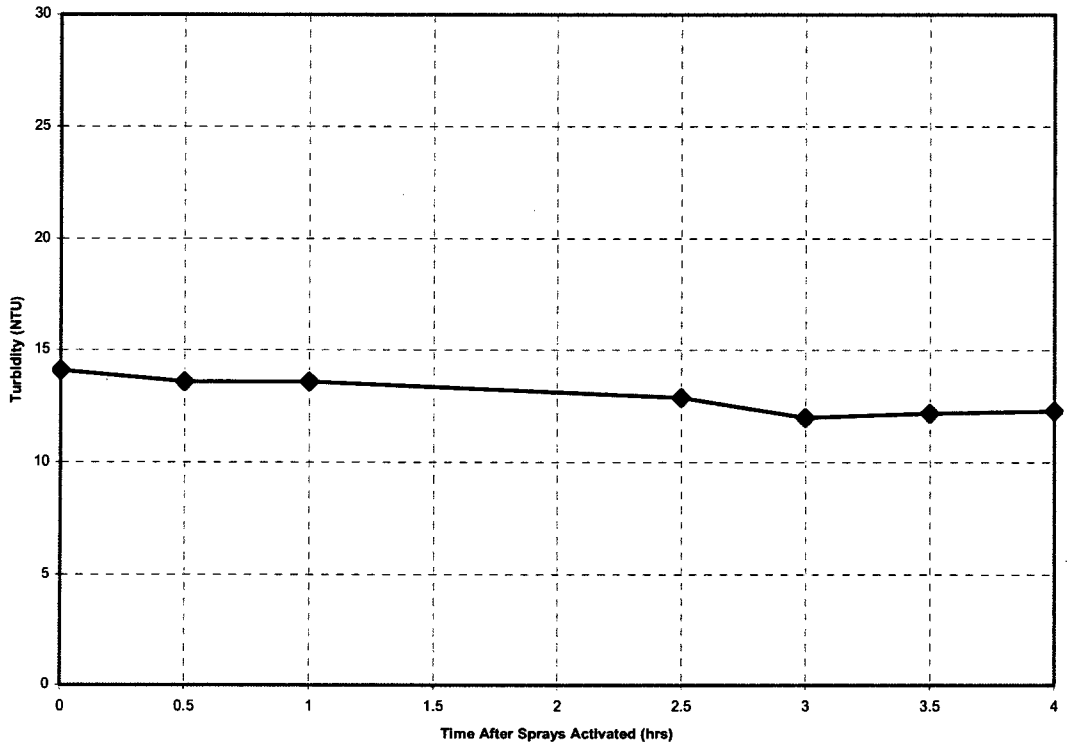


**Figure 3-4. Turbidity results during spray phase.**

Figure 3-5 shows the daily turbidity values at 23°C and 60°C throughout the test. The 60°C curve exhibited a steady decline over that time period. The 23°C turbidity curve exhibited a similar trend through the first seven days of the test. However, beginning on Day 8, the 23°C turbidity values began to deviate slightly, rising higher than the 60°C readings. From Day 8 through Day 30, the 23°C values were, on average, 2.95 NTU greater than the 60°C values. From Day 21 to Day 30, the mean turbidity measurements for the 60°C and 23°C samples were 0.7 NTU and 4.7 NTU, respectively.

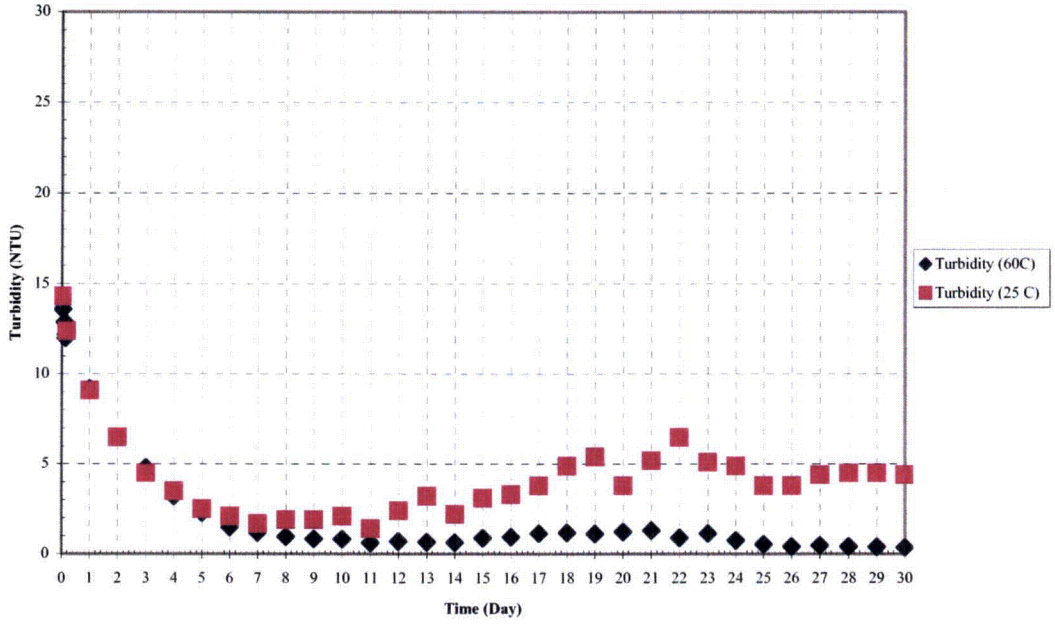


**Figure 3-5. Daily turbidity results.**

**Total Suspended Solids:** Total suspended solids (TSS) are measured by running a volume of approximately 500 mL through an in-line filter directly at the sample tap and measuring the dried mass added to the filter. The selected equipment assures that TSS measurements are not affected by temperature-dependent or time-dependent precipitation reactions that may occur once the process solution is removed from the tank. Figure 3-6 presents Test #5 TSS data as the experiment progressed. The baseline TSS measurement, taken before time zero, was 16.2 mg/L. At the end of the four-hour spray phase, the TSS value rose to 26.5 mg/L. Following the spray cycle and beginning at 24 hours, the TSS measurements were performed daily. TSS measurements gradually declined over the first seven days, with a Day 7 value of 17.6 mg/L, which is close to the baseline measurement. The TSS measurement remained constant through Days 7 through 9 but began increasing on Day 10 and continued increasing to Day 13. The measurements after Day 13 were somewhat erratic. This unexplained behavior in TSS occurred through Day 21. From Day 22 through the end of the test, the TSS measurements remained similar to the baseline measurement taken at time zero.

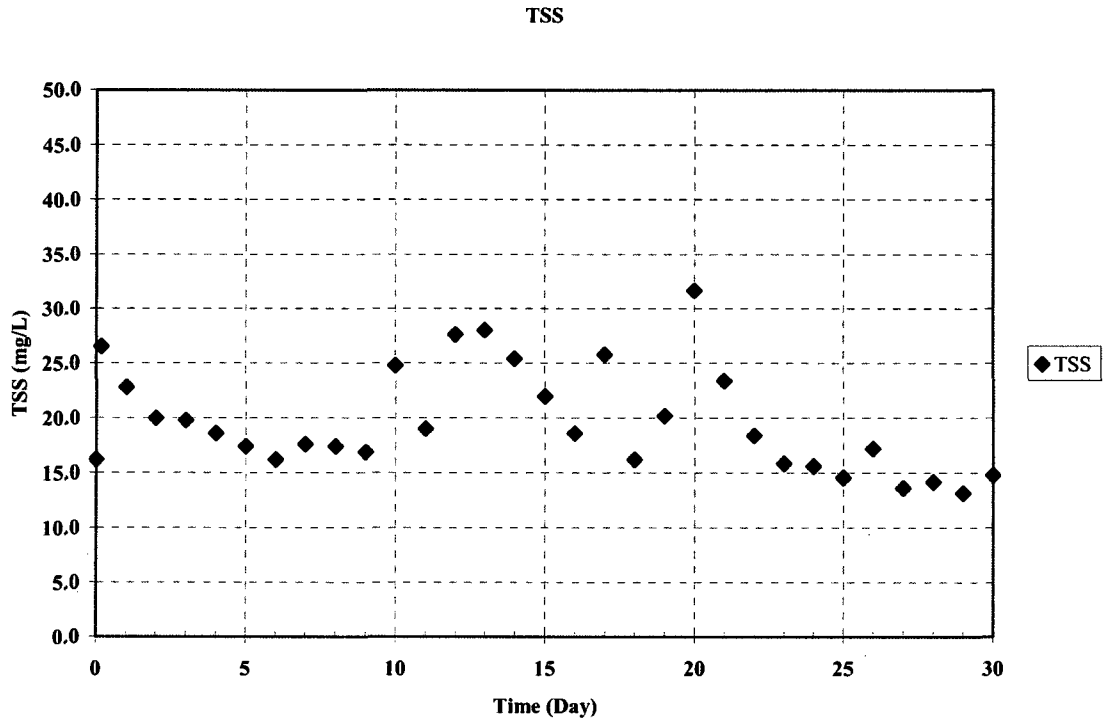


**Figure 3-6. Test #5 TSS results.**

**Kinematic Viscosity:** Kinematic viscosity was measured with a Cannon-Fenske capillary viscometer. Viscosity was measured on unfiltered samples, each at a temperature of 60°C (±1.0°C) [140°F (±1.8°F)] and 23°C (±2.0°C) [73.4°F (±3.6°F)]. Water's viscosity is highly sensitive to temperature, and the allowed temperature range results in a variation of viscosity of 2.9% between 59°C (138.2°F) and 61°C (141.8°F), and a 9.3% variation between 21°C (69.8°F) and 25°C (77.0°F). For this reason, temperature was measured to 0.1°C accuracy with a National Institute of Standards and Technology (NIST)-traceable thermometer for all viscosity measurements, and the measured viscosity values were corrected to a common temperature to facilitate comparisons. The corrected temperatures were 60.0°C (140°F) and 23.0°C (73.4°F). Throughout Test #5, the viscosity measurements remained relatively constant. The average viscosity for the 23°C measurement was 0.96 $mm^2/s$, and for the 60°C measurement, it was 0.50 $mm^2/s$. The viscosity values are shown in Figure 3-7.

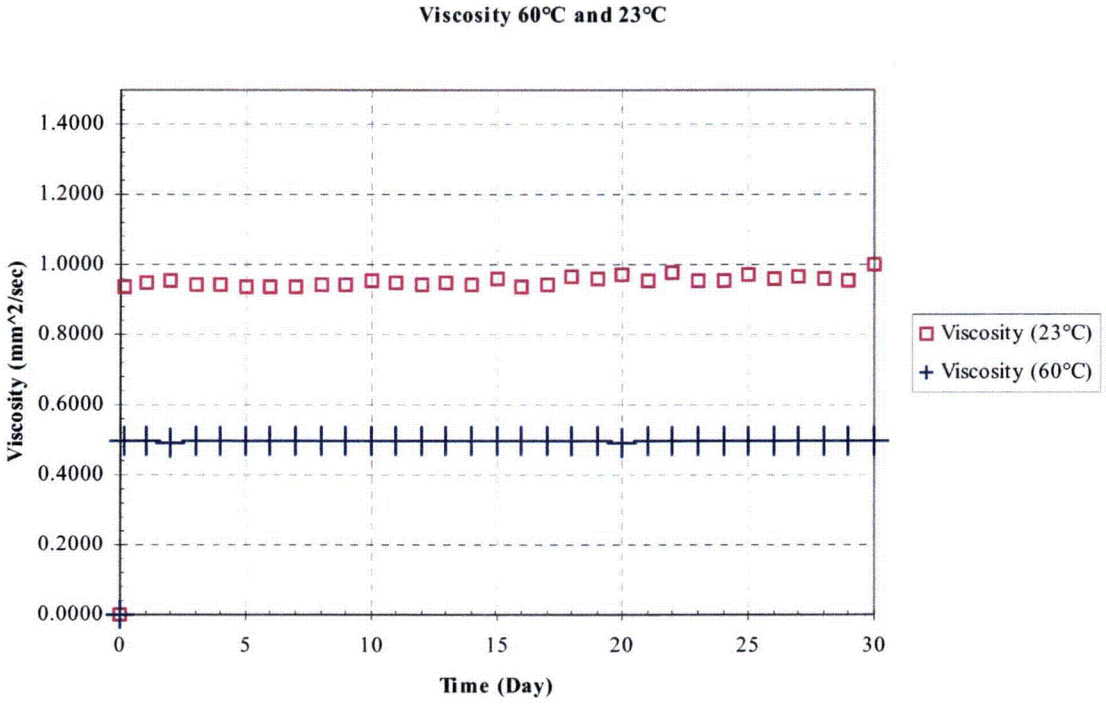


**Figure 3-7. Viscosity at 60°C and 23°C.**

### 3.2.2. Metal Ion Concentration

ICP results for daily water samples from Test #5 are displayed in Figures 3-8 through 3-15. Table 3-1 contains ICP results for elements that were analyzed at time zero and 4 hours and on Days 15 and 30. Table 3-1 shows the chloride, boron, lead, lithium, and potassium concentrations. An examination of the figures reveals that copper, iron, magnesium, and zinc were present in trace amounts, below 1 mg/L. It also can be seen that aluminum, calcium, silica, and sodium were present in higher concentrations. The concentrations of aluminum and calcium were verified by retesting, but the reason for their variations was not determined.

**Table 3-1. ICP Results for Selected Elements**

| Unfiltered Samples | | | | | |
|---|---|---|---|---|---|
| | Chloride | Boron | Lead | Lithium | Potassium |
| Sample Time | mg/L | | | | |
| Baseline | 1.5 | 2580 | 0.02 | 0.10 | 3.0 |
| 4 Hours | 40.0 | 2860 | 0.03 | 0.11 | 4.3 |
| Day 15 | 41.6 | 1920 | 0.02 | 0.11 | 5.2 |
| Day 30 | 36.6 | 2320 | 0.02 | 0.10 | 8.4 |

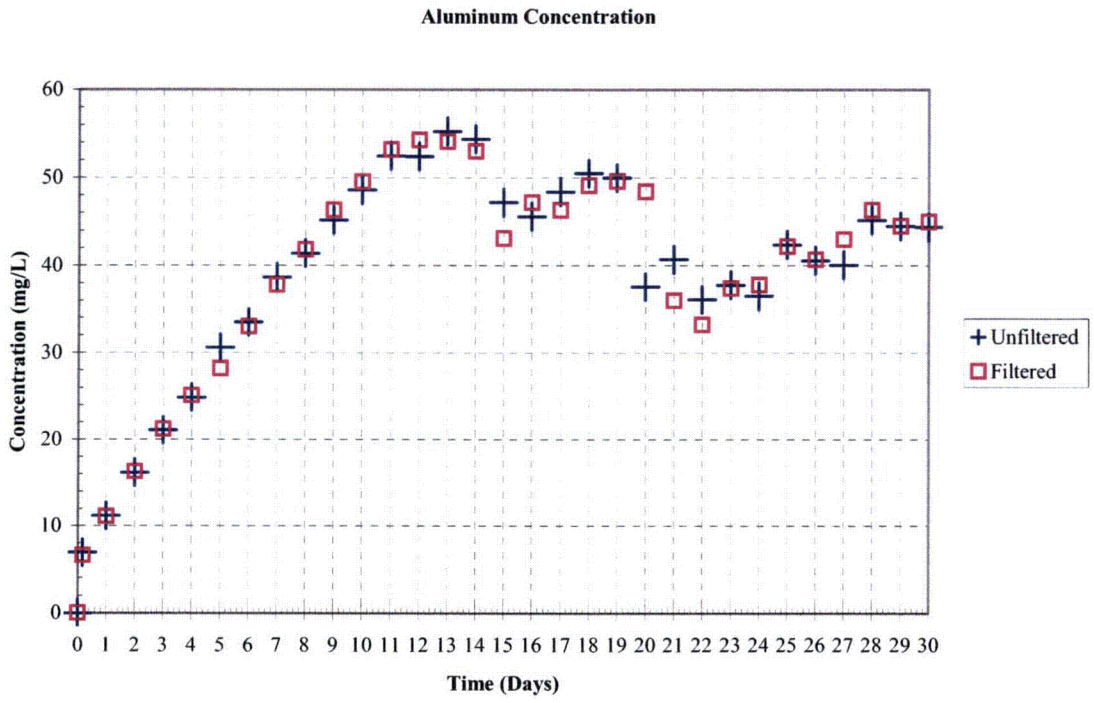


**Figure 3-8. Aluminum concentration.**

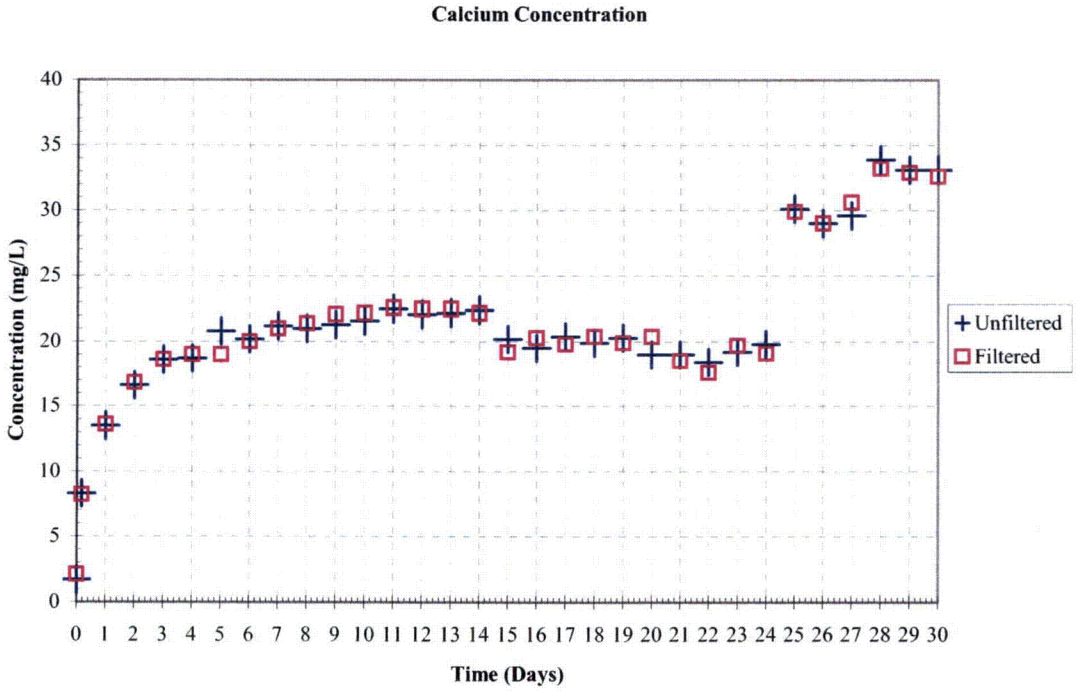


**Figure 3-9. Calcium concentration.**

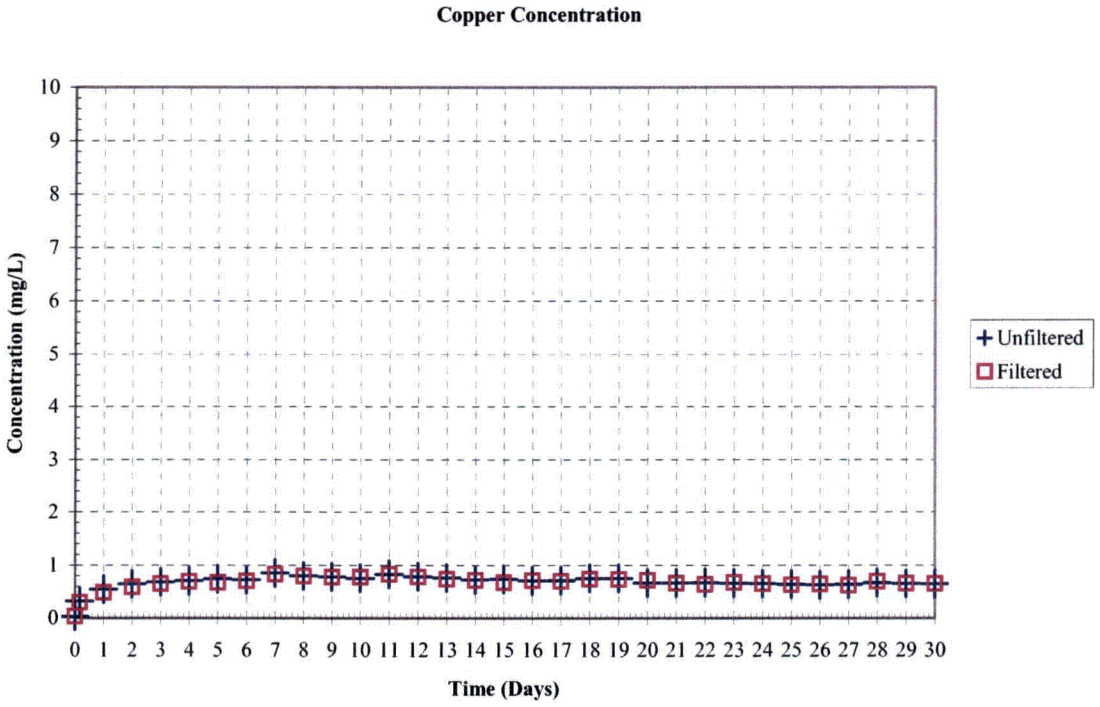


**Figure 3-10. Copper concentration.**

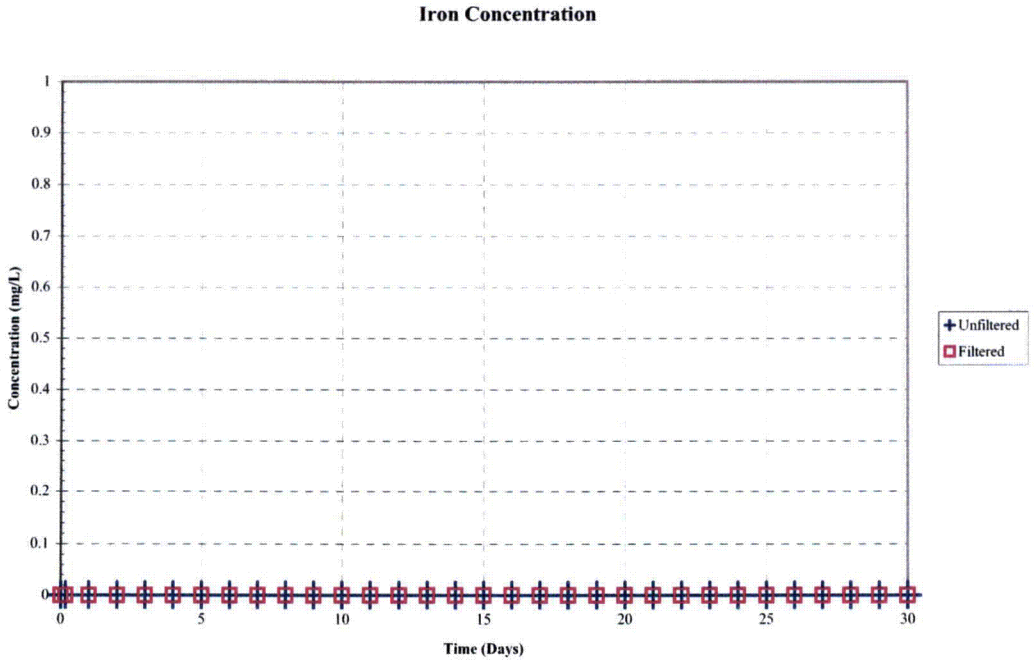


**Figure 3-11. Iron concentration.**

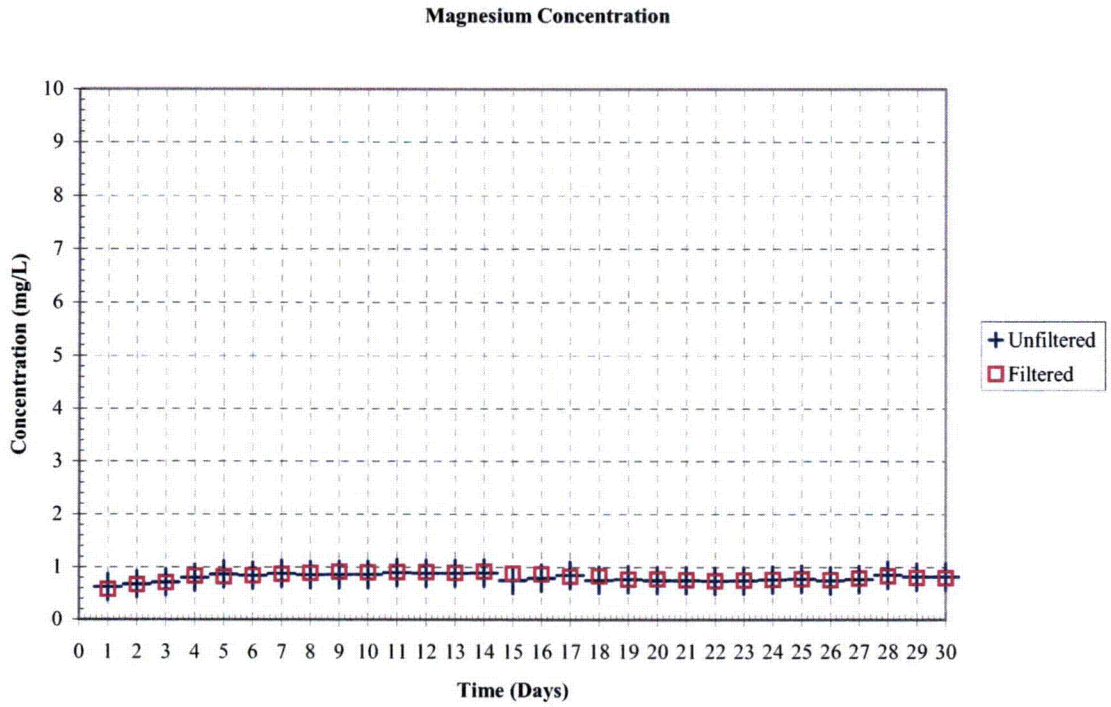


**Figure 3-12. Magnesium concentration.**

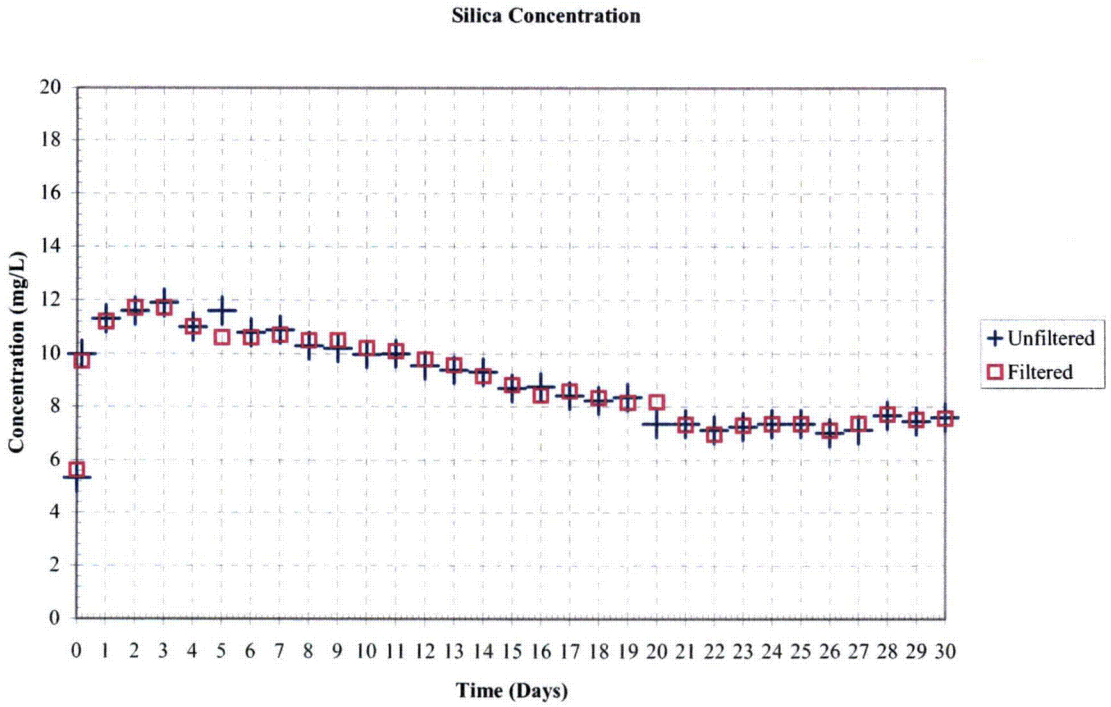


**Figure 3-13. Silica concentration.**

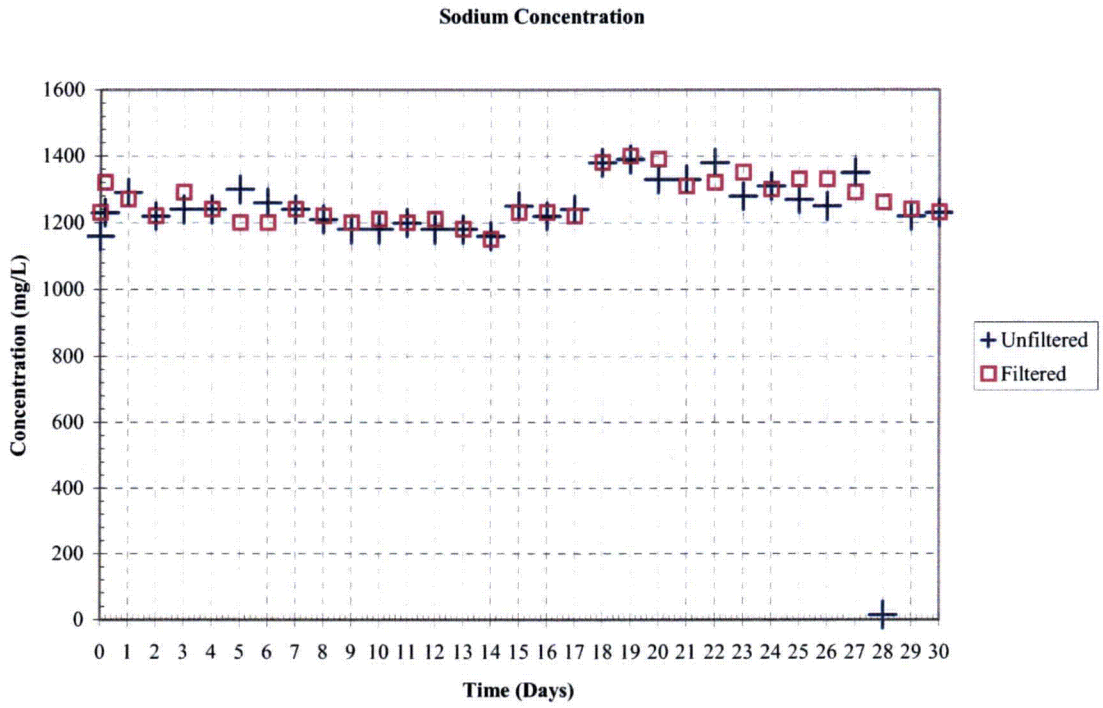


**Figure 3-14. Sodium concentration.**

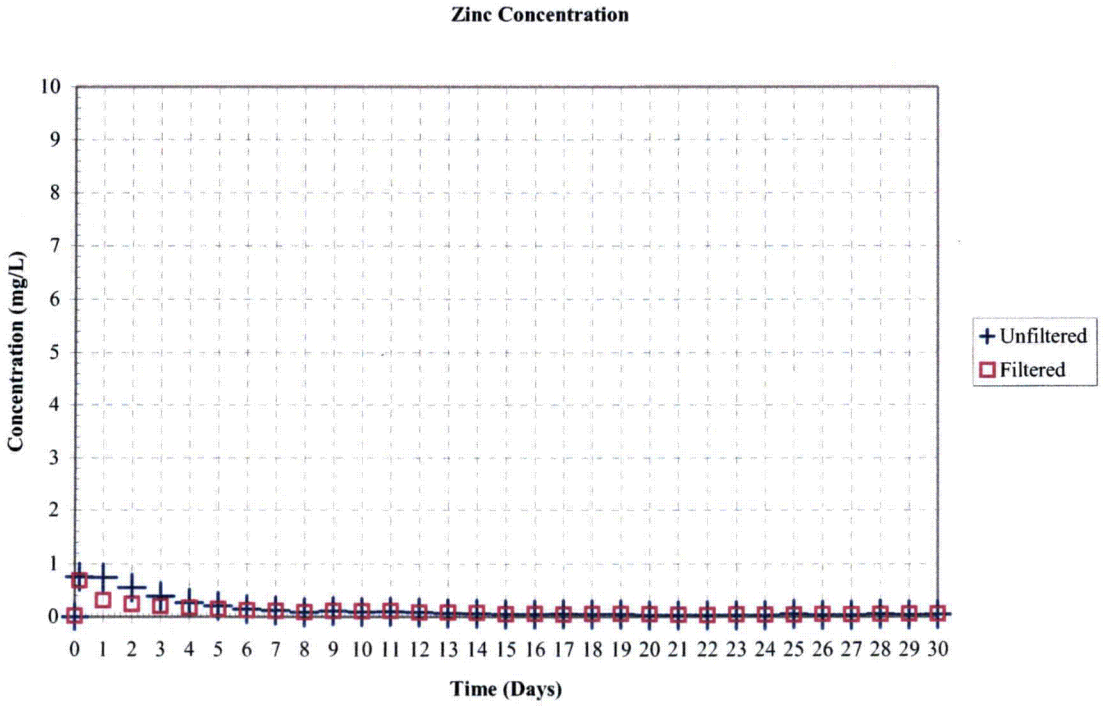


**Figure 3-15. Zinc concentration.**

## 3.3. Insulation

Test #5 contained NUKON™ fiberglass samples. The fiberglass samples were thoroughly investigated, with samples being removed from the tank on Days 4, 15, and 30.

### 3.3.1. Deposits in Fiberglass Samples

The fiberglass samples were contained in SS mesh bags to minimize migration of the fiberglass throughout the tank and piping. Small mesh envelopes, approximately 4 in. square, containing approximately 5 g of fiber, were pulled out of the tank periodically for SEM examination. These sample envelopes were placed in a range of water flow conditions, but none experienced direct water flow through the fiberglass. All were thoroughly immersed in the test solution until they were recovered from the tank.

There were four fiberglass locations in the tank that were examined in this test, including the low-flow areas, the high-flow areas, the drain collar, and the birdcage. (See Subsection 2.4.1.1 for descriptions of the fiberglass samples.) Both the exterior and the interior of the fiberglass samples from each location were examined. Subsections 3.3.1.1 through 3.3.1.10 give the ESEM/SEM/EDS results according to the location of the fiberglass samples in the tank and when the sample was removed from the tank. The different samples include Day-4 low-flow, Day-15 low-flow, Day-15 high-flow, Day-30 low-flow, Day-30 low-flow in a big envelope, Day-30 high-flow, Day-30 high-flow in front of a header, Day 30 in nylon mesh, Day-30 drain collar, and Day-30 birdcage. The corresponding figures are Figures 3-16 through 3-70. Additional micrographs of fiberglass samples are presented in Appendices A, B, and C.

In general, particulate deposits were found on only the exterior of the fiberglass. This result suggests that almost all of the particulate deposits were physically retained at the fiberglass exterior. Because there was no significant water flow directly through the fiber, the migration of particulate deposits into the fiberglass interior was insignificant. Comparing the amount of particulate deposits, the greatest amount was found on the drain collar exterior, especially the exterior farthest from the drain screen. Small amounts of particulate deposits were found on the fiberglass exterior within the birdcage and within the big envelope in a low-flow zone. All other fiberglass exteriors were relatively clean, and no significant particulate deposits were found. EDS shows that the particulate deposits on the drain collar exterior were mainly composed of O, Al, Na, Ca, Mg, C, and possibly Si. Unlike the exterior, the interior of the fiberglass samples at each location was relatively clean. Only flocculent and web-like deposits were observed. The web-like deposits were not present on Day-30 samples, which may be due to a change of the solution chemistry. There was no significant trend of the flocculent deposits with respect to either the location or time. The flocculent and web-like deposits were primarily composed of O, Na, Ca, Mg, Al, B, C, and possibly Si. These deposits were likely formed by chemical precipitation during dehydration of the samples after the samples were removed from the tank.

Results also show that the mesh material, i.e., stainless steel or nylon, did not significantly affect the deposits on the fiberglass. In addition, because of suspended particles settling out of the test solution, the Day-30 high-flow fiberglass (placed in front of a header on Day 6) sample exterior had much less particulate deposits attached/retained than did the high-flow samples put in the tank on Day 0.

#### 3.3.1.1. Day-4 Low-Flow Fiberglass Samples

Since there was no significant water flowing through the fiberglass samples during the test, the migration of particulate deposits from the solution into the fiberglass interior was insignificant. ESEM results revealed some deposits on both the exterior and the interior of the low-flow fiberglass samples after 4 days of the test. These deposits were either formed like a webbing among glass fibers (see Figures 3-17 and 3-21) or flocculent (see Figure 3-19). The deposits are likely of chemical origin instead of being physically attached/retained. They may be formed during the drying process (semi-dehydrated) of the samples during ESEM analysis. EDS results indicated that both types of deposits were commonly composed of O, Na, Ca, Mg, Al, B, C, and possibly Si. Comparing the amount of the deposits on fiberglass revealed no significant difference between the interior and exterior samples. Again, this fact may be explained by the likely chemical origin of the deposits, since chemical precipitation would occur to a similar degree on both the exterior and the interior fiberglass samples if the concentrations were similar. Figures 3-16 through 3-22 show the Day-4 low-flow fiberglass results.


**Figure 3-16. ESEM image magnified 100 times for a Test #5, Day-4 low-flow exterior fiberglass sample.**

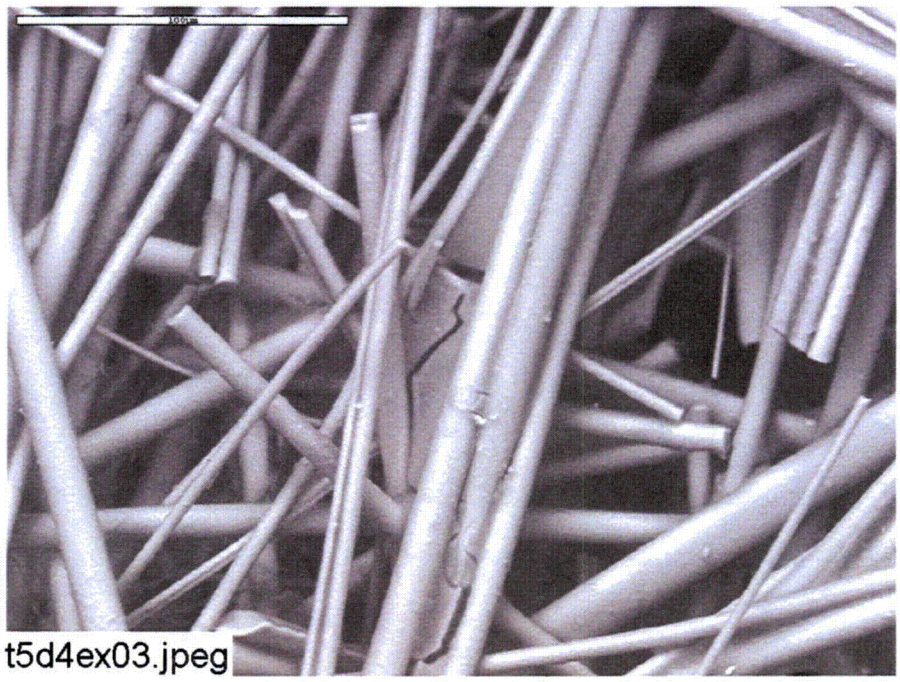


**Figure 3-17. ESEM image magnified 500 times for a Test #5, Day-4 low-flow exterior fiberglass sample.**

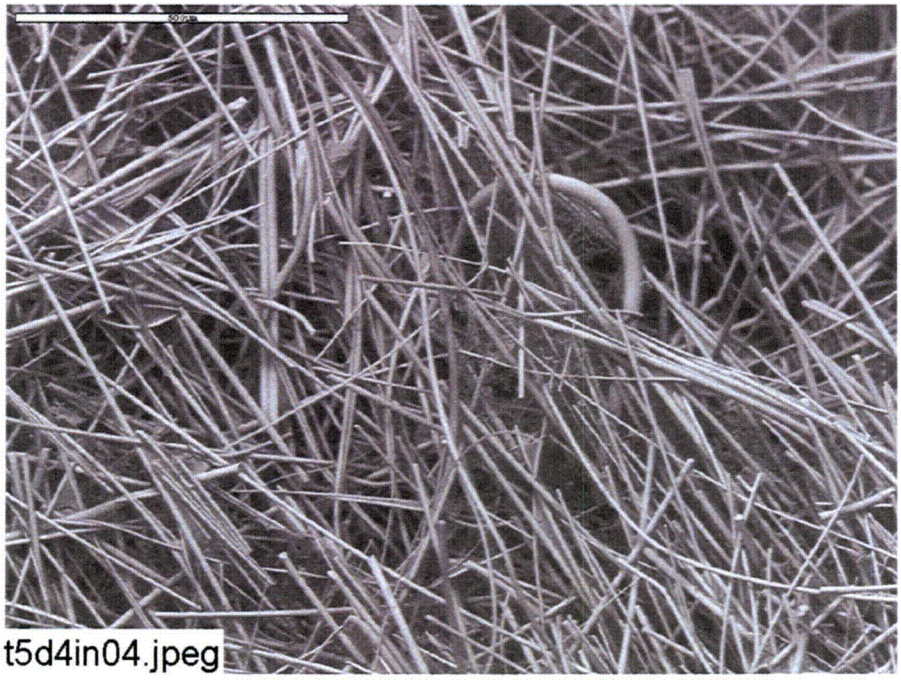


**Figure 3-18. ESEM image magnified 100 times for a Test #5, Day-4 low-flow interior fiberglass sample.**

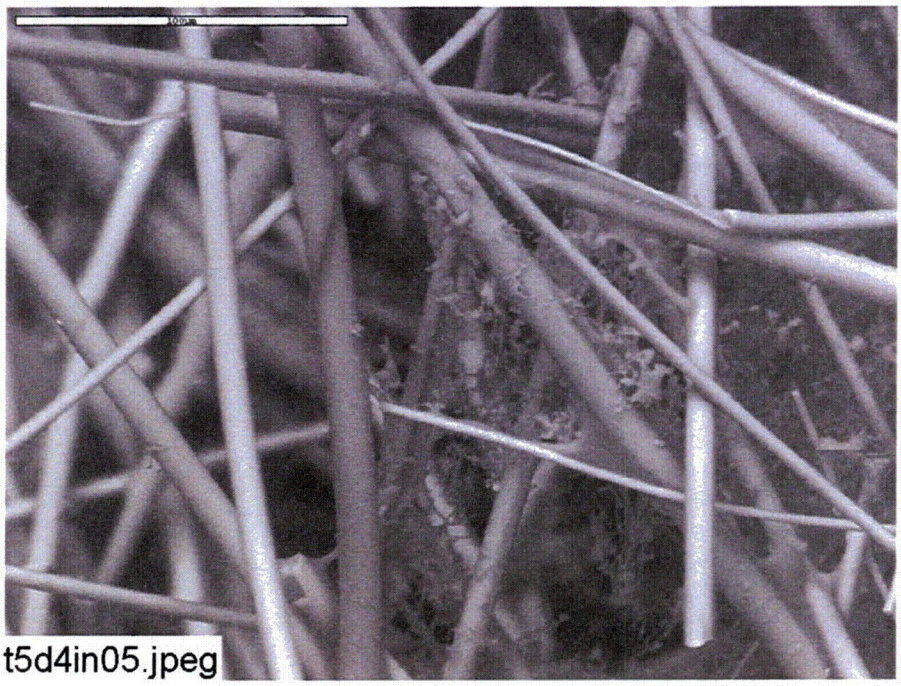


**Figure 3-19. ESEM image magnified 500 times for a Test #5, Day-4 low-flow interior fiberglass sample.**

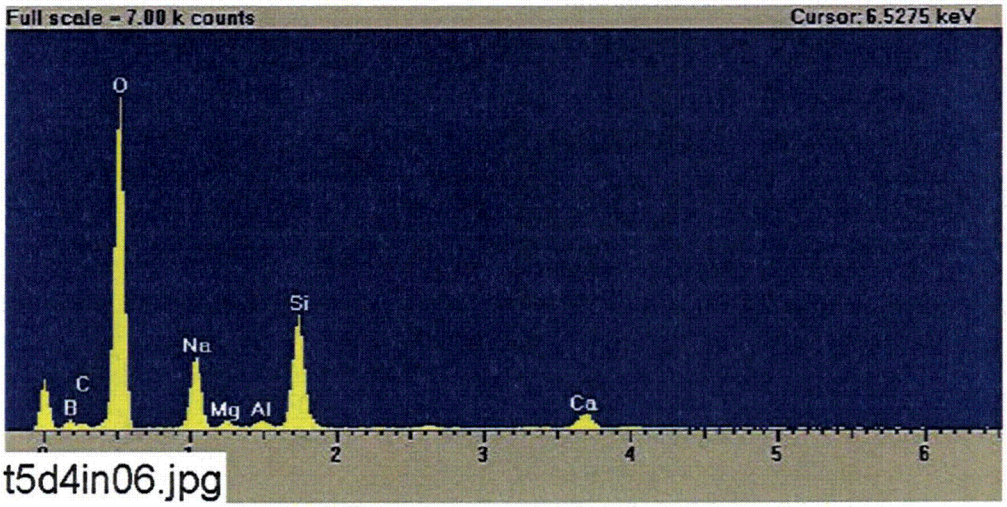


**Figure 3-20. EDS counting spectrum for the flocculence between the fibers shown in Figure 3-19.**

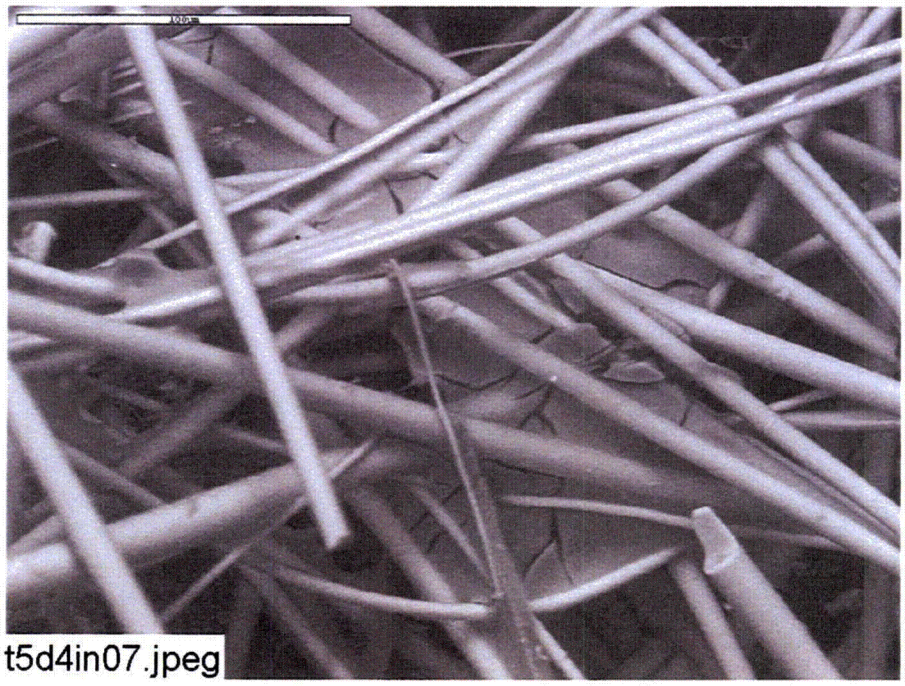


**Figure 3-21. ESEM image magnified 500 times for a Test #5, Day-4 low-flow interior fiberglass sample.**

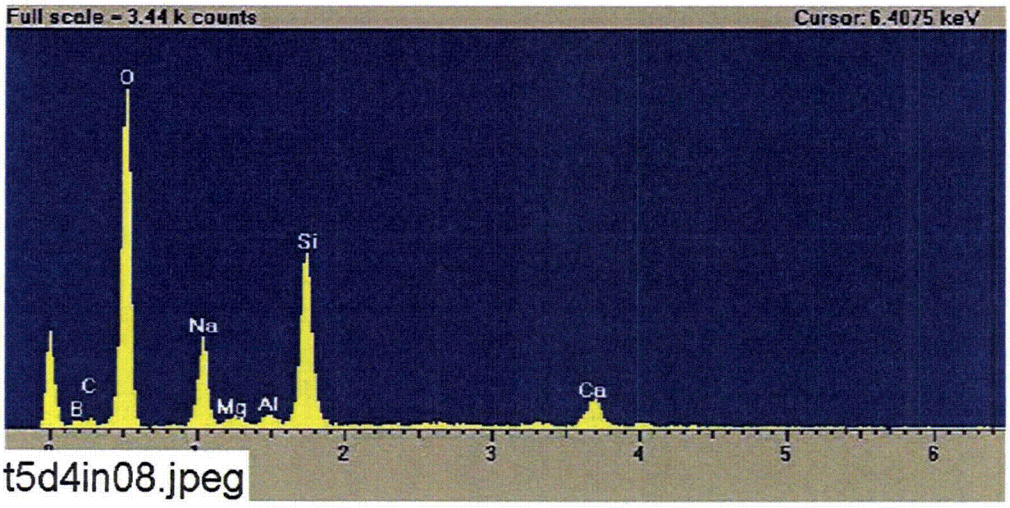


**Figure 3-22. EDS counting spectrum for the web-like deposits between the fibers in Figure 3-21.**

### 3.3.1.2. Day-15 Low-Flow Fiberglass Samples

Similar to the Day-4 samples, some flocculent and web-like deposits were found on the fiberglass exterior and interior of the Day-15 samples. EDS analyses showed that the deposits were mainly composed of O, Na, Ca, Mg, Al, B, C, and possibly Si. There was no significant increase in the amount of deposits on Day-15 samples compared with Day-4 samples. In addition, the difference in the amount of deposits on the exterior and the

interior Day-15 low-flow fiberglass samples was insignificant. Figures 3-23 through 3-28 show the Day-15 low-flow fiberglass results.


**Figure 3-23. ESEM image magnified 100 times for a Test #5, Day-15 low-flow exterior fiberglass sample.**

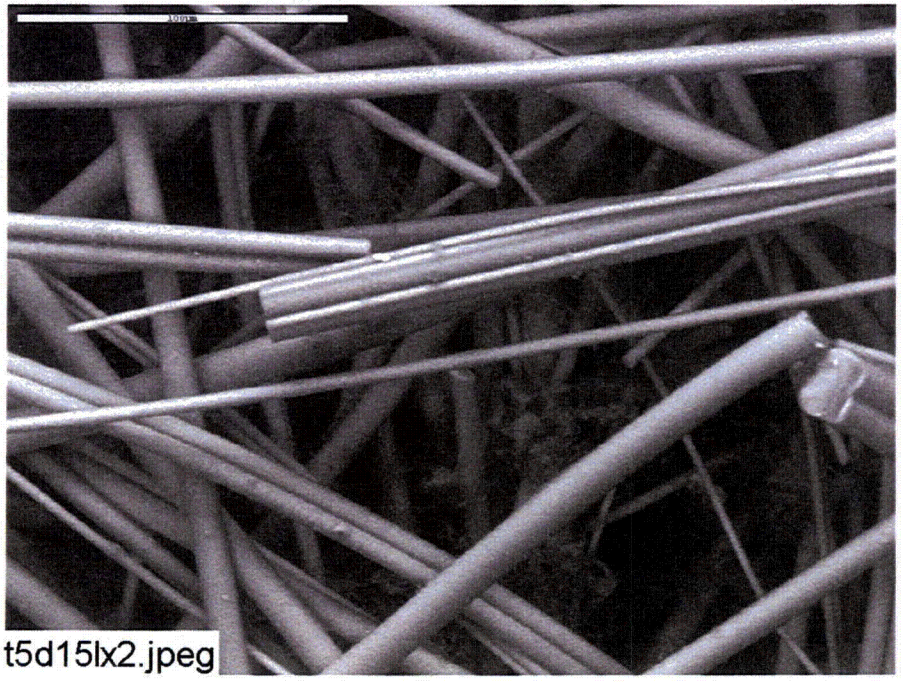


**Figure 3-24. ESEM image magnified 500 times for a Test #5, Day-15 low-flow exterior fiberglass sample.**

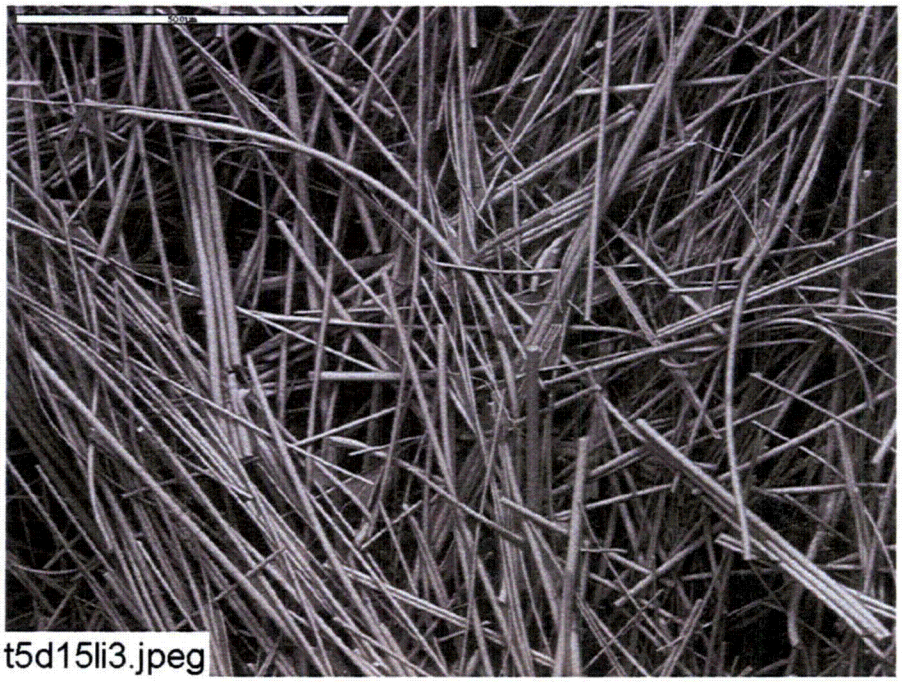


**Figure 3-25. ESEM image magnified 100 times for a Test #5, Day-15 low-flow interior fiberglass sample.**

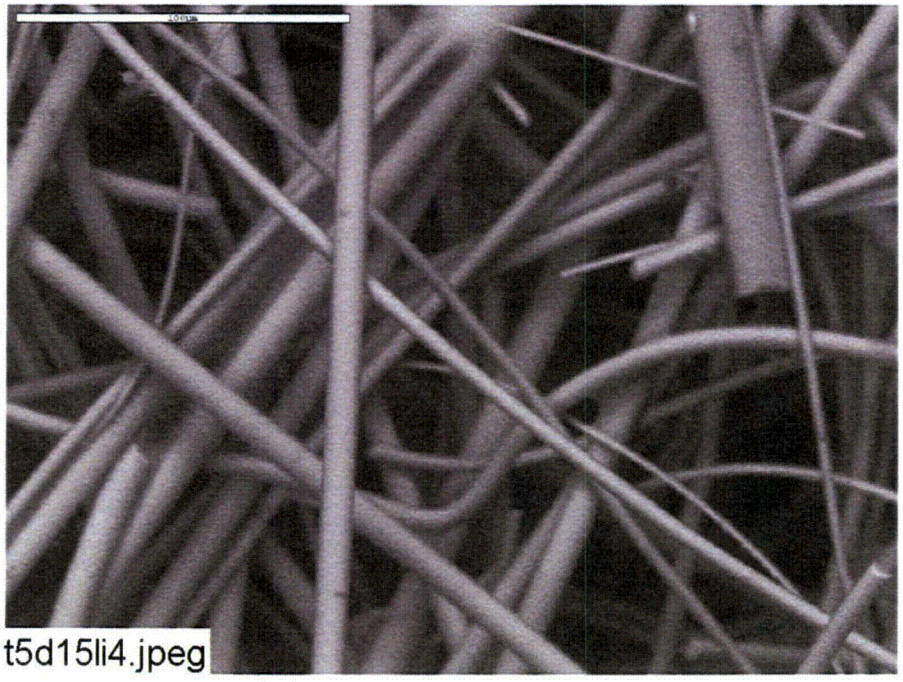


**Figure 3-26. ESEM image magnified 500 times for a Test #5, Day-15 low-flow interior fiberglass sample.**

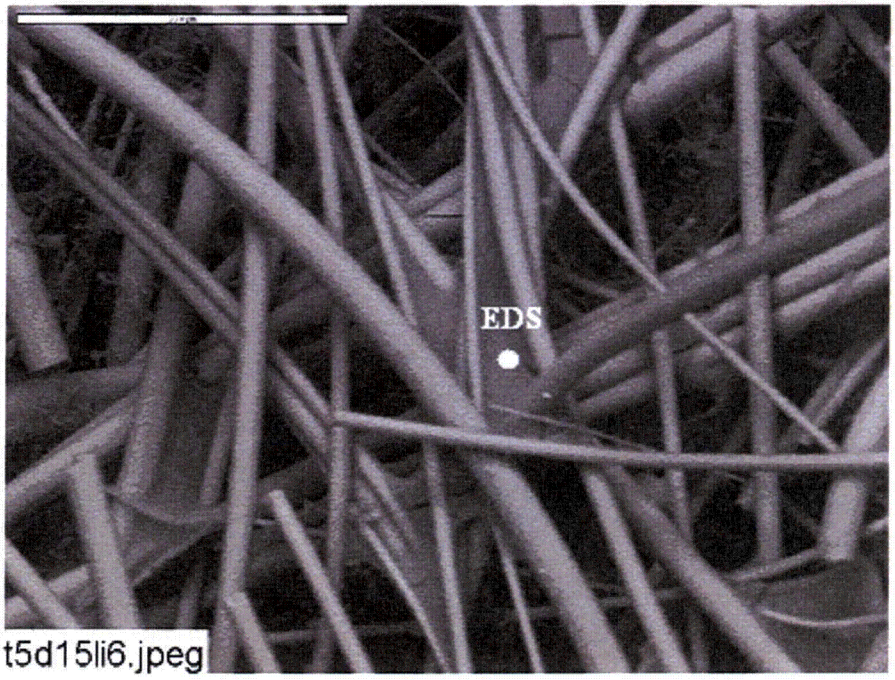


**Figure 3-27. Annotated ESEM image magnified 500 times for a Test #5, Day-15 low-flow interior fiberglass sample.**

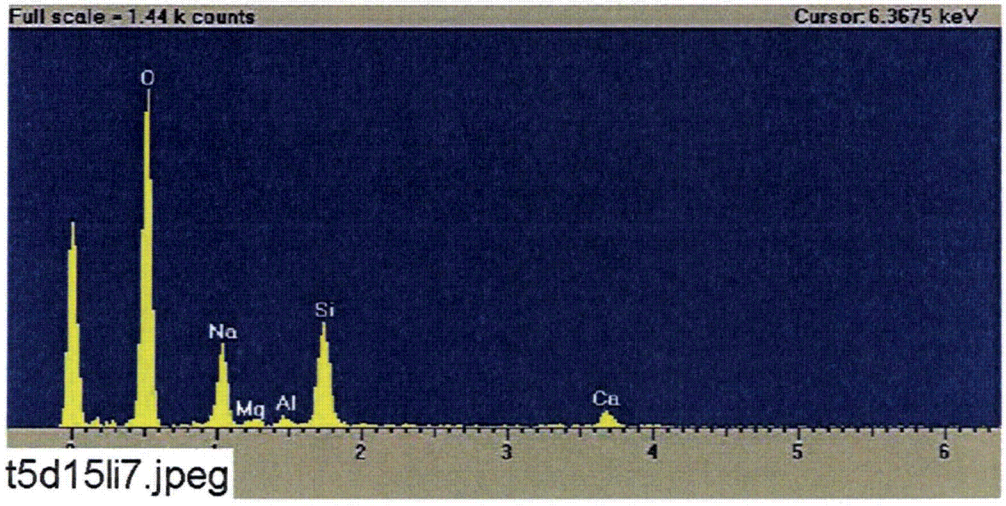


**Figure 3-28. EDS counting spectrum for the web-like deposits between the fibers in Figure 3-27.**

### 3.3.1.3. Day-15 High-Flow Fiberglass Samples

In contrast to the Day-15 low-flow samples, no web-like deposits were found in the Day-15 high-flow fiberglass samples. However, flocculent deposits were found on both the exterior and interior Day-15 high-flow fiberglass samples. There was no significant difference regarding the amount of the flocculent deposits between the exterior and the interior fiberglass samples, suggesting the deposits' likely chemical origin. The visual

appearance of the flocculent deposits was similar to other fiberglass samples, so no additional EDS was performed. In addition, no particulate deposits were observed on either the exterior or interior fiberglass samples. Figures 3-29 through 3-32 show the Day-15 high-flow fiberglass results.

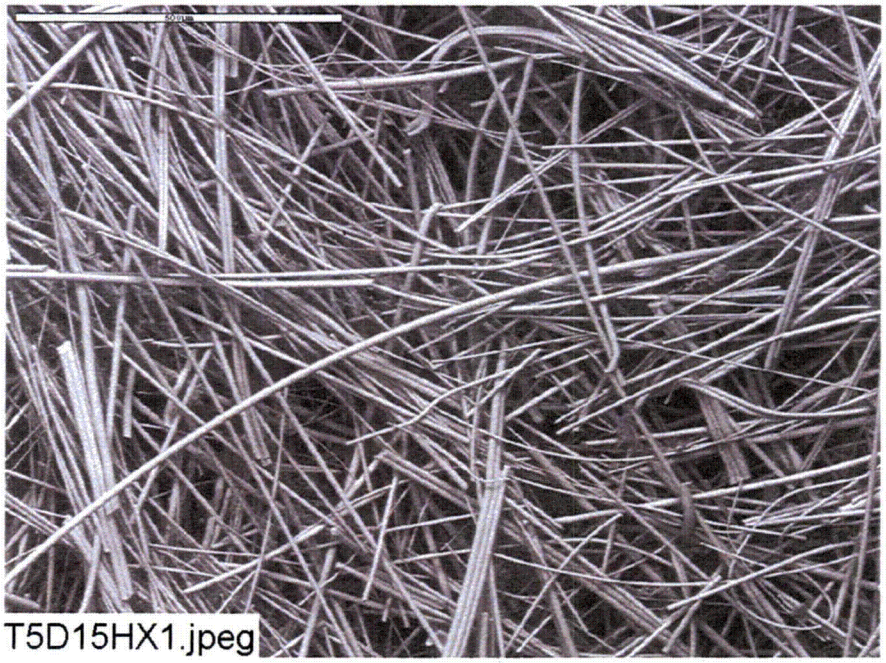


**Figure 3-29. ESEM image magnified 100 times for a Test #5, Day-15 high-flow exterior fiberglass sample.**

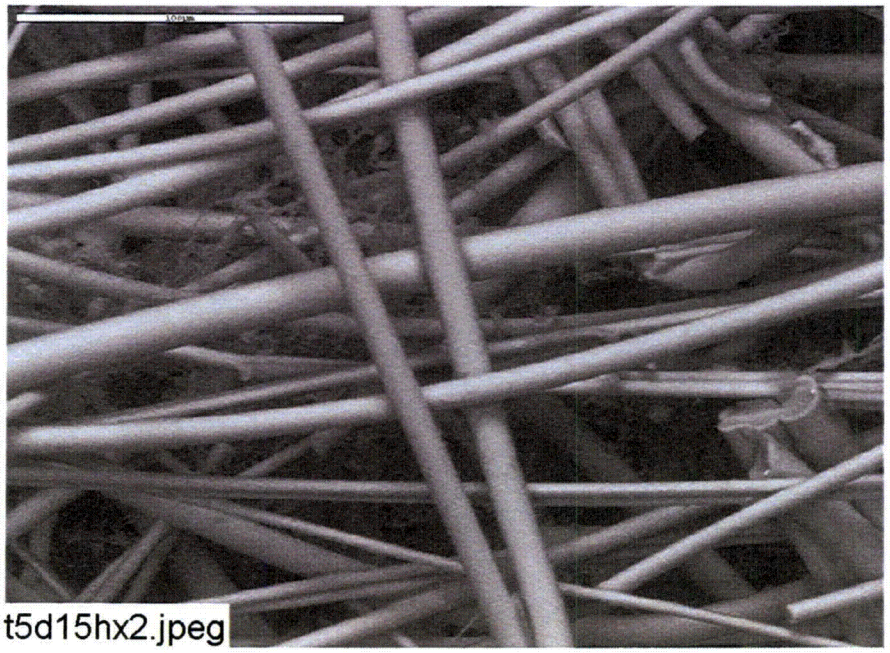


**Figure 3-30. ESEM image magnified 500 times for a Test #5, Day-15 high-flow exterior fiberglass sample.**

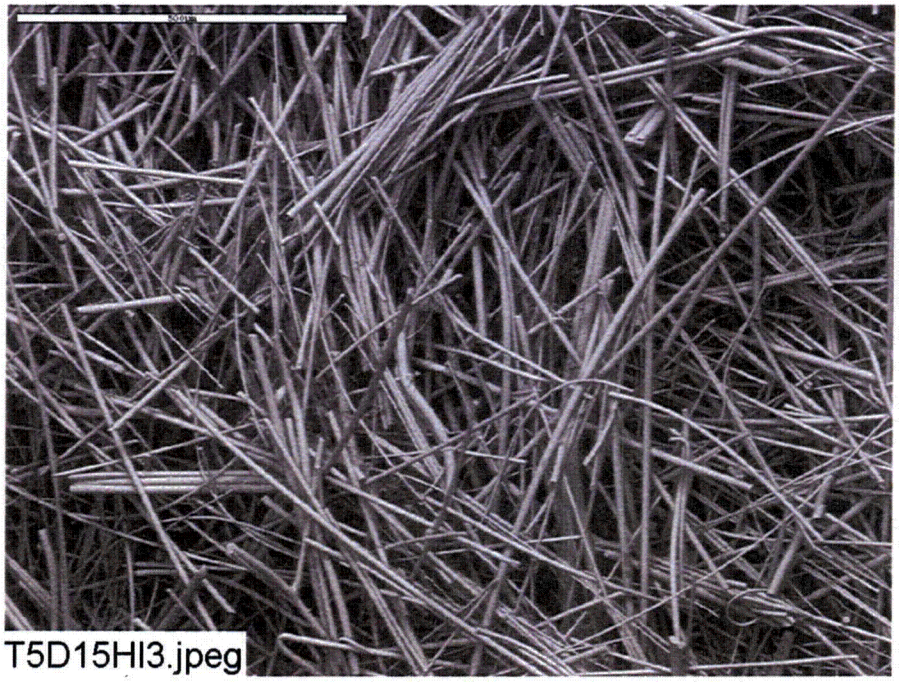


**Figure 3-31. ESEM image magnified 100 times for a Test #5, Day-15 high-flow interior fiberglass sample.**

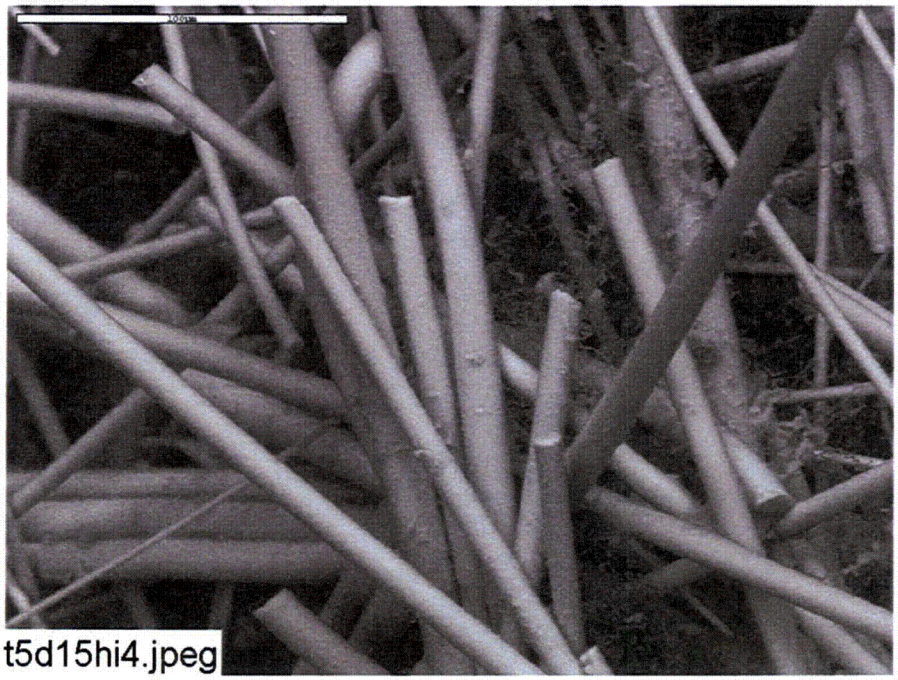


**Figure 3-32. ESEM image magnified 500 times for a Test #5, Day-15 high-flow interior fiberglass sample.**

### 3.3.1.4. Day-30 Low-Flow Fiberglass Samples

No observable increase in the flocculent deposits was found with the Day-30 low-flow fiberglass samples compared with Day-4 and Day-15 low-flow fiberglass samples. No significant difference was found regarding the amount of the flocculent deposits between the exterior and the interior of the Day-30 low-flow fiberglass samples. No web-like deposits were found on either the exterior or interior of the Day-30 low-flow fiberglass samples. Furthermore, no particulate deposits were observed on either the exterior or interior fiberglass samples. Figures 3-33 through 3-36 show the Day-30 low-flow fiberglass results.

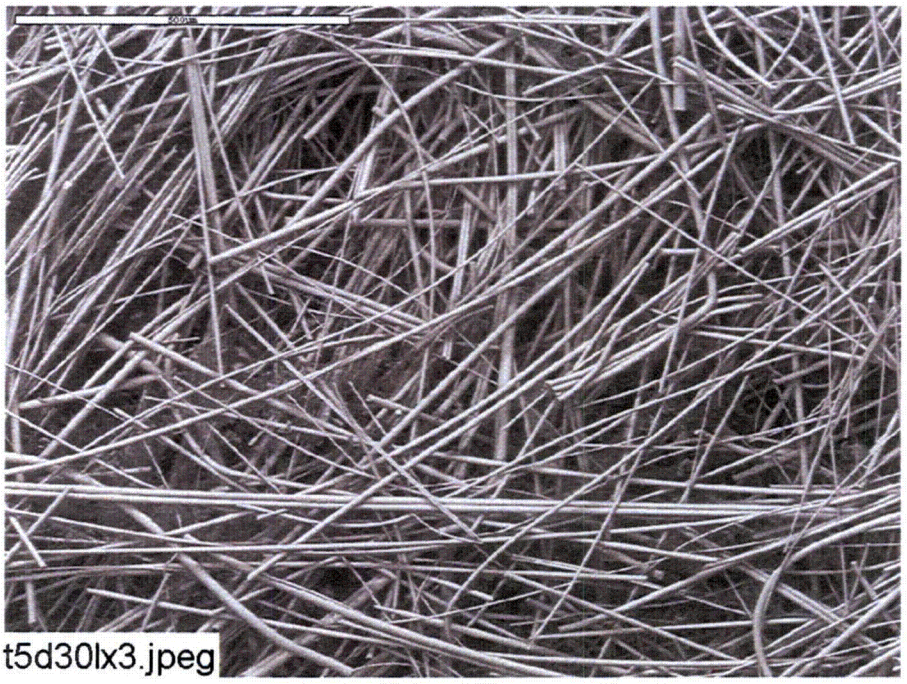


**Figure 3-33. ESEM image magnified 100 times for a Test #5, Day-30 low-flow exterior fiberglass sample.**

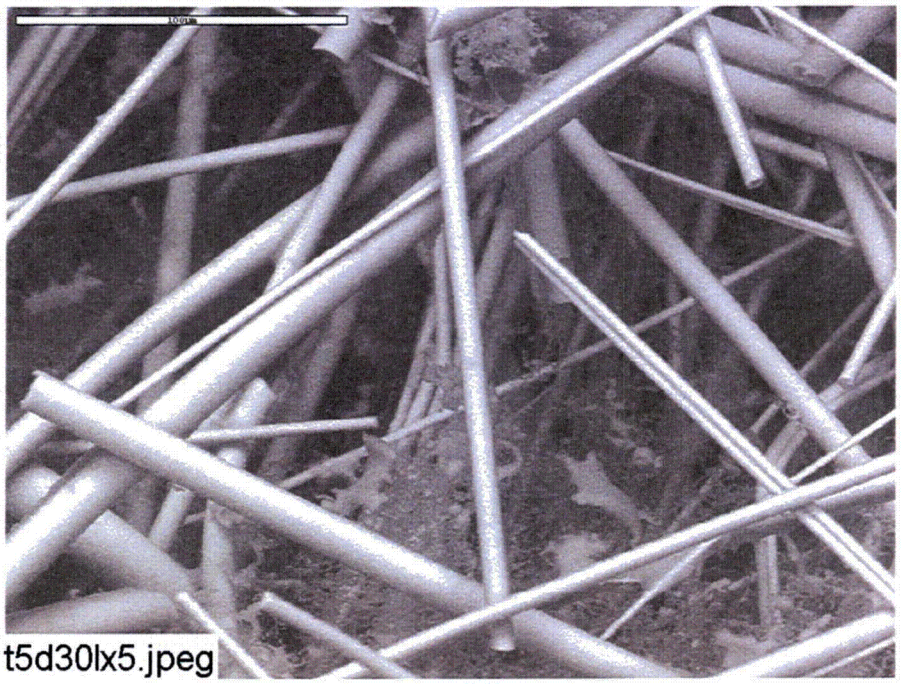


**Figure 3-34. ESEM image magnified 500 times for a Test #5, Day-30 low-flow exterior fiberglass sample.**


**Figure 3-35. ESEM image magnified 100 times for a Test #5, Day-30 low-flow interior fiberglass sample.**

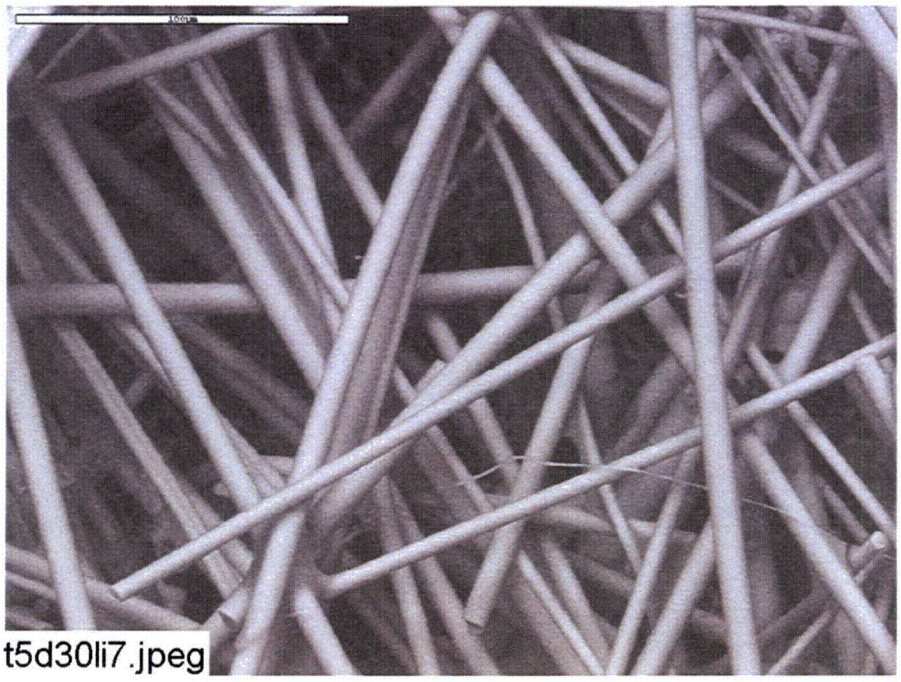


**Figure 3-36. ESEM image magnified 500 times for a Test #5, Day-30 low-flow interior fiberglass sample.**

### 3.3.1.5. Day-30 Low-Flow Fiberglass Samples in the Big Envelope

The big envelope was located on the tank bottom, contacting the test sediment on the bottom of the tank. In contrast to Day-4, Day-15, and other Day-30 low-flow fiberglass samples, a small amount of particulate deposits were observed on the fiberglass exterior of the Day-30 low-flow samples in the big envelope. EDS results show that the particulate deposits (see Figure 3-39) were composed of O, Na, Ca, Mg, Al, and possibly Si. However, no particulate deposits were observed on the fiberglass interior. Instead, flocculent deposits were found on the fiberglass interior, as they were with other interior fiberglass samples. Figures 3-37 through 3-41 illustrate these deposits for the Day-30 low-flow fiberglass in the big envelope.

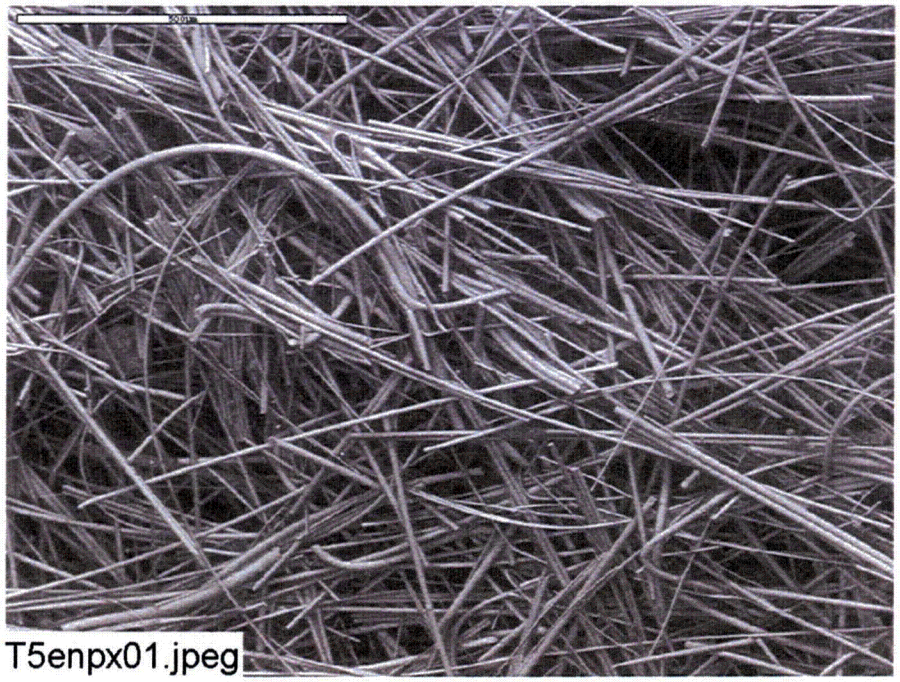


**Figure 3-37. ESEM image magnified 100 times for a Test #5, Day-30 low-flow exterior fiberglass sample in a big envelope.**

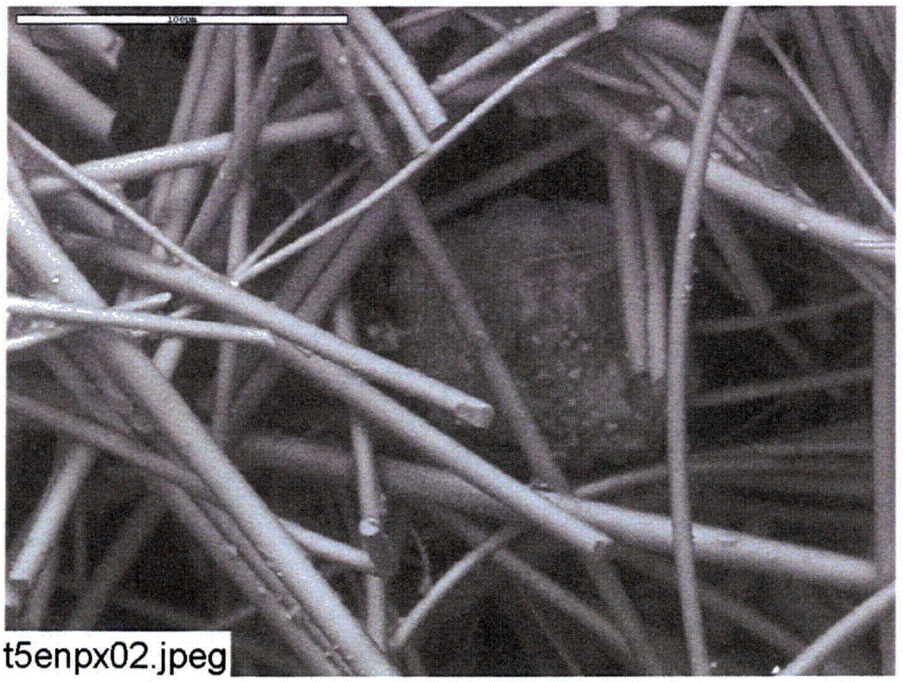


**Figure 3-38. ESEM image magnified 500 times for a Test #5, Day-30 low-flow exterior fiberglass sample in a big envelope.**

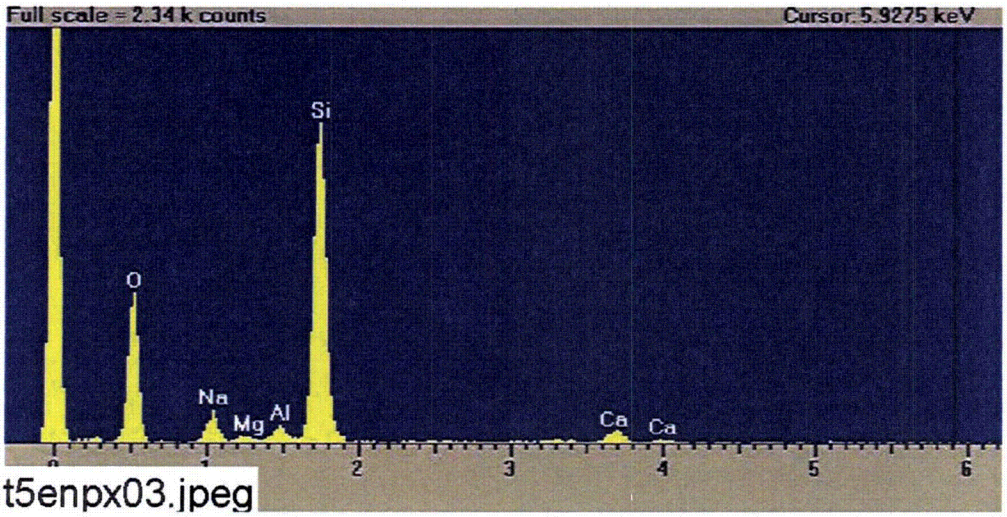


**Figure 3-39. EDS counting spectrum for the particulate deposit between the fibers in Figure 3-38.**


**Figure 3-40. ESEM image magnified 100 times for a Test #5, Day-30 low-flow interior fiberglass sample in a big envelope.**

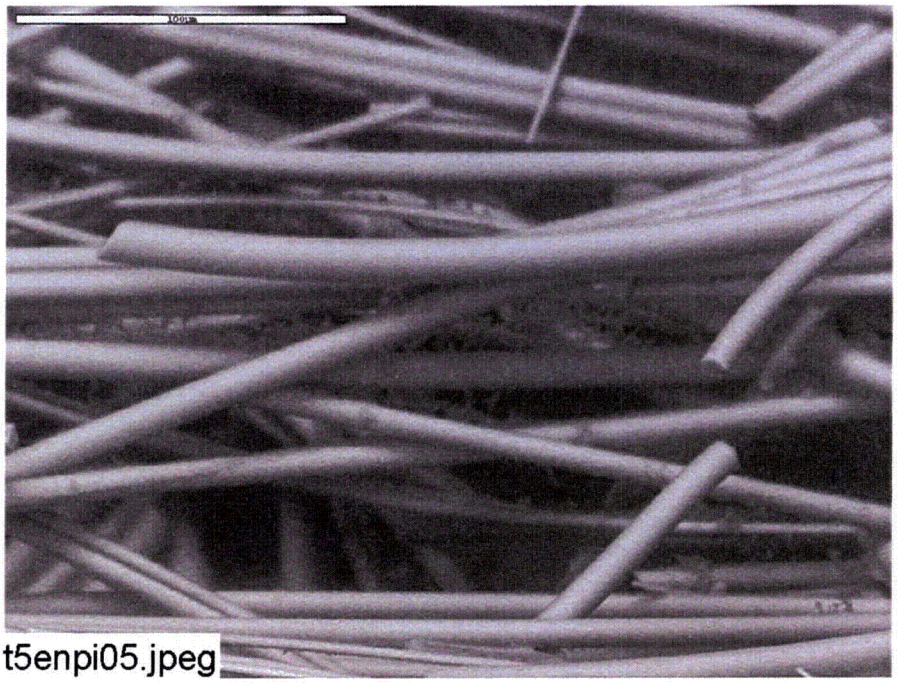


**Figure 3-41. ESEM image magnified 500 times for a Test #5, Day-30 low-flow interior fiberglass sample in a big envelope.**

### 3.3.1.6. Day-30 High-Flow Fiberglass Samples

Compared with the Day-30 low-flow fiberglass samples, no significant amount of particulate deposits was found on high-flow exterior samples. In addition, consistent with the findings for other fiberglass interior samples, no particulate deposits were found on the interior. However, similar flocculent deposits were found on both the fiberglass exterior and interior. Figures 3-42 through 3-45 show the Day-30 high-flow fiberglass results.

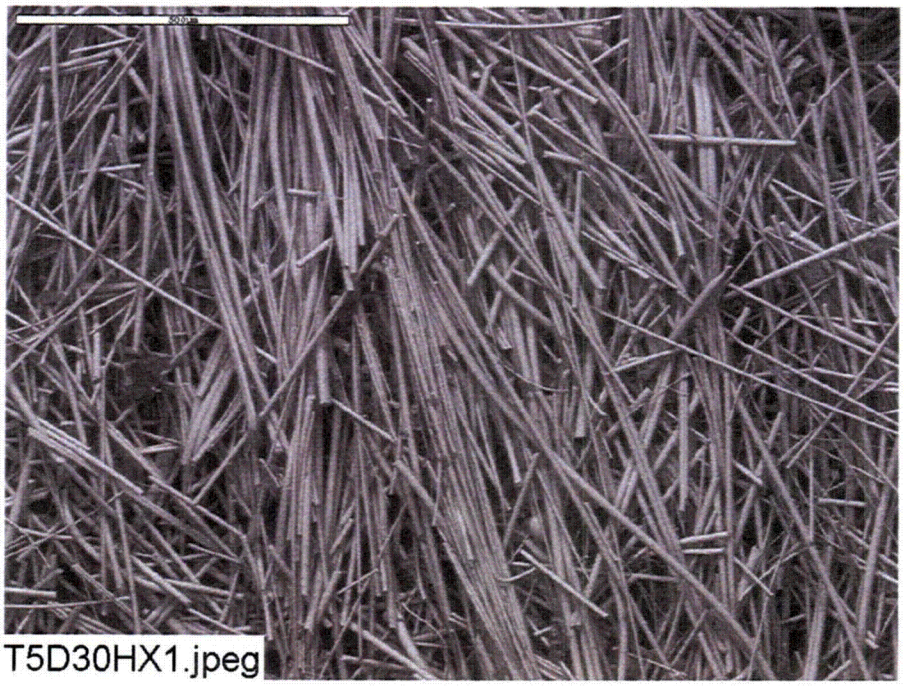


**Figure 3-42. ESEM image magnified 100 times for a Test #5, Day-30 high-flow exterior fiberglass sample.**

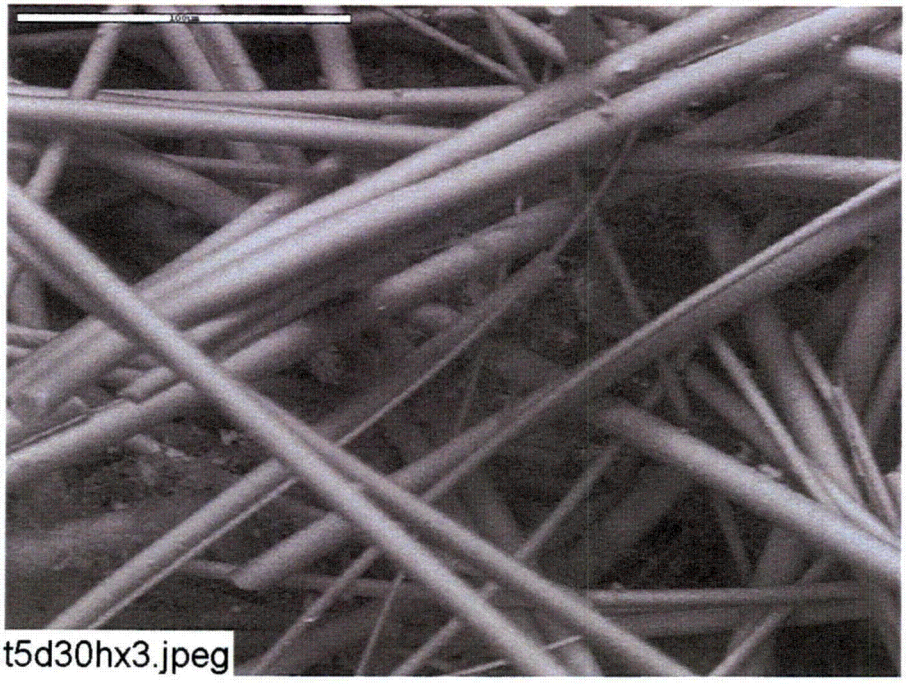


**Figure 3-43. ESEM image magnified 500 times for a Test #5, Day-30 high-flow exterior fiberglass sample.**


**Figure 3-44. ESEM image magnified 100 times for a Test #5, Day-30 high-flow interior fiberglass sample.**

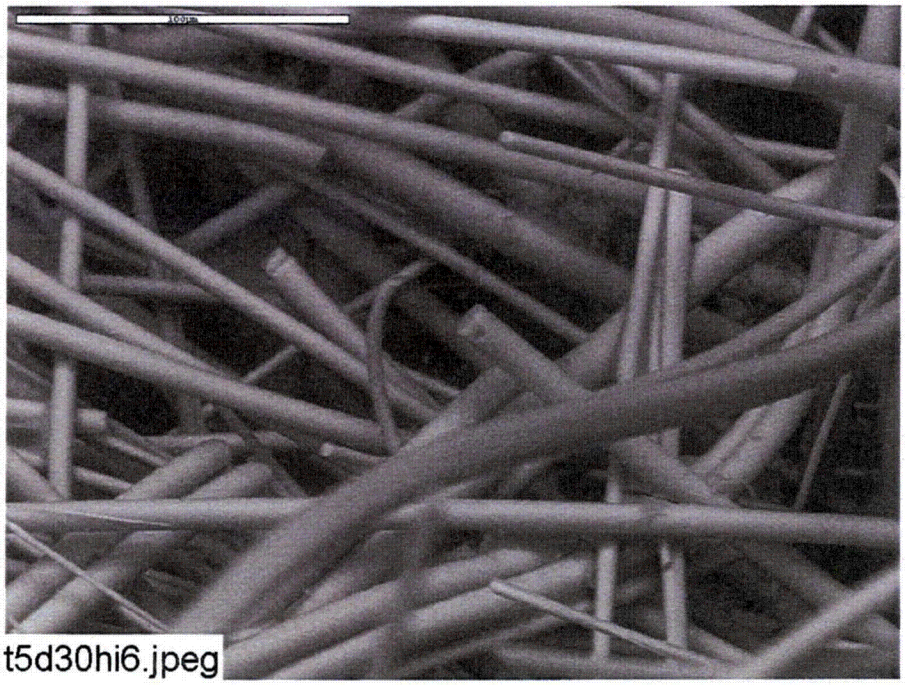


**Figure 3-45. ESEM image magnified 500 times for a Test #5, Day-30 high-flow interior fiberglass sample.**

### 3.3.1.7. Day-30 High-Flow Fiberglass Samples in Front of a Header

The fiberglass sample in front of a header was different from the conventional high-flow fiberglass samples discussed in Subsections 3.3.1.3 and 3.3.1.6; the header sample was put in the tank on Day 6. By placing the sample in the tank on Day 6, turbidity and TSS would be much less than on Day 0, and deposits on the sample would be from the tank solution over the last 3 weeks of the test. Due to the settling of suspended particles and the decrease in turbidity during the first several days of the test, no significant particulate deposits were found on the header fiberglass exterior, as shown by ESEM images. However, flocculent deposits were found on both the exterior and the interior of the header samples. This result suggests again that the flocculent deposits were likely caused by chemical precipitation and may have formed when the samples were partially dehydrated. Figures 3-46 through 3-49 show the results from the Day-30 high-flow fiberglass in front of a header.

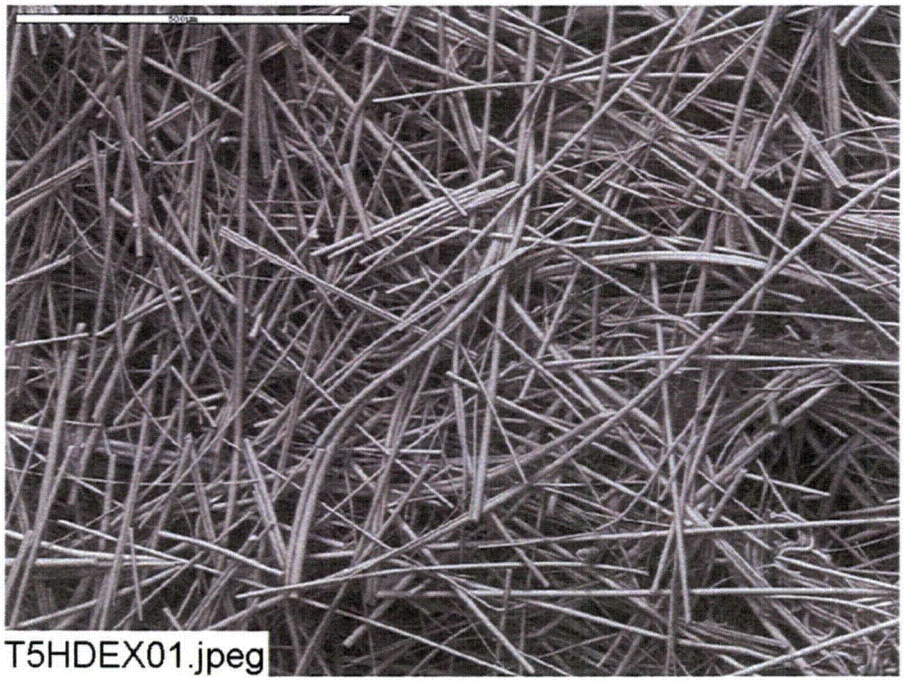


**Figure 3-46. ESEM image magnified 100 times for a Test #5, Day-30 high-flow exterior fiberglass sample in front of the header.**

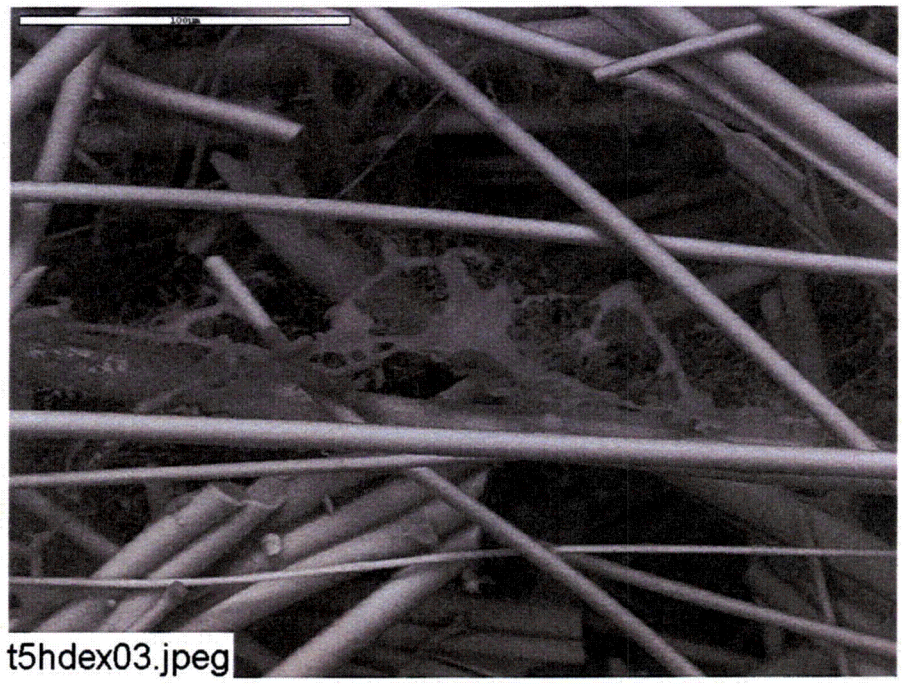


**Figure 3-47. ESEM image magnified 500 times for a Test #5, Day-30 high-flow exterior fiberglass sample in front of the header.**

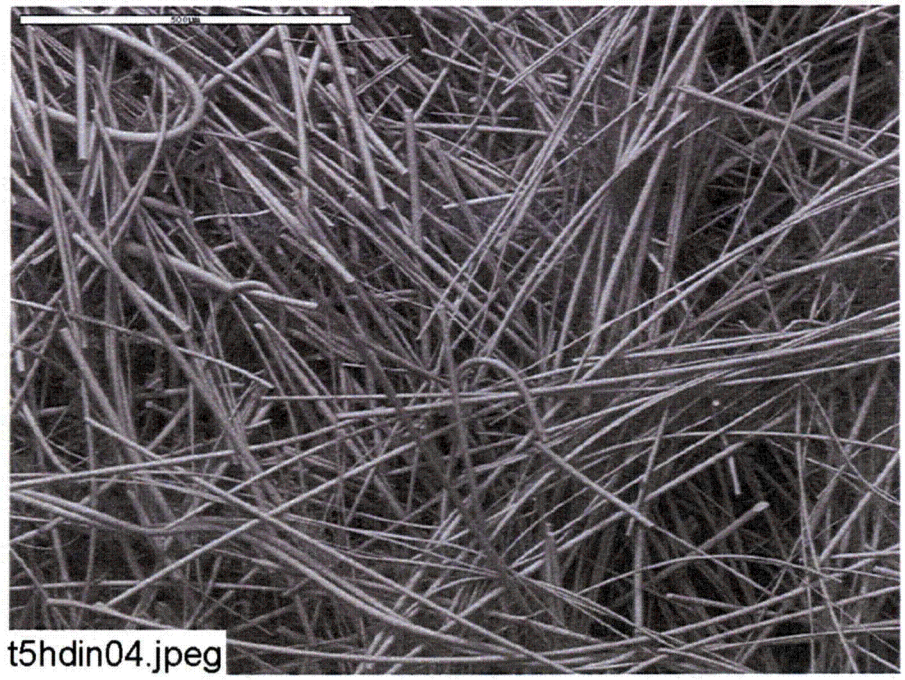


**Figure 3-48. ESEM image magnified 100 times for a Test #5, Day-30 high-flow interior fiberglass sample in front of the header.**

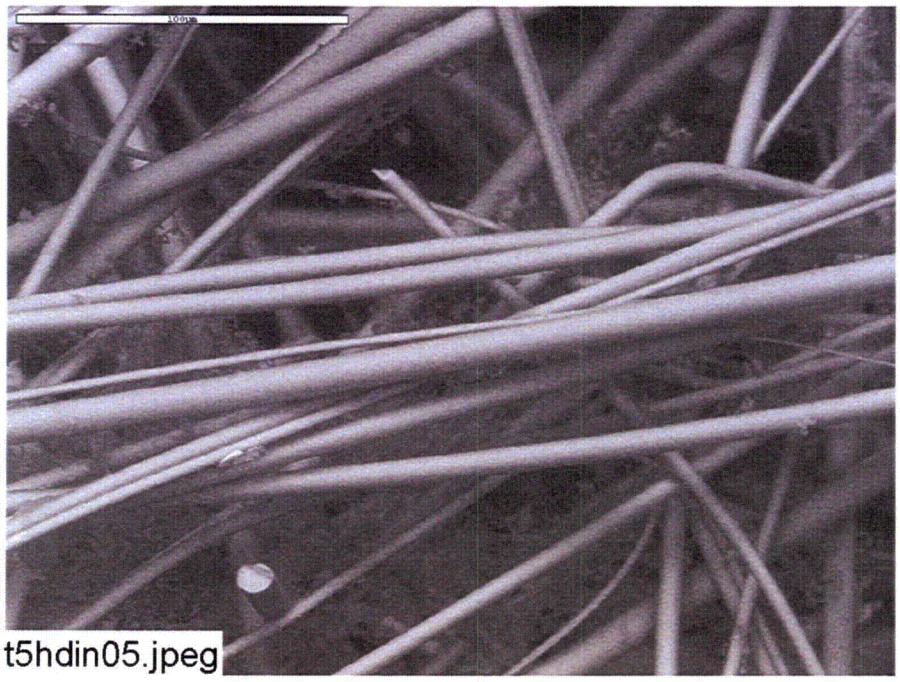


**Figure 3-49. ESEM image magnified 500 times for a Test #5, Day-30 high-flow interior fiberglass sample in front of the header.**

### 3.3.1.8. Day-30 Low-Flow Fiberglass Samples in Nylon Mesh

A 5-g fiberglass sample was enclosed in nylon mesh and submerged in a low-flow zone of the tank on Day 6. This sample provided a comparison with all other fiberglass samples, which were enclosed in stainless steel mesh. The purpose of using a nylon mesh was to see if the mesh material (i.e., stainless steel or nylon) affects the deposits on the fiberglass samples. Comparing the sample in nylon mesh with Day-30 low-flow fiberglass samples contained in stainless steel mesh revealed no significant difference. Flocculent deposits were still the dominant deposit on both the exterior and interior samples. No particulate deposits were found on fiberglass. This result suggests that the mesh material did not significantly affect the deposits on fiberglass. Even though the nylon mesh sample was put in the tank on Day 6, no significant difference was observed between these samples and the low-flow fiberglass samples in the stainless steel mesh put into the tank on Day 0. This result is likely due to the low turbidity and low debris concentration in the test solution. Figures 3-50 through 3-54 show the Day-30 low-flow fiberglass in nylon mesh results.

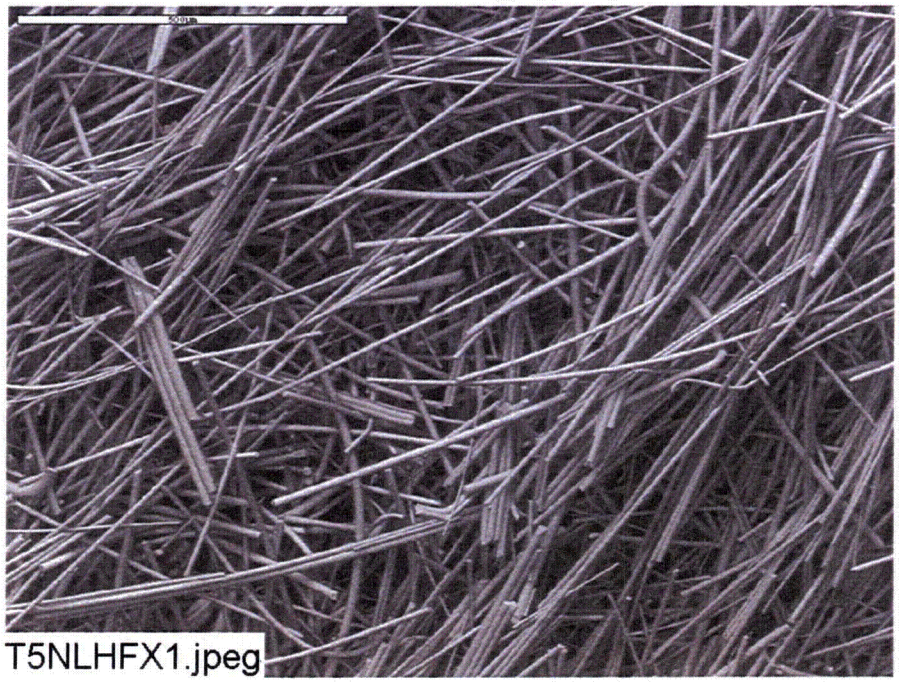


**Figure 3-50. ESEM image magnified 100 times for a Test #5, Day-30 low-flow exterior fiberglass sample in a nylon mesh.**

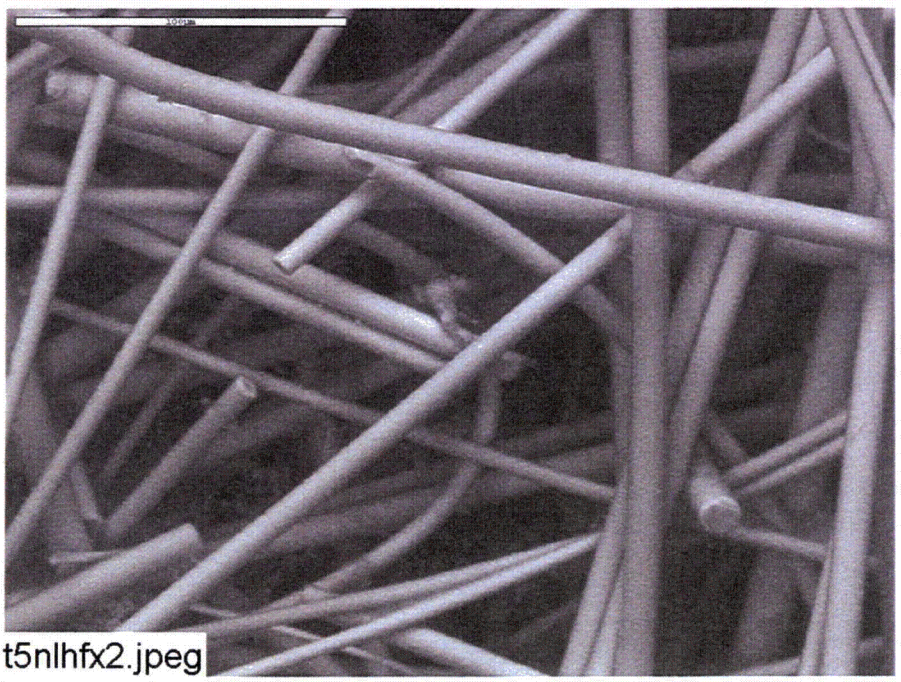


**Figure 3-51. ESEM image magnified 500 times for a Test #5, Day-30 low-flow exterior fiberglass sample in a nylon mesh.**


**Figure 3-52. ESEM image magnified 100 times for a Test #5, Day-30 low-flow interior fiberglass sample in a nylon mesh.**

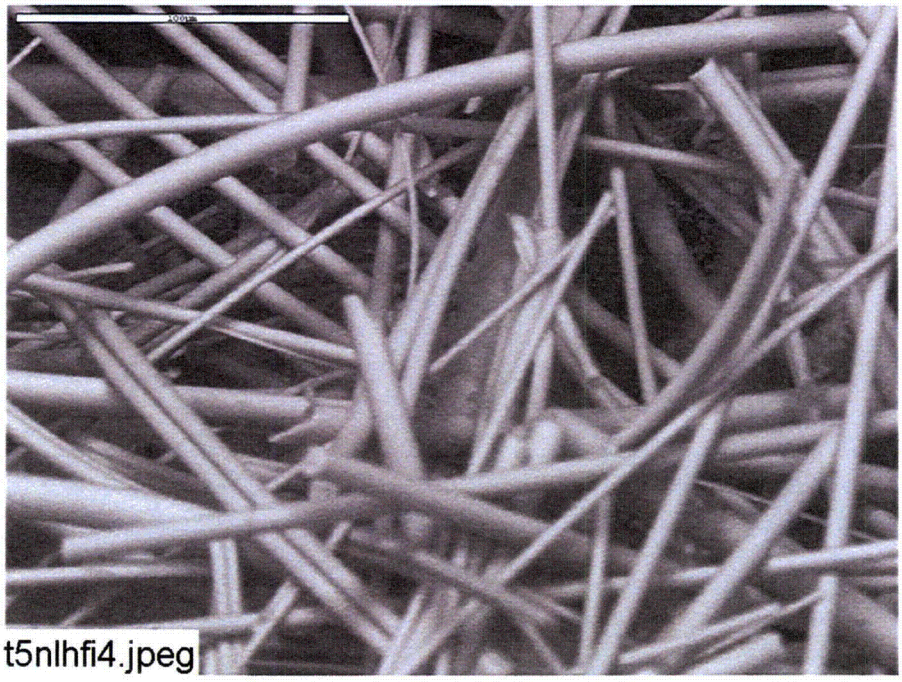


**Figure 3-53. ESEM image magnified 500 times for a Test #5, Day-30 low-flow interior fiberglass sample in a nylon mesh.**

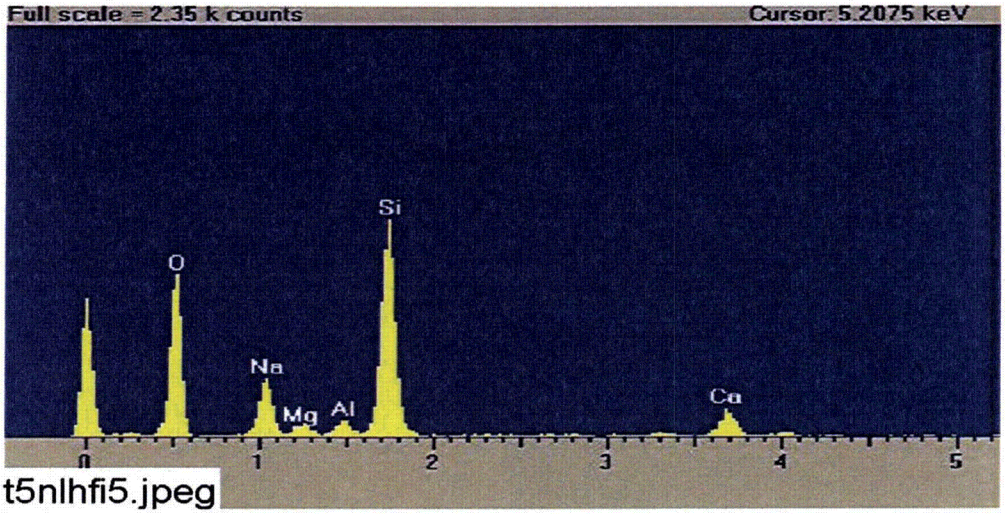


**Figure 3-54. EDS counting spectrum for the deposits between the fibers shown in Figure 3-53.**

### 3.3.1.9. Day-30 Drain Collar Fiberglass Samples

Figure 3-94 shows the drain collar after it was removed from the tank. Both the exterior fiberglass sample that was farthest from the drain screen and the exterior sample that was next to the drain screen have significant amounts of particulate deposits. The amount of deposits on the drain collar exterior was much greater than on the high- and low-flow fiberglass samples. However, the exterior farthest from the drain screen had the most particulate deposits. ESEM results show that the development of a continuous coating on the drain collar exterior farthest from the drain screen, which includes particulate deposits that were likely physically retained or attached. EDS results indicate that the particulate deposits were composed mainly of O, Al, Na, Ca, Mg, C, and possibly Si, for both the drain collar exterior farthest from the drain screen and the exterior next to the drain screen. In addition to the particulate deposits, deposits rich in carbon were also found on the exterior farthest from the drain screen (see Figure 3-57). In contrast to the exterior, no significant particulate deposits were found in the drain collar interior sample, and only flocculent deposits were found (see image Figure 3-64). The drain collar interior is as clean as other high- or low-flow fiberglass interior samples. This result suggests that almost all of the particulate deposits were physically retained at the fiberglass exterior. Figures 3-55 through 3-64 show the drain collar fiberglass results.


**Figure 3-55. ESEM image magnified 100 times for a Test #5, Day-30 exterior drain collar fiberglass sample farthest from the drain screen.**


**Figure 3-56. ESEM image magnified 100 times for a Test #5, Day-30 exterior drain collar fiberglass sample farthest from the drain screen.**

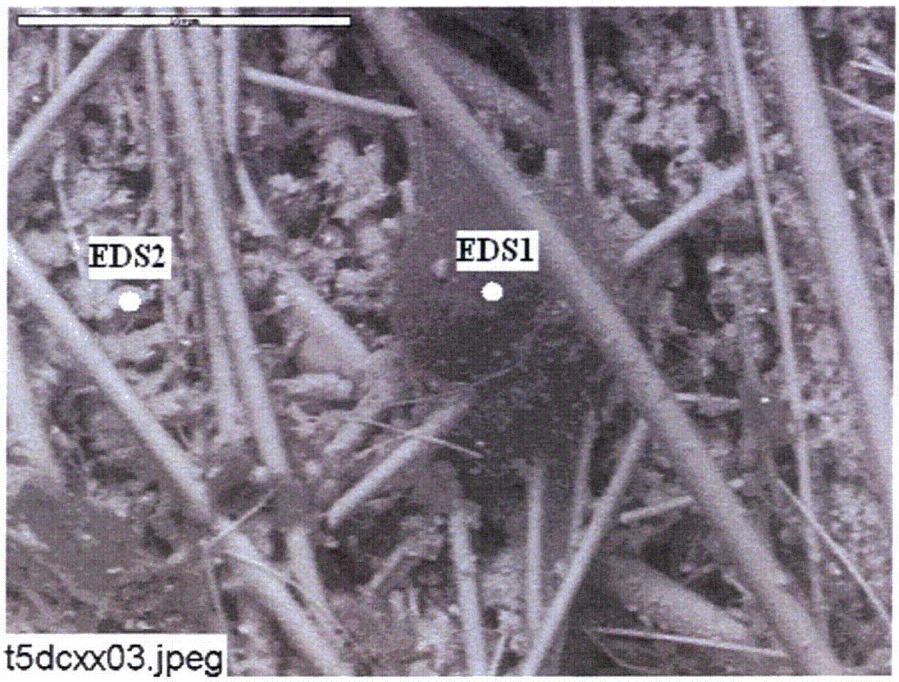


**Figure 3-57. Annotated ESEM image magnified 500 times for a Test #5, Day-30 exterior drain collar fiberglass sample farthest from the drain screen.**

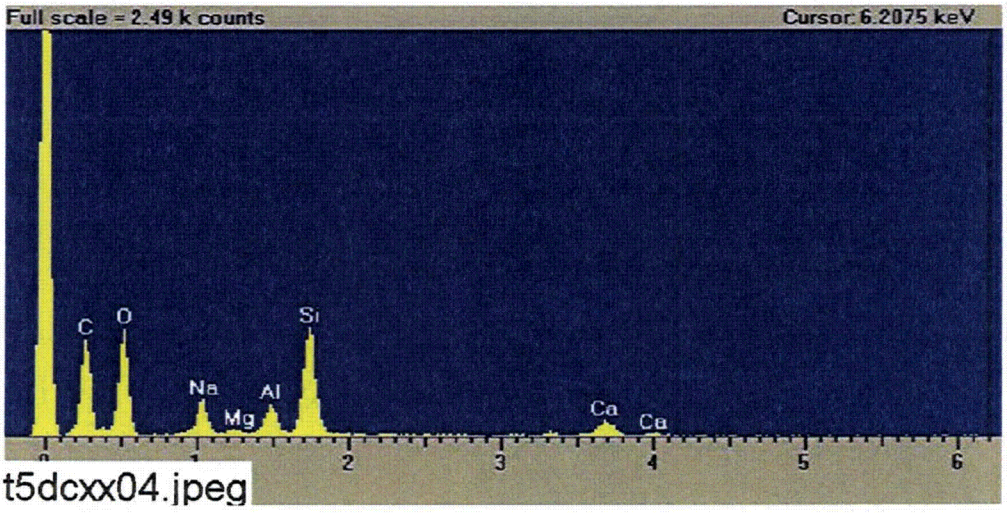


**Figure 3-58. EDS counting spectrum for the large mass of particulate deposits (EDS1) on fiberglass shown in Figure 3-57.**

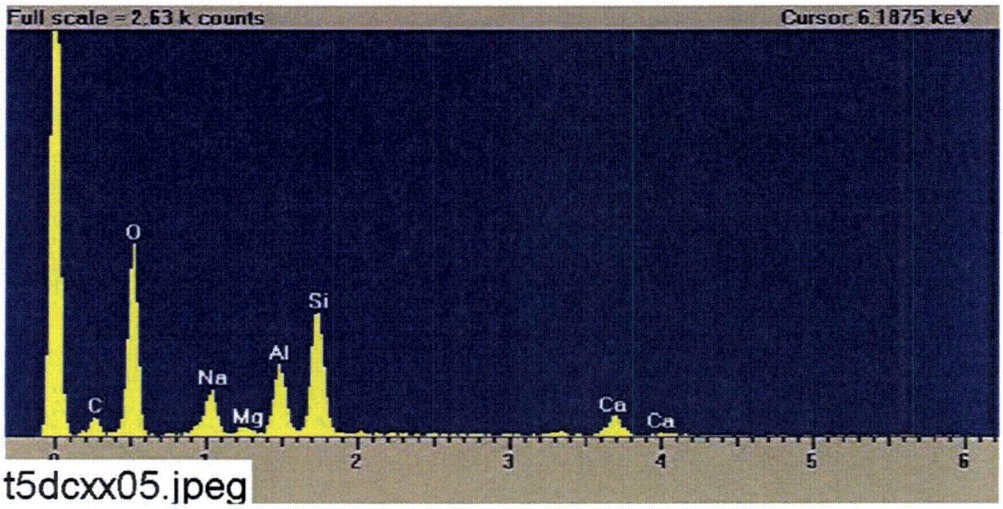


**Figure 3-59. EDS counting spectrum for the small particulate deposits (EDS2) between fibers shown in Figure 3-57.**

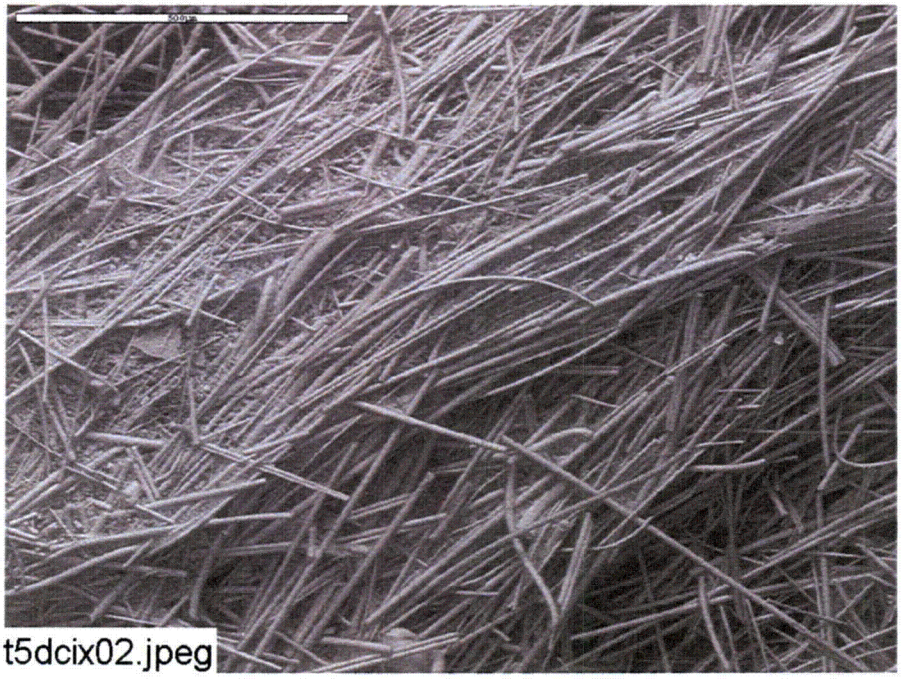


**Figure 3-60. ESEM image magnified 100 times for a Test #5, Day-30 exterior drain collar fiberglass sample next to the drain screen.**

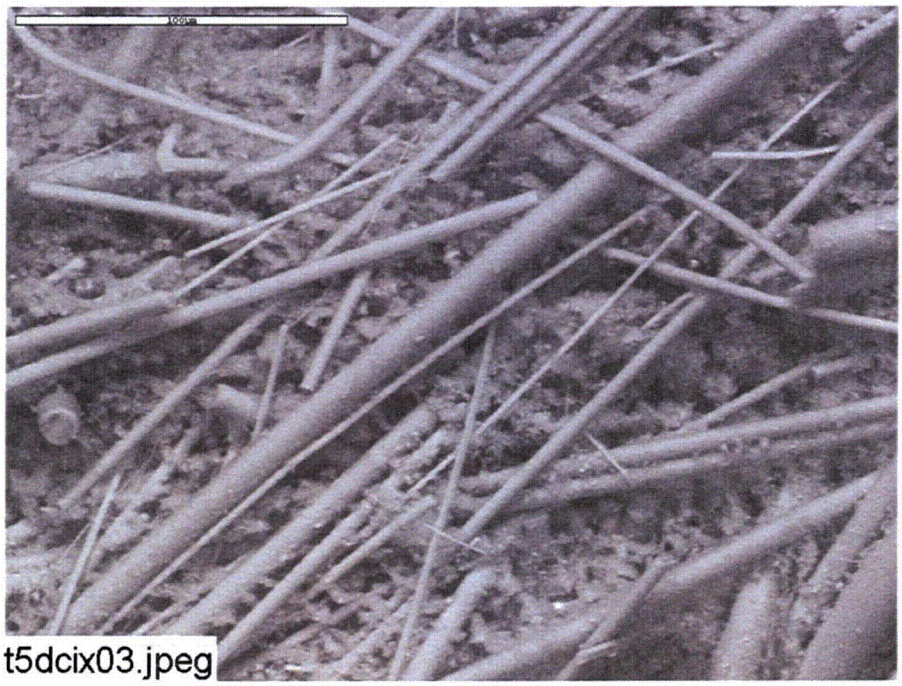


**Figure 3-61. ESEM image magnified 500 times for a Test #5, Day-30 exterior drain collar fiberglass sample next to the drain screen.**

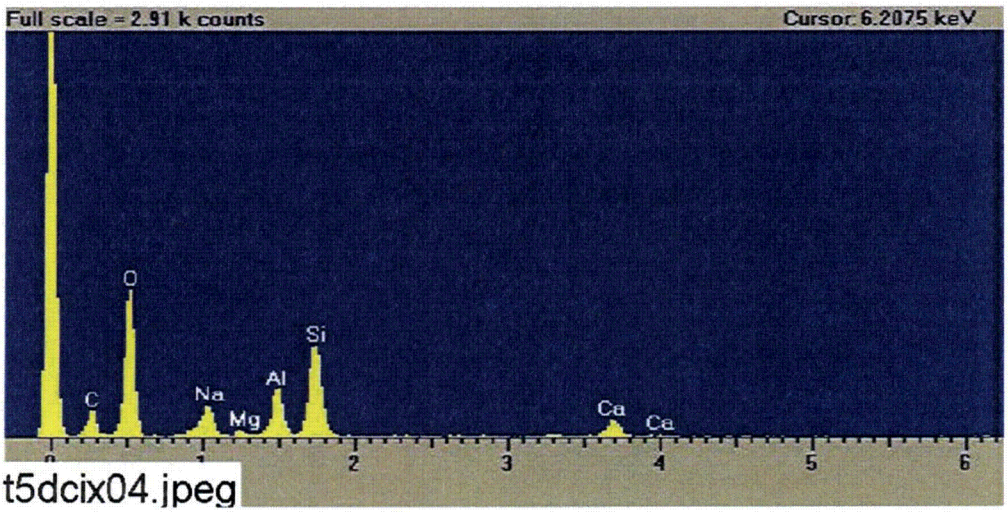


**Figure 3-62. EDS counting spectrum for the particulate deposits between fibers in Figure 3-61.**

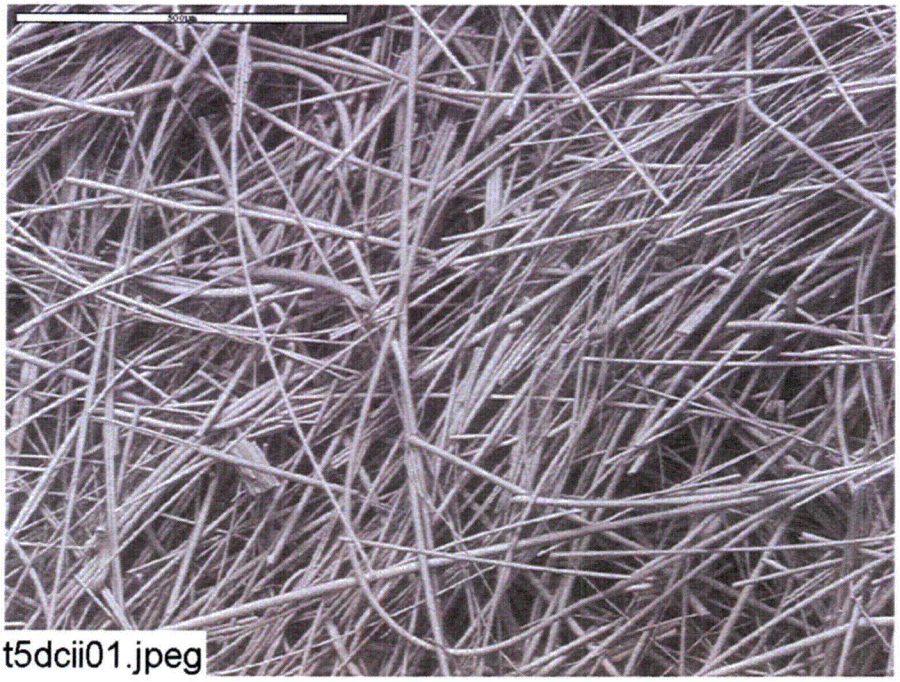


**Figure 3-63. ESEM image magnified 100 times for a Test #5, Day-30 interior drain collar fiberglass sample.**

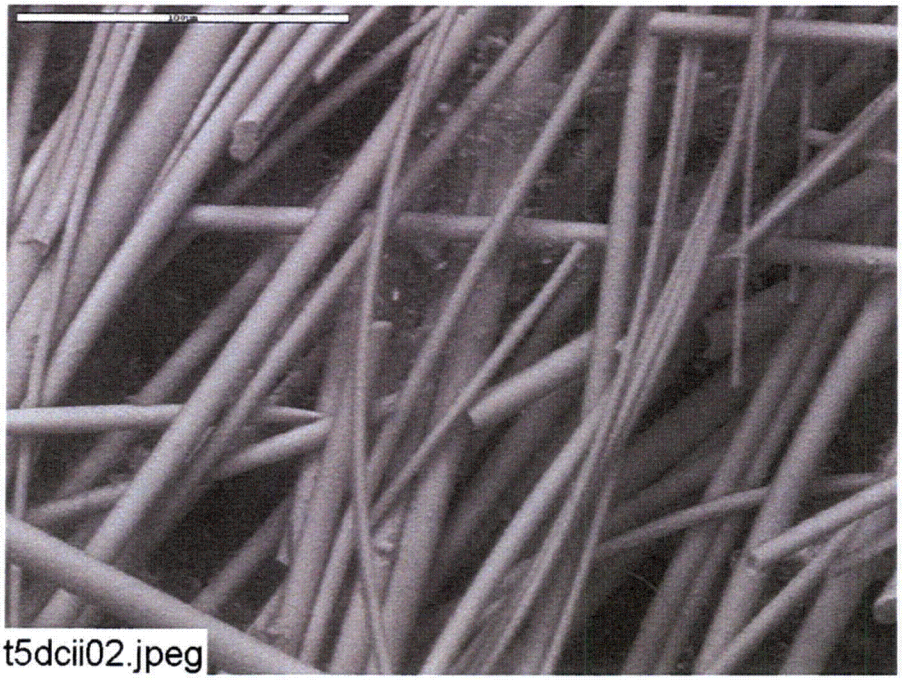


**Figure 3-64. ESEM image magnified 500 times for a Test #5, Day-30 interior drain collar fiberglass sample.**

### 3.3.1.10. Day-30 Fiberglass Sample within the Birdcage

For the Day-30 fiberglass sample within the birdcage, the SEM images indicate that a small amount of particulate deposit (see Figure 3-65) was on the exterior of the fiberglass. The amount of particulate deposits was slightly greater than on high- and low-flow fiberglass samples but much less than on the drain collar exterior. The EDS result shows that the particulate deposits were composed of O, Na, Ca, Zn, Al, Mg, and possibly Si. The presence of Zn is inconsistent with the drain collar exterior. Compared with other fiberglass interior samples, the interior birdcage sample was relatively clean. Only flocculent deposits were found. These flocculent deposits were similar to those observed on the high- and low-flow fiberglass samples, which was likely caused by chemical precipitation during the drying process. Again, this result suggests that almost all of the particulate deposits were physically retained at the fiberglass exterior, consistent with findings for the Day-30 high-flow and drain collar fiberglass samples. Figures 3-65 through 3-70 show the birdcage fiberglass results.

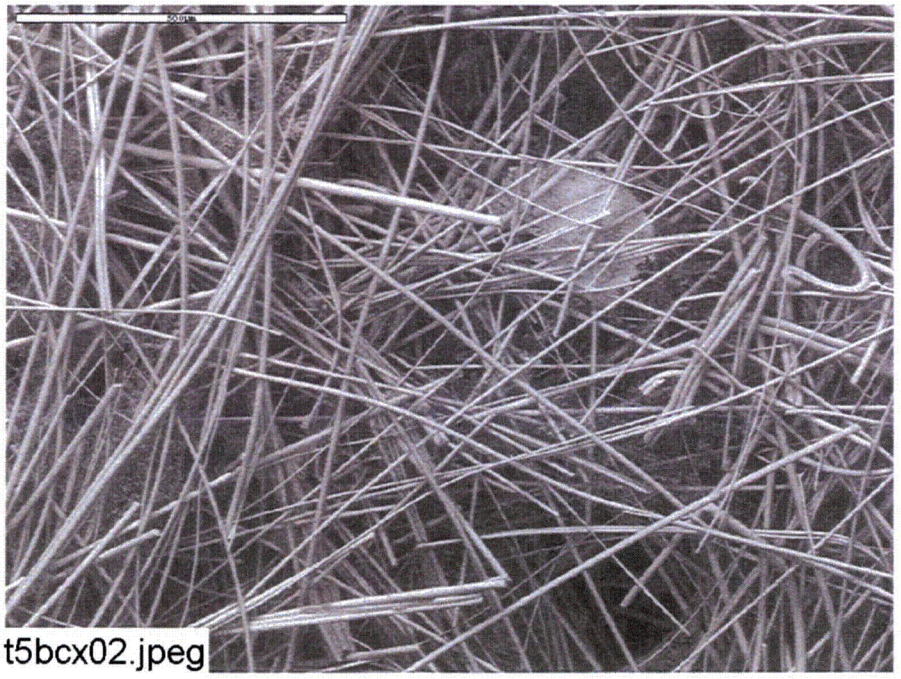


**Figure 3-65. ESEM image magnified 100 times for a Test #5, Day-30 exterior fiberglass sample in the bird cage.**

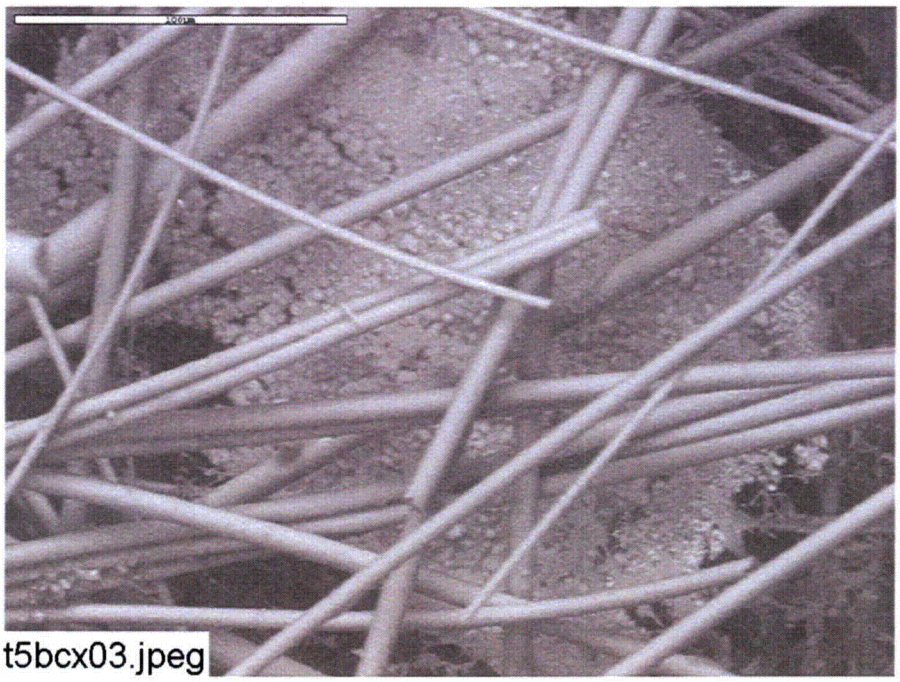


**Figure 3-66. ESEM image magnified 500 times for a Test #5, Day-30 exterior fiberglass sample in the birdcage.**

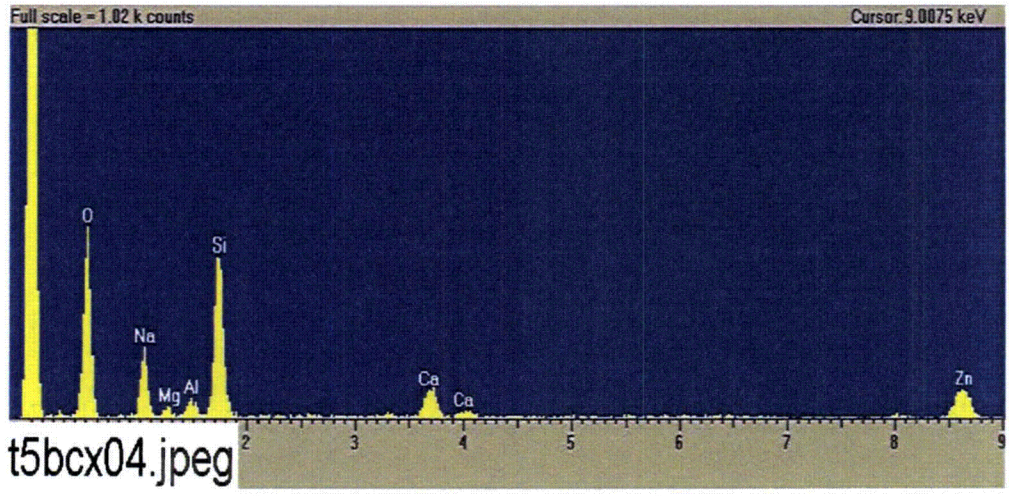


**Figure 3-67. EDS counting spectrum for the deposits between fibers shown in Figure 3-66.**

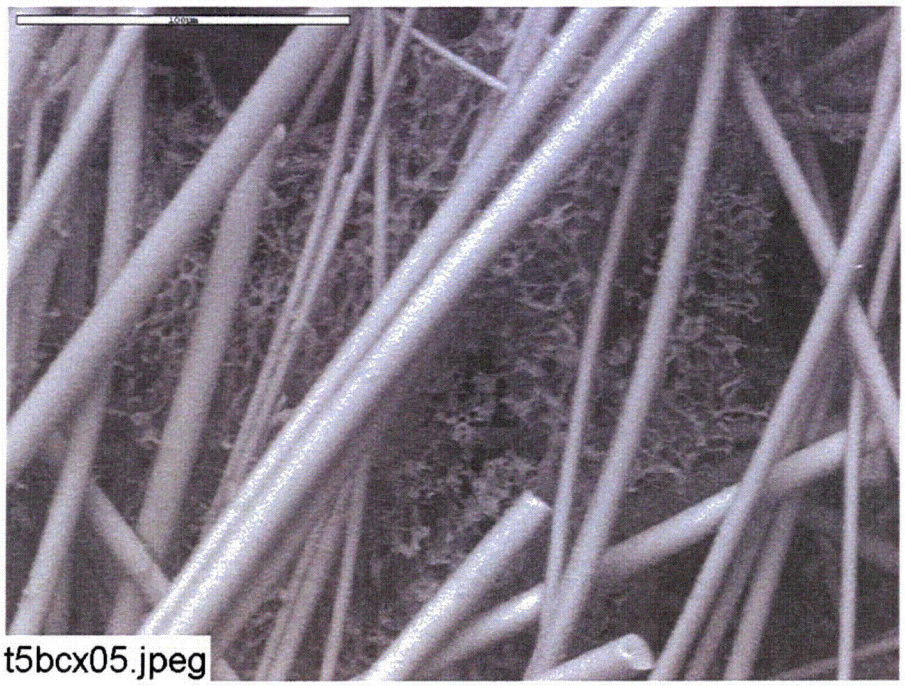


**Figure 3-68. ESEM image magnified 500 times for a Test #5, Day-30 exterior fiberglass sample in the birdcage.**

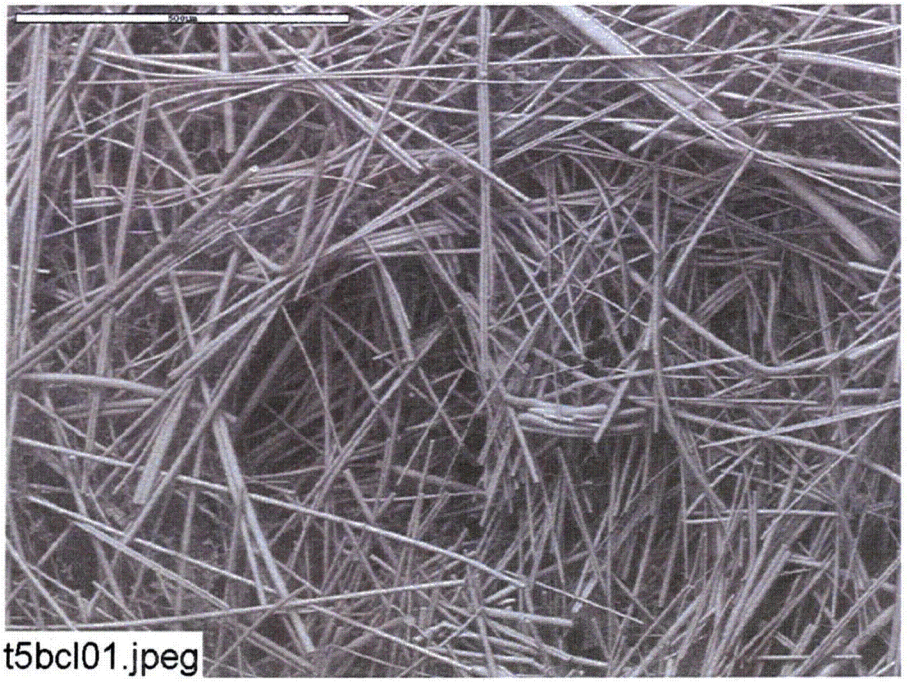


**Figure 3-69. ESEM image magnified 100 times for a Test #5, Day-30 interior fiberglass sample in the birdcage.**

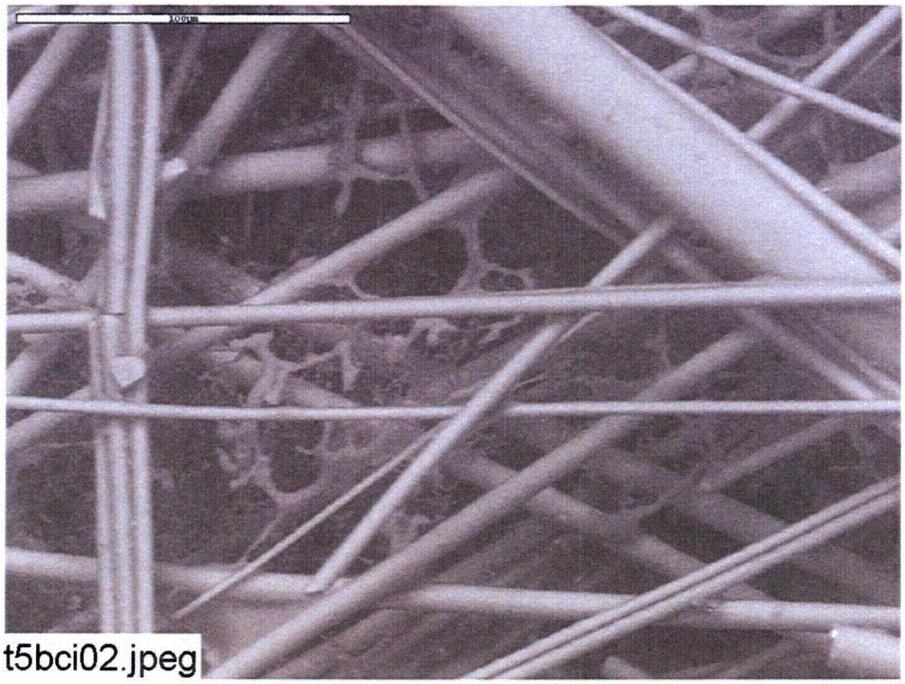


**Figure 3-70. ESEM image magnified 500 times for a Test #5, Day-30 interior fiberglass sample in the birdcage.**

## 3.4. Metallic and Concrete Coupons

### 3.4.1. Weights and Visual Descriptions

#### 3.4.1.1. Submerged Coupons

Examination of the 40 submerged coupons provides insights into the nature of the chemical kinetics that occurred during this 30-day test. The physical change that these coupons experienced is determined through both visual evidence and weight measurement of each coupon before and after the test. Pre-test pictures were taken of the coupons when they were received and before they were inserted into the racks. Post-test pictures were taken several days after the racks had been removed from the tank. All racks with coupons still inserted were staged to allow the coupons to dry completely before the post-test pictures were taken. The coupons were placed in a low-humidity room and allowed to air dry. All coupons were also weighed before they were inserted into the tank and after the 30-day test was completed.

There are three submerged aluminum coupons in each test. Figures 3-71 through 3-73 are the pre- and post-test pictures of the Test #5 coupons. The aluminum coupons A1-240, A1-241, and A1-242 (see Figures 3-71 through 3-73) were located from east to west, respectively, in the tank. The submerged aluminum coupons turned brown, and they developed a brown, powdery film on the surface. The film resulted in the surface of the coupon becoming rough to the touch.


**Figure 3-71. Al-240 submerged, pre-test (left) and post-test (right).**


**Figure 3-72. Al-241 submerged, pre-test (left) and post-test (right).**


**Figure 3-73. Al-242 submerged, pre-test (left) and post-test (right).**

Figures 3-74 through 3-76 present the pre- and post-test pictures of three submerged galvanized steel coupons. The galvanized steel coupons developed a white precipitate on the surface of the coupons, which caused the surfaces to have a coarse feel. The surfaces of the coupons had horizontal lines composed of this same white precipitate. The horizontal deposits may have been left during the slow draining of the tank solution.


**Figure 3-74. GS-137 submerged, pre-test (left) and post-test (right).**


**Figure 3-75. GS-140 submerged, pre-test (left) and post-test (right).**


**Figure 3-76. GS-141 submerged, pre-test (left) and post-test (right).**

Figures 3-77 and 3-78 present the pre- and post-test pictures of two submerged IOZ-coated steel coupons. Both submerged IOZ-coated steel coupons have similar light particulate deposits. These coupons were covered with a brown coating over their entire surfaces.


**Figure 3-77. IOZ-310 submerged, pre-test (left) and post-test (right).**


**Figure 3-78. IOZ-312 submerged, pre-test (left) and post-test (right).**

Figures 3-79 and 3-80 present the pre- and post-test pictures of two submerged copper coupons. The submerged copper coupons developed very light horizontal white deposits, which may be due to the slow tank draining process.

Figure 3-81 presents the pre- and post-test pictures of the submerged carbon steel coupon. The surface of the coupon was roughened by the deposition of white precipitate. There were also areas of rust on the coupon.

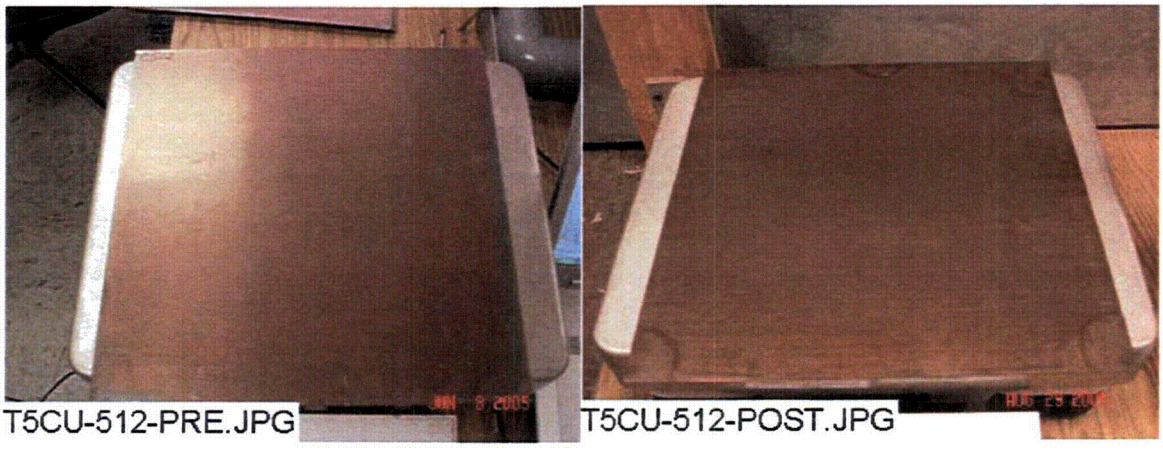


**Figure 3-79. CU-512 submerged, pre-test (left) and post-test (right).**

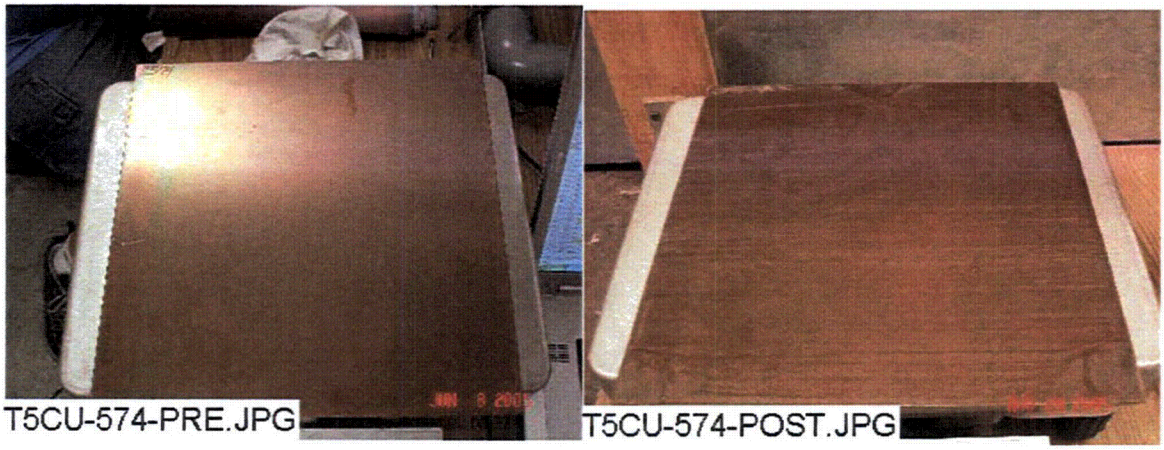


**Figure 3-80. CU-574 submerged, pre-test (left) and post-test (right).**


**Figure 3-81. US-14 submerged, pre-test (left) and post-test (right).**

Figure 3-82 presents the pre- and post-test pictures of the submerged concrete coupon. The post-test concrete coupon exhibits a brownish color.

Table 3-2 presents the pre- and post-test weight data for each representative submerged coupon.

The aluminum coupons' average weight differential was -11.2 g. The galvanized steel coupons' average weight gain was less than 0.1 g, and the coated steel coupons gained an average of 1.5 g. The representative copper coupons lost an average of 0.5 g, and the carbon steel coupon had no weight change. The concrete coupon gained 225.9 g, a gain of 3% of its original weight, which was likely due to post-test water retention.


**Figure 3-82. Conc-003 submerged, pre-test (left) and post-test (right).**

**Table 3-2. Weight Data for Submerged Coupons**

| Type | Coupon No. | Pre-Test Wt. (g) | Post-Test Wt. (g) | Net Gain/Loss |
|---|---|---|---|---|
| Al | 240 | 391.7 | 378.6 | -13.1 |
| Al | 241 | 391.7 | 379.6 | -12.1 |
| Al | 242 | 392.1 | 383.6 | -8.5 |
| GS | 137 | 1043.2 | 1043.1 | -0.1 |
| GS | 140 | 1067.5 | 1067.7 | 0.2 |
| GS | 141 | 1069.9 | 1070.0 | 0.1 |
| IOZ | 310 | 1652.9 | 1654.5 | 1.6 |
| IOZ | 312 | 1610.3 | 1611.6 | 1.3 |
| CU | 512 | 1322.6 | 1322.2 | -0.4 |
| CU | 574 | 1306.0 | 1305.4 | -0.6 |
| US | 14 | 1022.2 | 1022.2 | 0.0 |
| Conc | 003 | 7627.8 | 7853.7 | 225.9 |

### 3.4.1.2. Unsubmerged Coupons

Figures 3-83 and 3-84 show the pre- and post-test pictures of two unsubmerged aluminum coupons. Each unsubmerged aluminum coupon accumulated a white particle deposition along with some brownish areas. Also, the texture of each coupon is coarser, and the surface quality of each coupon is less lustrous than before the test. The reddish-brown color that was observed on the submerged coupons is absent on the unsubmerged coupons. The Al-247 coupon was loaded in Rack 2, which was located in the southern position of the middle tier of the tank. The Al-294 coupon was loaded in Rack 7, which was located in the northern position of the top tier of the tank.

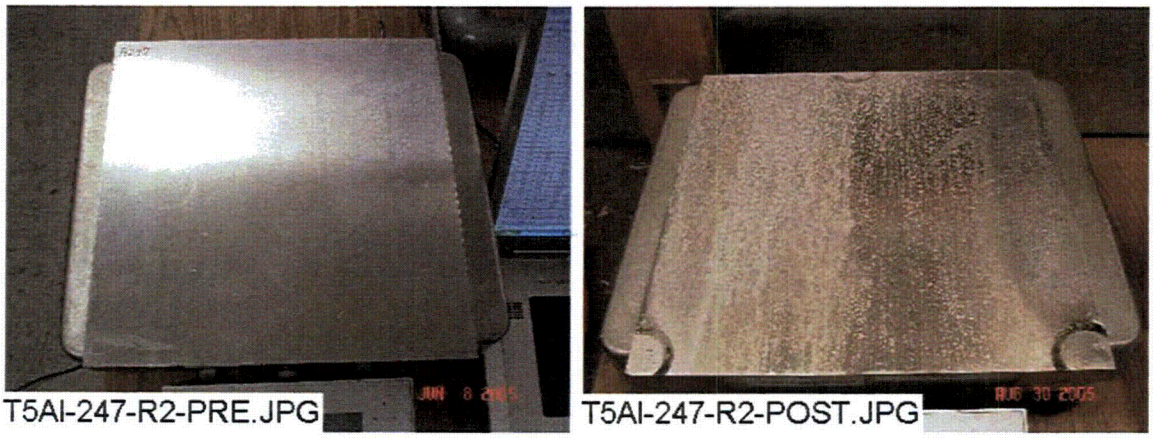


**Figure 3-83. Al-247 unsubmerged, pre-test (left) and post-test (right).**


**Figure 3-84. Al-294 unsubmerged, pre-test (left) and post-test (right).**

Figures 3-85 and 3-86 show the pre- and post-test pictures of two unsubmerged galvanized steel coupons. There was some white deposition on the surface of these coupons, although it was in small amounts. This deposition is visibly different and less concentrated than that of the submerged coupons. The GS-167 coupon was loaded in Rack 3, which was located in the center position of the middle tier of the tank. The GS-638 coupon was loaded in Rack 6, which was located in the middle position of the top tier of the tank.


**Figure 3-85. GS-167 unsubmerged, pre-test (left) and post-test (right).**

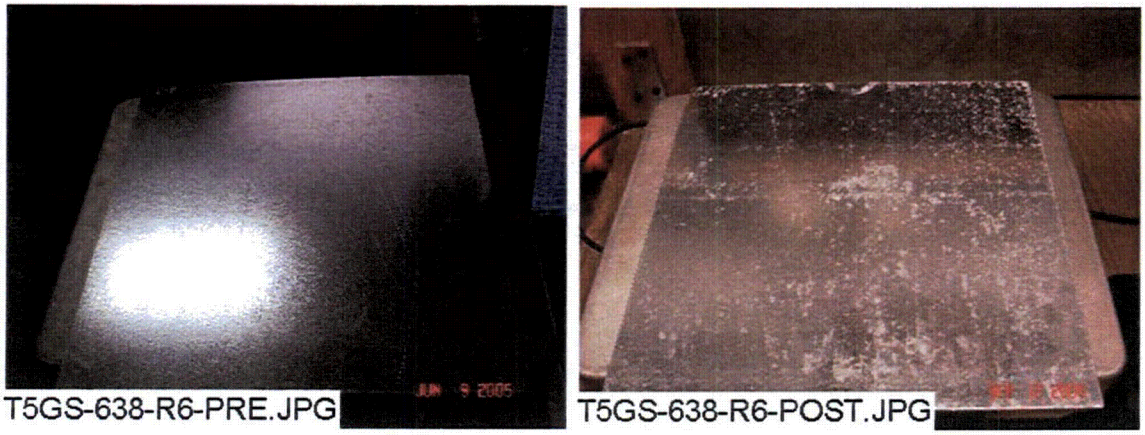


**Figure 3-86. GS-638 unsubmerged, pre-test (left) and post-test (right).**

Figures 3-87 and 3-88 present the pre- and post-test pictures of two unsubmerged copper coupons. All of the copper coupons had vertical water marks that were likely caused by water flowing downward on the coupon surface during the spray portion of the test. The copper coupons did not appear to accumulate any particle deposition. The CU-430 coupon was loaded in Rack 2, which was located in the southern position of the middle tier of the tank. The CU-587 coupon was loaded in Rack 7, which was located in the northern position of the top tier of the tank.

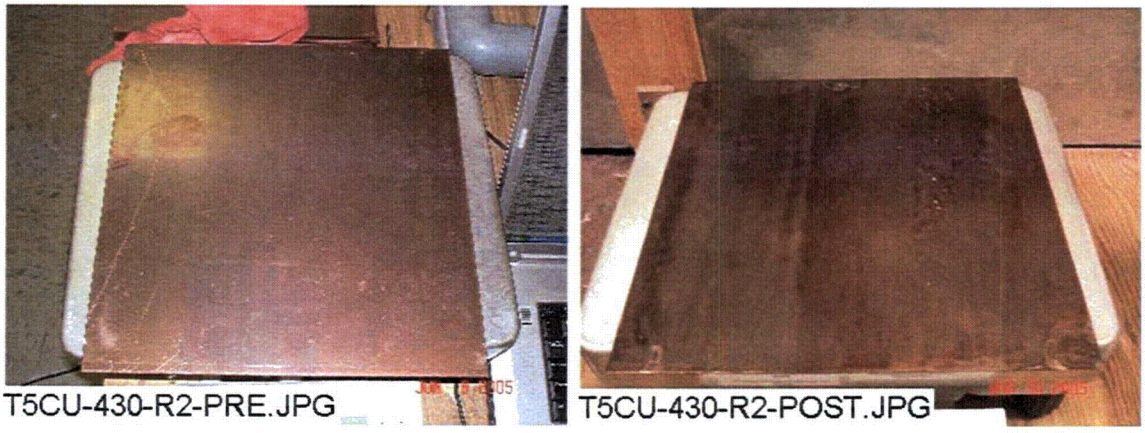


**Figure 3-87. CU-430 unsubmerged, pre-test (left) and post-test (right).**

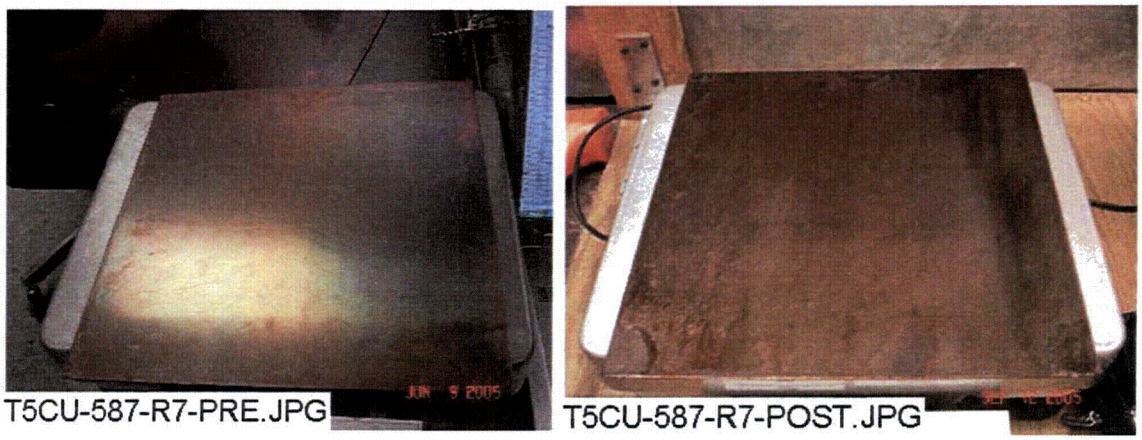


**Figure 3-88. CU-587 unsubmerged, pre-test (left) and post-test (right).**

Figures 3-89 and 3-90 present the pre- and post-test pictures of two unsubmerged IOZ-coated steel coupons. Each post-test coated steel coupon exhibits a similar pattern of deposition, which is less concentrated than that of the submerged coupons. The IOZ-342 coupon was loaded in Rack 4, which was located in the northern position of the middle tier of the tank. The IOZ-356 coupon was loaded in Rack 5, which was located in the southern position of the top tier of the tank.


**Figure 3-89. IOZ-342 unsubmerged, pre-test (left) and post-test (right).**


**Figure 3-90. IOZ-356 unsubmerged, pre-test (left) and post-test (right).**

Figure 3-91 presents the pre- and post-test pictures of one unsubmerged carbon steel coupon. The post-test carbon steel coupon exhibits rust along its center line and around its bottom edge. The deposition concentration is greater than that of the submerged carbon steel coupon. The US-18 coupon was loaded in Rack 6, which was located in the center position of the top tier of the tank.

Table 3-3 presents the pre- and post-test weight data for each representative unsubmerged coupon.

The aluminum coupons gained an average of 1.3 g, and the galvanized steel coupons lost an average of 0.2 g. The coated steel coupons' average weight gain was 1.6 g, and the copper coupons' average weight gain was 0.5 g. The carbon steel coupon lost 0.2 g.

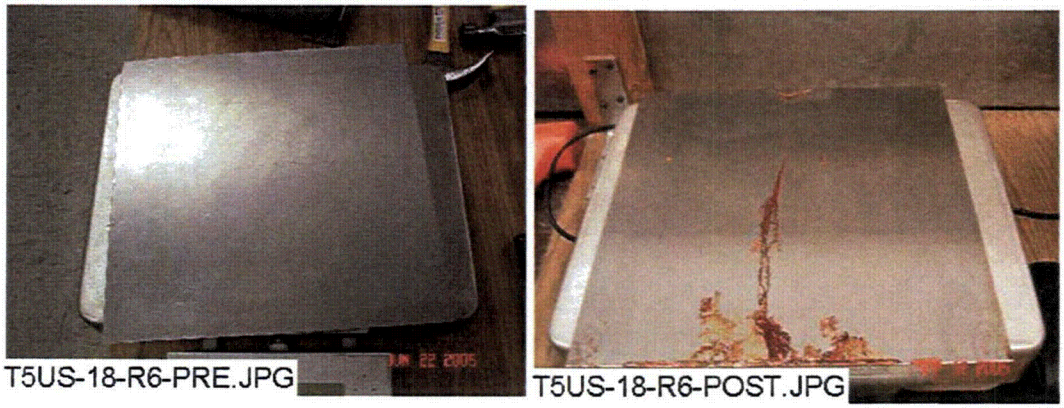


**Figure 3-91. US-18 unsubmerged, pre-test (left) and post-test (right).**

**Table 3-3. Weight Data for Unsubmerged Coupons**

| Type | Coupon No. | Pre-Test Wt. (g) | Post-Test Wt. (g) | Net Gain/Loss |
|---|---|---|---|---|
| Al | 247 | 390.2 | 391.6 | 1.4 |
| Al | 294 | 390.6 | 391.8 | 1.2 |
| GS | 167 | 1051.6 | 1051.5 | -0.1 |
| GS | 638 | 1067.5 | 1067.3 | -0.2 |
| IOZ | 342 | 1656.0 | 1658.3 | 2.3 |
| IOZ | 356 | 1621.5 | 1622.5 | 1.0 |
| CU | 430 | 1319.8 | 1320.6 | 0.8 |
| CU | 587 | 1328.0 | 1328.2 | 0.2 |
| US | 18 | 1032.1 | 1032.3 | 0.2 |

Table 3-4 displays the mean weight gain/loss summary in grams for all of the submerged coupons. Table 3-5 displays the mean weight gain/loss summary in grams for all of the unsubmerged coupons by rack.

**Table 3-4. Mean Gain/Loss Data for All Submerged Coupons (g)**

| Coupon Type | AL | GS | CU | IOZ | US | Concrete |
|---|---|---|---|---|---|---|
| Mean Gain - Loss (g) | -11.2 | 0.1 | -0.2 | 1.6 | 0.0 | 225.9 |

**Table 3-5. Mean Gain/Loss Data for All Unsubmerged Coupons (g)**

| | Mean Gain-Loss Per Coupon Type (g) | | | | |
|---|---|---|---|---|---|
| Rack No. | AL | GS | CU | IOZ | US |
| 2 | 0.8 | 0.6 | 0.4 | 1.4 | n/a |
| 3 | 0.1 | <0.1 | 0.1 | 0.2 | n/a |
| 4 | 0.4 | 0.1 | <0.1 | 1.1 | 0.2 |
| 5 | 0.9 | <0.1 | <0.1 | 1.1 | n/a |
| 6 | 0.4 | 0.1 | 0.1 | 1.5 | 0.2 |
| 7 | 1.2 | 0.3 | 0.2 | 1.8 | n/a |
| Overall | 0.4 | 0.2 | 0.2 | 1.2 | 0.2 |

### 3.4.2. SEM Analyses of Coupons

#### 3.4.2.1. Submerged Coupons

During the ICET tests, trace metal cations may be released from the submerged metal coupon surfaces due to corrosion effects. Subsequently, the released metal cations may form complexes in solution through electrostatic interactions with anions such as $OH^-$,

$B_4O_7^{2-}$, $H_2BO_3^-$, $SiO_3^{2-}$, and $CO_3^{2-}$. In addition, the complexed anions may attract other cations from the solution, such as $Ca^{2+}$, $Mg^{2+}$, $Al^{3+}$, $Cu^{2+}$, $Zn^{2+}$, and $H^+$. As a result, corrosion products (deposits) are formed and may continuously grow on the metal coupon surfaces. The thickness of the deposits was observed to be in the range of millimeters. The adherence between the metal coupons and the deposits is through chemical bonds, which are much stronger than van der Waals forces. Due to the vertical orientation of the metal coupons in the tank (with a small horizontal cross-sectional area), the deposits on the metal coupon surface are likely of chemical origin, rather than being the result of particulate deposits settling on the surface.

According to the SEM/EDS results, the dominant corrosion products on the submerged Al coupons are likely aluminum hydroxide with other substances containing Si, Ca, O, C, Fe, and Cu. For submerged Cu coupons, the possible corrosion products include CuO, $Cu_2(CO_3)(OH)_2$, and substances containing Cu, Ca, Si, Al, O, and C. For the submerged galvanized steel coupons, the possible corrosion products are oxides, hydroxides, silicate, and carbonate compounds of Zn, Ca, and Al. For the submerged steel coupon, the possible corrosion products include oxide, hydroxide, silicate, and carbonate compounds of Fe and Ca and compounds composed of Fe, Si, Ca, O, and Al.

#### 3.4.2.2. Unsubmerged Coupons

The physical and chemical changes that the unsubmerged coupons experienced during Test #5 are less significant than the changes experienced by the submerged coupons. The unsubmerged coupons were affected by the test solution only during the initial 4-hour spray phase. They were also exposed to moisture vapor throughout the test.

According to SEM/EDS results, the dominant corrosion products on the unsubmerged Al coupons are likely aluminum hydroxide and/or aluminum oxide. For unsubmerged Cu, the corrosion products on the coupon surface are likely CuO; $Cu_2(CO_3)(OH)_2$; and the corrosion products containing Al, Si, O, Ca, Cu, Na, Fe, and C. The corrosion products on the unsubmerged galvanized steel coupon surface are composed of C, O, and Zn. They are likely ZnO and $ZnCO_3$. For the unsubmerged steel coupon, the likely corrosion products are $Fe_2O_3$, $Fe(OH)_3$, $Fe_2(CO_3)_3$, and compounds containing small amounts of Si.

The complete listing of Day-30 coupon analysis is shown in Appendix E.

## 3.5. Sedimentation

Sediment was collected from the tank bottom after the test solution was drained. The entire amount recovered was 89 g, wet, as shown in Figure 3-92. Figure 3-93 shows the tank bottom with the sediment, after the test solution was drained and the samples were removed. Figure 3-94 shows the top of the drain screen with the drain collar still attached.

Figures 3-95 through 3-99 and Table 3-6 provide SEM/EDS and XRD/XRF analysis results. The SEM/EDS and XRD/XRF analyses provided information on the morphology and composition of Test #5 sediment. SEM images show that the sediments were mainly

composed of fiberglass debris, which mixed with some particulate deposits. Consistently, the XRF result shows that $SiO_2$ was about 64% of the total mass of the dried sediments. In addition, the XRD result indicates the presence of quartz crystal in the sediments. The quartz is likely from a crystalline form of fiberglass debris. The particulate deposits in the sediments possibly originated from the corrosion products, chemical precipitates, concrete debris, and dust.

It should be noted that the XRD result also shows the possible crystalline match of cobalt and uranium compounds in the sediments. However, cobalt and uranium were unlikely present in the testing material. Their match patterns are likely due to the variety of species contained within the sediment. As a result, these compounds may be excluded from the sediment compositions.

The complete Day-30 sediment analyses are given in Appendix F.

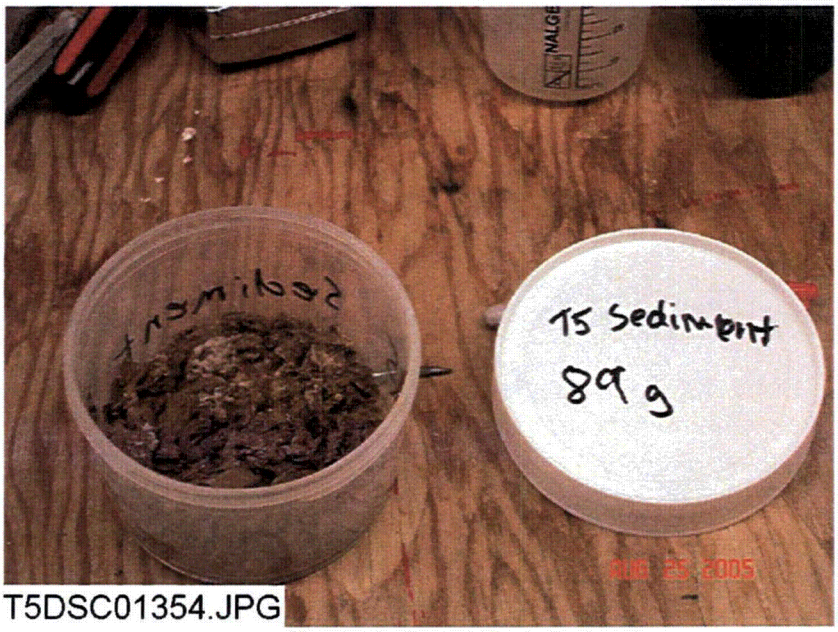


**Figure 3-92. Sediment removed from the tank.**


**Figure 3-93. Tank bottom after draining.**

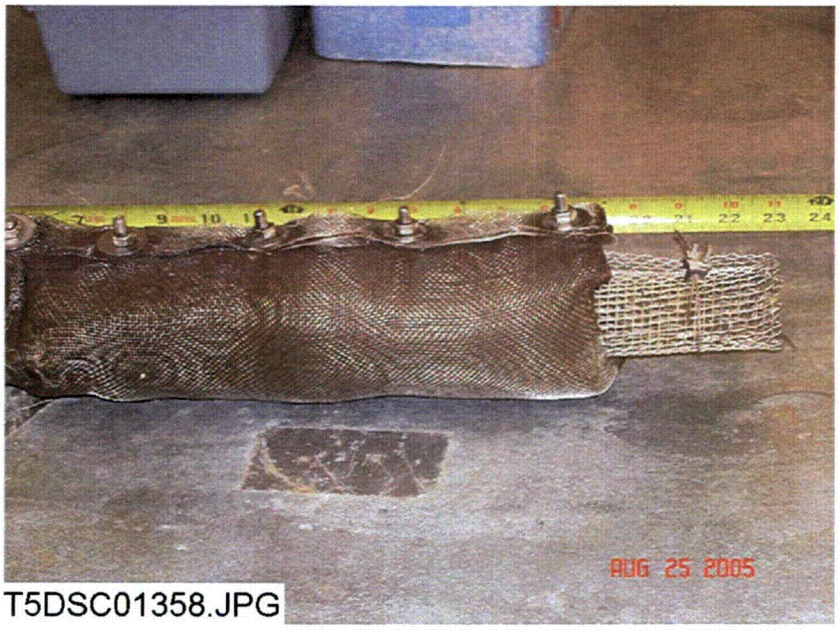


**Figure 3-94. Drain collar removed from the tank bottom.**

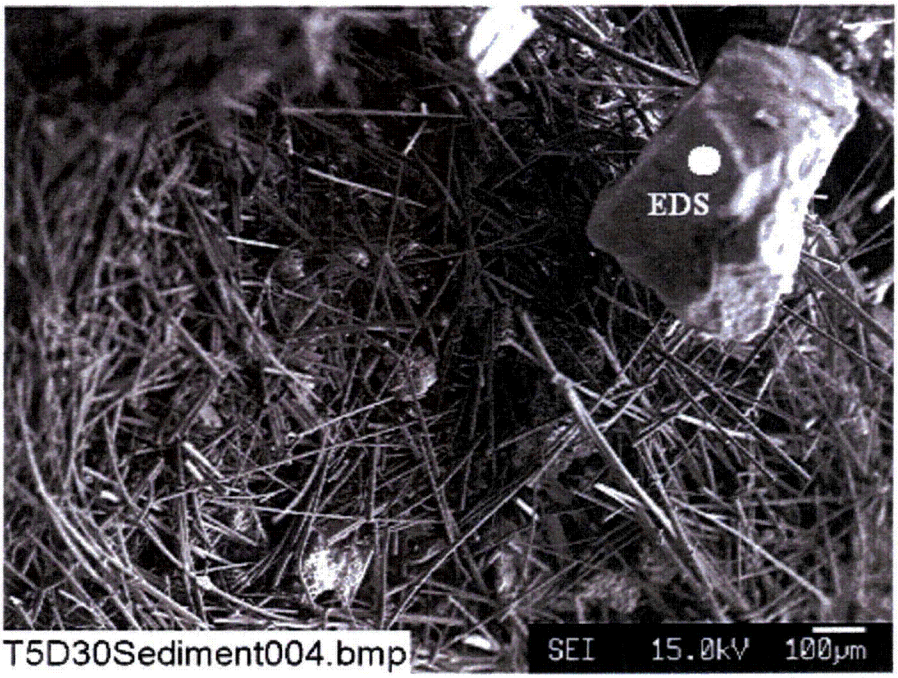


**Figure 3-95. SEM image magnified 70 times for the Test #5, Day-30 sediment at the bottom of the tank.**

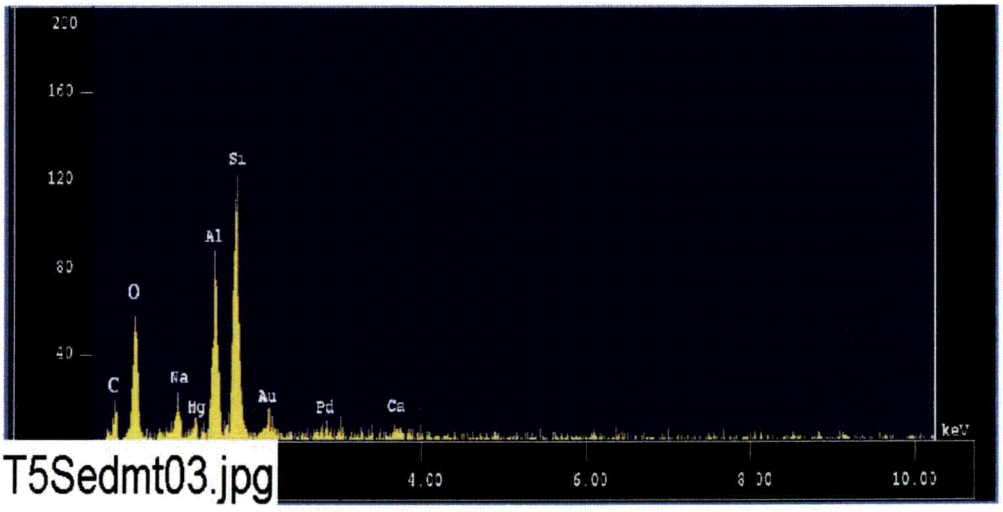


**Figure 3-96. EDS counting spectrum for the big particulate deposit shown in Figure 3-95.**

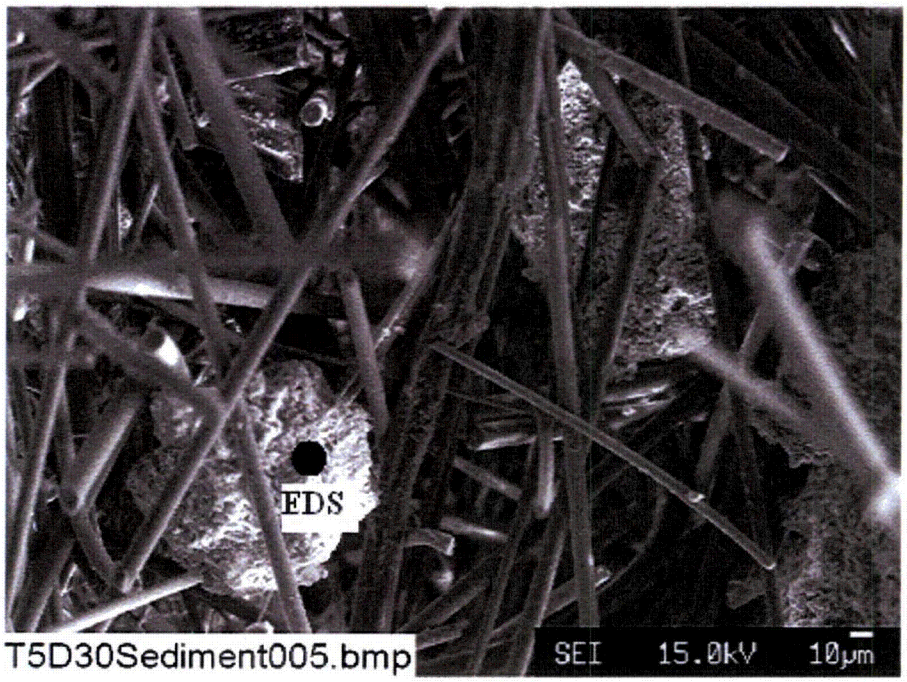


**Figure 3-97. SEM image magnified 300 times for the Test #5, Day-30 sediment at the bottom of the tank.**

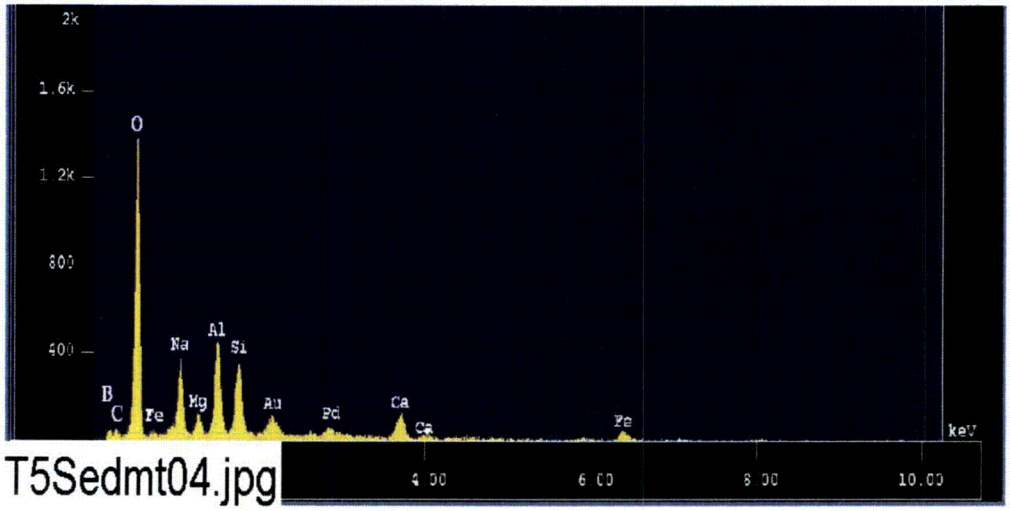


**Figure 3-98. EDS counting spectrum for the particulate deposit shown in Figure 3-97.**

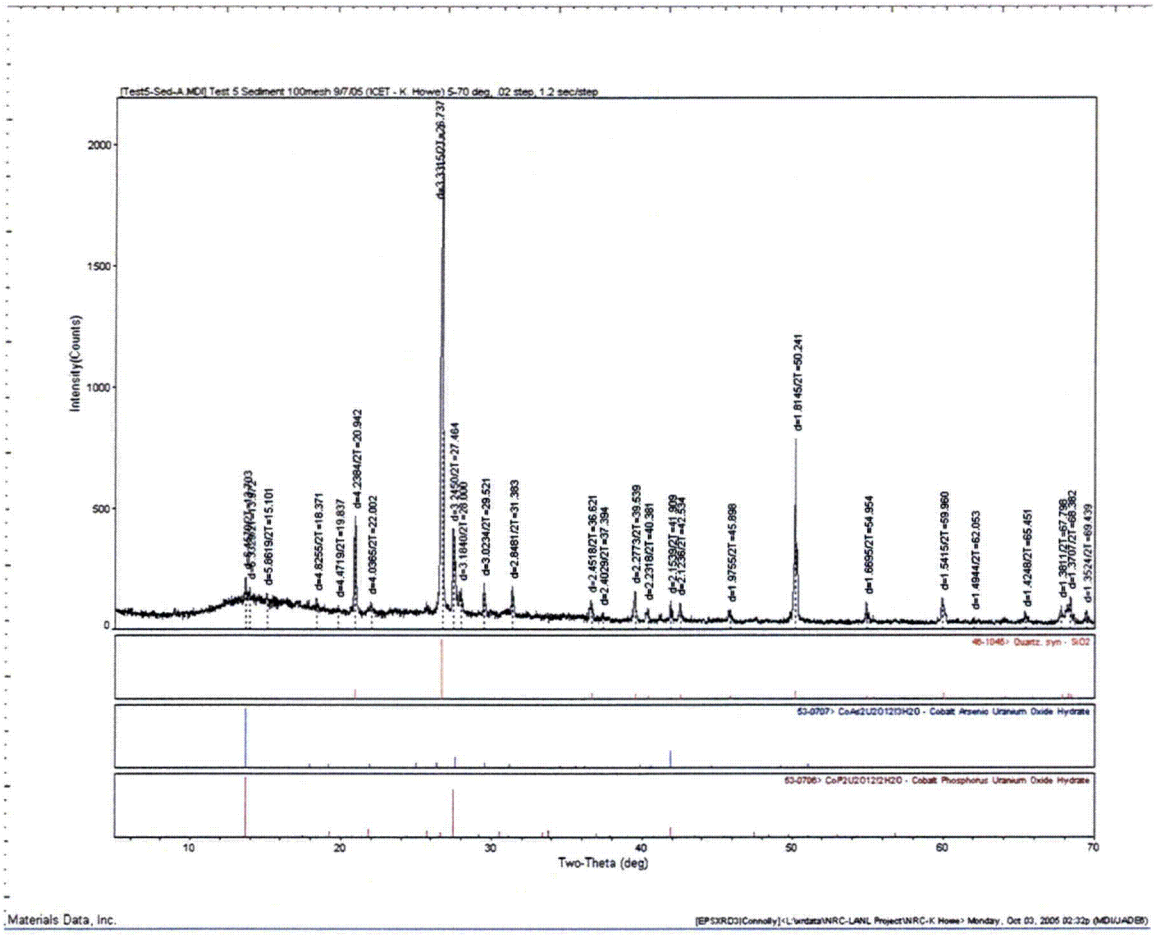


**Figure 3-99. XRD result of the possible matching crystalline substances in Test #5, Day-30 sediment.**

**Table 3-6. Dry Mass Composition of Test #5, Day-30 Sediment by XRF Analysis**

**First row is chemical component; second row is mass composition (%).**

| $SiO_2$ | $TiO_2$ | $Al_2O_3$ | $Fe_2O_3$ | FeO | MnO | MgO | CaO | $Na_2O$ | $K_2O$ | $H_20(-)$ | $H_2O(+)CO_2$ | $P_2O_5$ | Total |
|---|---|---|---|---|---|---|---|---|---|---|---|---|---|
| 63.76 | 0.18 | 6.00 | 1.34 | 0.00 | 0.07 | 1.78 | 5.49 | 9.28 | 1.09 | 0.69 | 3.27 | 0.07 | 93.02 |

## 3.6. Deposition Products

For the ICET tests, one concern is the deposition of debris/corrosion products in the tank. To help understand this problem, the corrosion/deposition products were collected after completion of the test. These products are fine yellow powders removed from the submerged CPVC rack. SEM/ EDS results shown in Figures 3-100 through 3-102 indicate that the fine yellow powders were mainly composed of fiberglass debris and particulate deposits containing O, Na, Al, C, Ca, Mg, and possibly Si.

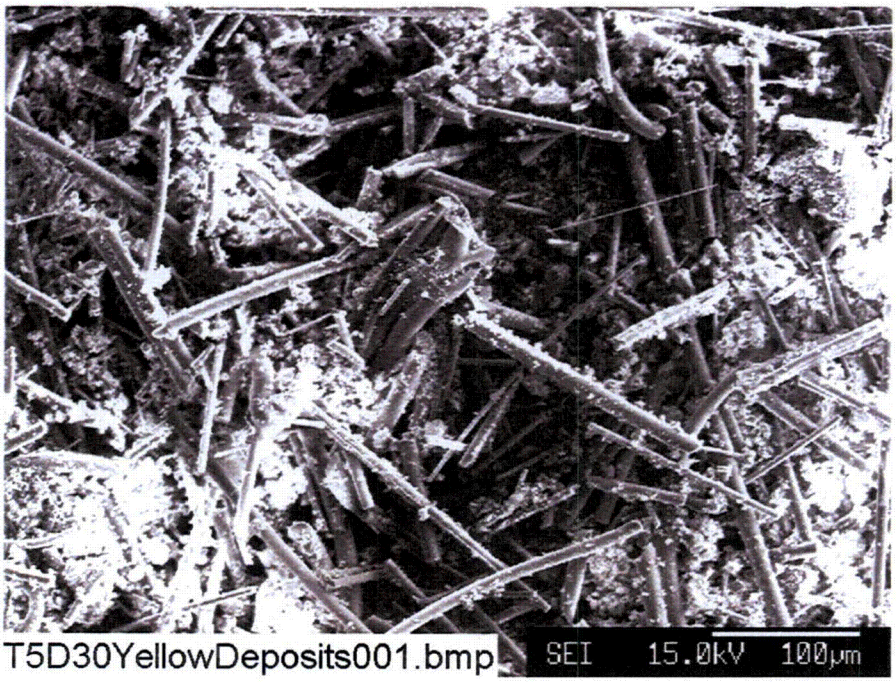


**Figure 3-100. SEM image magnified 200 times for the Test #5, Day-30 fine yellow powder on the submerged rack.**


**Figure 3-101. Annotated SEM image magnified 1000 times for the Test #5, Day-30 fine yellow powder on the submerged rack.**

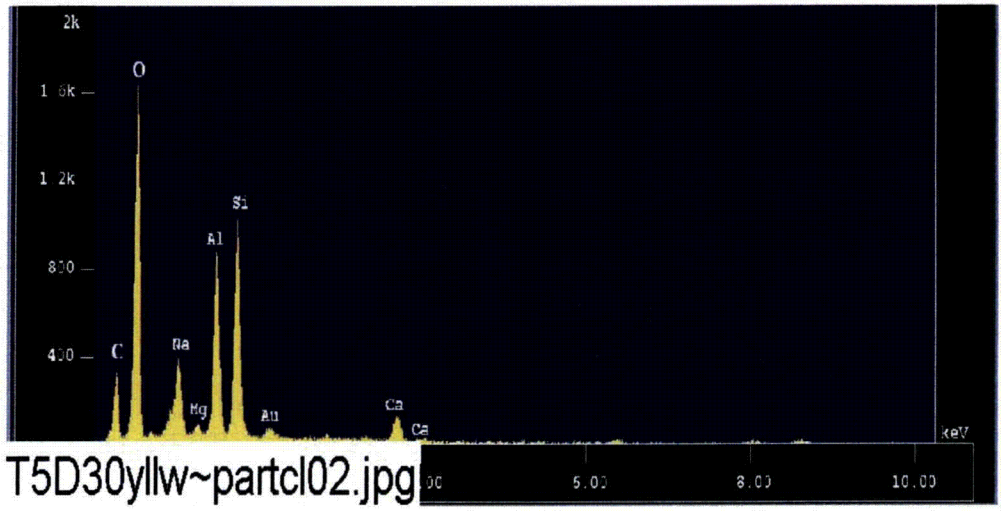


**Figure 3-102. EDS counting spectrum for the particulate deposit shown in Figure 3-101.**

## 3.7. Optical/TEM Images

The TEM images and EDS results for Test #5, Day-4, Day-15, and Day-30 unfiltered solution samples are shown in Appendix G. The unfiltered solution samples were extracted from the tank directly. A tiny drop of the test solution was transferred to a copper mesh and dried in air for TEM analysis.

TEM results show the presence of submicron-size colloidal particles in the samples (see Figures 3-103 through 3-105). However, it is unclear if the colloidal particles originally existed in the test solution or were formed during the drying process before TEM examination.

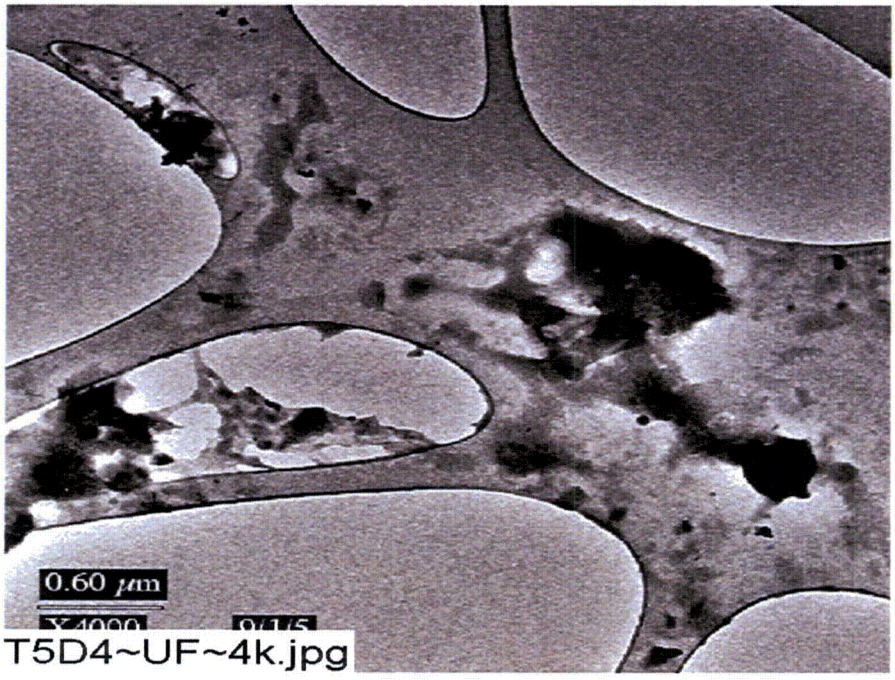


**Figure 3-103. TEM magnified 4000 times for one Test #5, Day-4 unfiltered sample location.**

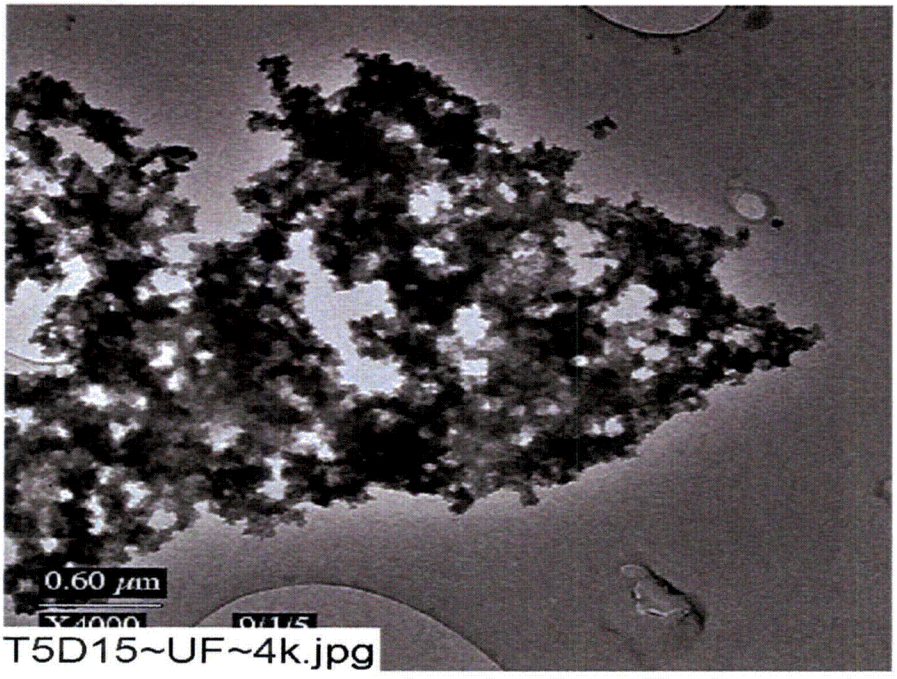


**Figure 3-104. TEM magnified 4000 times for one Test #5, Day-15 unfiltered sample location.**

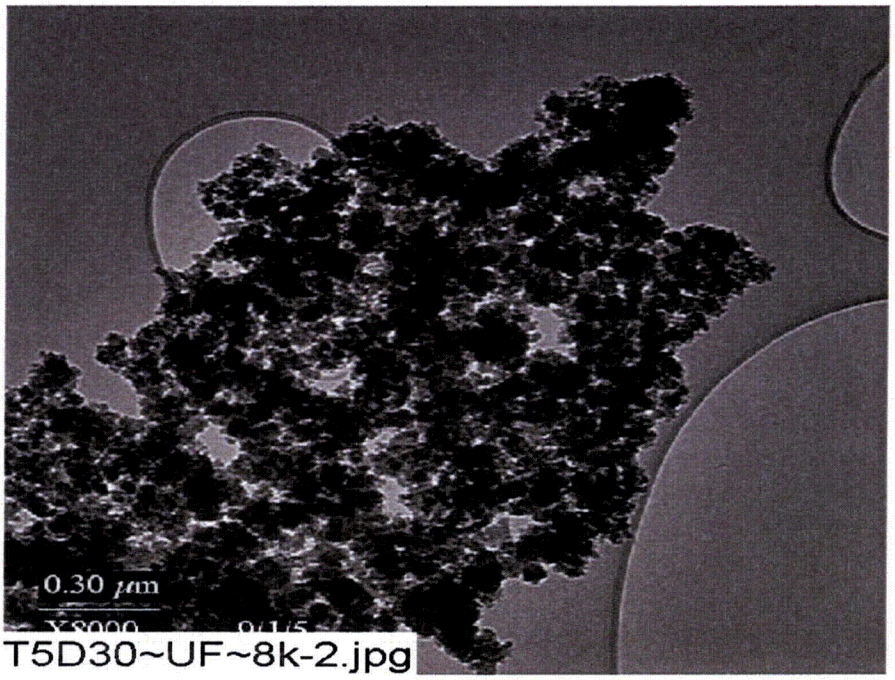


**Figure 3-105. TEM magnified 8000 times for one Test #5, Day-30 unfiltered sample location.**

## 3.8. UV Absorbance Spectrum

UV absorbance was measured for the Day-30 filtered solution sample and is shown in Appendix H. The purpose of this analysis was to identify the presence of any distinguished absorbance peaks that may identify organics present in the solution. However, based on the result, no distinguished absorbance peaks were found due to the heterogeneous nature of the test solution.

## 3.9. Shear-Dependent Viscosity

As explained in the Test #1 data report (Ref. 2), shear-rate viscosity measurements were taken weekly on test solution samples. The Test #1 solution at 25°C exhibited shear-thinning behavior, indicative of a non-Newtonian fluid. The solutions for Tests #2, #3, and #4 were all Newtonian fluids at 25°C.

As with Test #1, the Test #5 solution at 25°C exhibited shear-thinning behavior, as shown in Figure 3-106. The legend for the symbols gives the date the samples were remove from the solution. For example, "072705" is Day 2, and "082505" is Day 30. Shear thinning is indicated by the decrease in viscosity as the shear rate is increased to 20 1/s. Additionally, the solution's viscosity increases at all shear rates with time over the test duration, with one exception. The last sample taken on Day 30 (082505-0900-U) decreased to a value similar to that of the mid-test sample. While there is no definitive explanation for the decrease, it may be related to the late-test behavior of the turbidity, TSS, and aluminum and calcium concentrations.

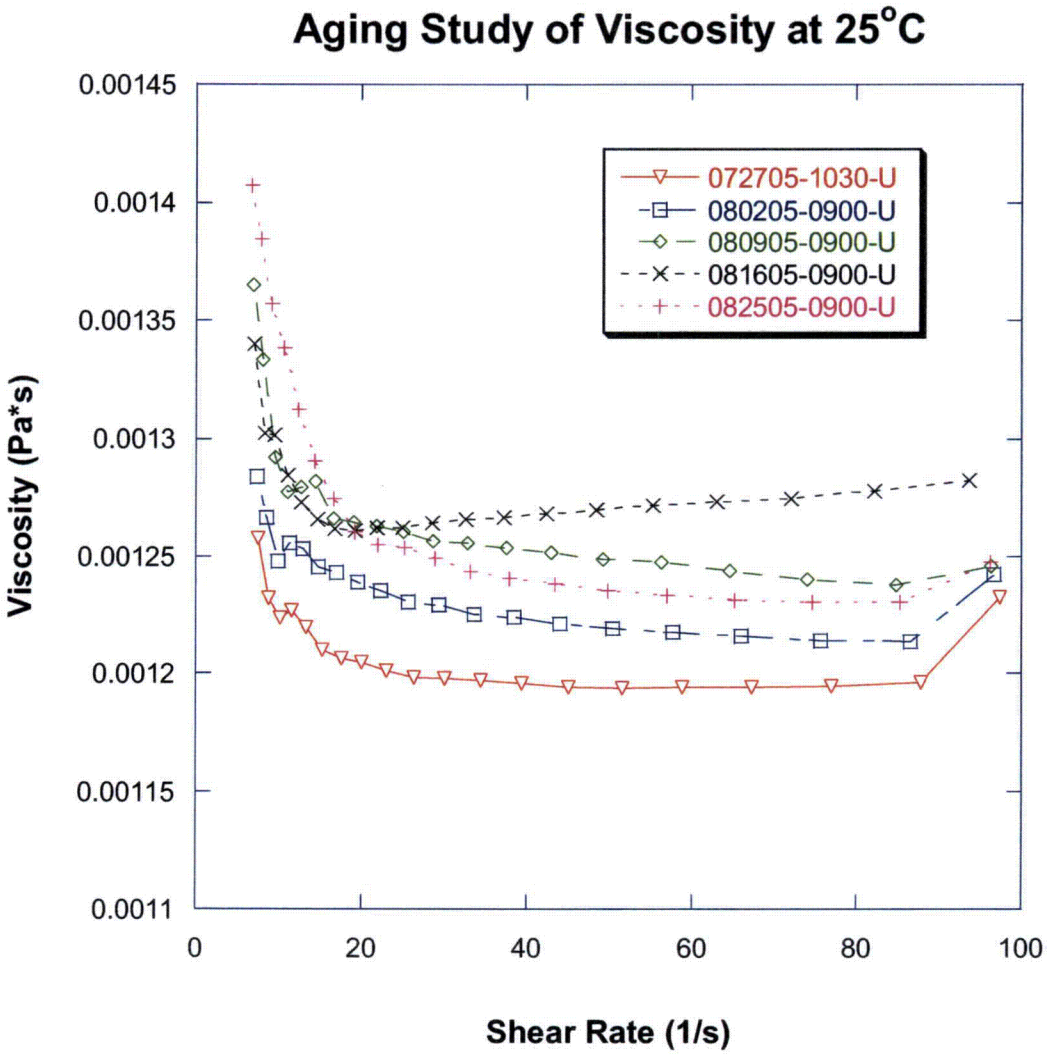


**Figure 3-106. Shear-rate viscosity measurements at 25°C.**

# 4. SUMMARY OF KEY OBSERVATIONS

ICET Test #5 ran for 30 days, and all conditions were maintained within the accepted flow and temperature ranges, with one exception. On Day 5, the addition of cold makeup water caused the test solution temperature to drop to 57.7°C, which is 0.3°C below the target minimum. The minimum temperature was below 58.0°C for less than 10 minutes. At the start of the test, the measured pH was 8.4. During the addition of hydrochloric acid, the pH dropped slightly to 8.3, and it remained between 8.2 and 8.4 for the duration of the test. The test solution turbidity decreased to approximately 2 NTU after 7 days. The turbidity at 60°C decreased to approximately 1 NTU the following day and remained near 1 NTU for the duration of the test. However, when the solution was cooled to 23°C, the turbidity increased to 5 NTU at Day 19 and remained near that value for the duration of the test.

Samples of the solution were taken daily. Analyses of the test solution showed that aluminum in the solution rose above 50 mg/L on Day 11 and fluctuated between 33 and 55 mg/L for the duration of the test. Calcium, silica, sodium, chloride, and boron were also prevalent in the solution.

Daily measurements of the constant-shear kinematic viscosity of the test solution revealed an approximately constant value at both test temperature and room temperature. Measurements of the shear-dependent viscosity indicated that at 60°C the test solution remained Newtonian for the entire test. At 25°C, the test solution exhibited shear-thinning behavior, and the viscosity generally increased at all shear rates as the test progressed. Light, wispy precipitates were visible after the test solution sat at room temperature for several days.

Examinations of fiberglass taken from the test apparatus revealed chemical byproducts and web-like deposits that spanned individual fibers. Flocculent deposits were also observed. The amounts of these deposits did not appear to increase significantly over the duration of the test, and the web-like deposits were absent in the Day-30 samples. The deposits were likely formed by chemical precipitation. In addition to these deposits, some samples had significant amounts of particulate deposits on their exteriors that were likely physically attached.

The submerged metallic coupons all developed thin particulate deposits that dulled their color and roughened their surface. Post-test examinations showed that the submerged aluminum coupons lost approximately 3% of their weight, but there were very little weight changes on the other coupons. The unsubmerged coupons exhibited some streaking but little or no weight change.

After the tank was drained, there was very little sediment on the tank bottom, but powdery deposition products were present on the submerged objects.

## REFERENCES


1. "Test Plan: Characterization of Chemical and Corrosion Effects Potentially Occurring Inside a PWR Containment Following a LOCA, Rev. 13," July 20, 2005.

2. J. Dallman, J. Garcia, M. Klasky, B. Letellier, and K. Howe, "Integrated Chemical Effects Test Project: Test #1 Data Report," LA-UR-05-0124, June 2005.

3. "Pre-Test Operations, Test #5," ICET-PI-017, Rev. 0, July 22, 2005.

4. "Test Operations, Test #5 (fiberglass and sodium tetraborate at pH 8)," ICET-PI-018, Rev. 0, July 22, 2005.

5. "Post-Test Operations, Test #3," ICET-PI-008, Rev. 3, May 2, 2005.